MODELLING WATER QUALITY OF THE PIKE RIVER WATERSHED UNDER FOUR CLIMATE CHANGE SCENARIOS

By

Colline Gombault
Department of Bioresource Engineering
McGill University, Montreal

October 2012

A thesis submitted to McGill University
in partial fulfilment of the requirements of the Degree of
Master of Science

ABSTRACT

Master of Science Colline Gombault **Bioresource Engineering**

Modelling Water Quality of the Pike River Watershed Under Climate Change Scenarios

The impacts of climate change on the hydrology and water quality of the Pike River watershed, an important contributor of nutrient loads to northern Lake Champlain, were predicted for the time horizon 2041-2070. Four water quality scenarios were simulated using a version of the Soil and Water Assessment Tool (SWAT) modified to suit Québec's agroclimatic conditions. Three of the scenarios were generated using climates simulated with the Fourth Canadian Regional Climate Model (CRCM4). The fourth scenario was generated using the climate simulated with the Arpege Regional Climate Model. SWAT was independently calibrated for the period 2001-2003, and then validated for the periods of 2004-2006 and 1980-2000, before inputting the climate scenarios. Potential mean changes predicted by these scenarios were then analysed for the evapotranspiration, surface and subsurface runoff, stream flow, sediment yields, and total phosphorus and nitrogen.

After calibration, mean annual evapotranspiration, surface and subsurface flow as well as water percolation were found to correspond satisfactorily with the hydrology of the basin. Likewise, monthly predicted stream flow compared reasonably well with observed stream flow. The performance of SWAT in simulating sediment and nutrient yields was clearly improved after calibration but did not always reach standards of acceptability. As for climate change results, only one scenario predicted a significant increase in mean annual stream flow and nutrient loadings. However, when considering shorter time spans, simulations predicted significant changes including a winter stream flow two to three times greater than current stream flow and earlier spring floods. The identified causes are the early onset of spring snowmelt, a greater number of rainfall events and snowmelt episodes caused by higher winter and spring temperatures. In contrast, peak flows in April, as well as summer stream flow, appear to decrease but not always significantly. Nutrient delivery to the lake significantly increased in winter and occurred earlier in the year as a consequence of hydrological changes. A three- to four-fold increase in subsurface flow was also observed in winter which may increase nutrient losses through this pathway.

RÉSUMÉ

Maîtrise ès Sciences Colline Gombault **Génie des bioressources**

Modélisation de la qualité de l'eau du bassin versant de la rivière Aux Brochets sous quatre scenarios de changement climatique

L'impact des changements climatiques sur l'hydrologie et la qualité de l'eau du bassin versant de la rivière Aux Brochets, un tributaire contribuant substantiellement à l'apport de nutriments au Nord du lac Champlain, a été prédit pour l'horizon 2041-2070. Quatre scénarios de qualité de l'eau ont été simulés avec une version du Soil And Water Assesment Tool (SWAT) adaptée aux conditions agro-climatiques du Québec. Trois de ces scénarios ont été produits en utilisant des climats simulés avec la quatrième version du Modèle Régional Canadien du Climat (MRCC4). Le quatrième scénario a été produit en utilisant un climat simulé par le modèle régional de climat Arpège**.** SWAT a d'abord été calibré pour la période 2001-2003, puis validé sur les périodes 2004-2006 et 1980-2000 avant d'y intégrer les scénarios climatiques. Ensuite, les changements moyens potentiels causés par ces scénarios ont été analysés pour l'évapotranspiration, le ruissellement, les écoulements souterrains, le débit et la charge en sédiments et nutriments (phosphore et nitrogène total).

Après calage, les valeurs annuelles et moyennes prédites d'évapotranspiration, de ruissellement de surface, d'écoulement souterrain ainsi que de percolation correspondaient à l'hydrologie du bassin. De même, les débits prédits mensuellement correspondaient aux débits mesurés. Le calage du modèle améliore clairement la capacité de SWAT à simuler les charges de sédiments et de nutriments. Cependant SWAT n'atteint pas systématiquement les standards de performance. En ce qui a trait aux changements climatiques, un seul scenario a prédit une hausse significative des débits et des charges annuelles en nutriments. Cependant, sur des périodes de plus courte durée des changements significatifs tels que des débits hivernaux deux à trois fois plus élevés que les débits actuels ont été simulés. De plus les crues printanières démarrent plus tôt dans la saison. Ces faits sont causés par la hausse des températures hivernales et printanières qui déclenche de nombreux épisodes de fonte de neige ainsi que de nombreux épisodes de pluie. À l'opposé, le pic des crues printanières en avril ainsi que les débits estivaux semblent diminuer, mais pas toujours significativement.

Sous l'effet des changements hydrologiques prédits, l'apport des nutriments au lac augmente significativement en hiver et se fait plus tôt dans l'année. Il a aussi été observé que le volume des écoulements souterrains triplait voire quadruplait en hiver ce qui pourrait augmenter la proportion des nutriments qui est perdue via la voie souterraine.

ACKNOWLEDGEMENTS

I would like to thank the Natural Sciences and Engineering Research Council of Canada (NSERC) which sponsored this study. I also thank Consortium Ouranos for providing data and funding for the realisation of the project. All the people listed below made this thesis possible and I am truly grateful to them. First, thank you to my supervisor Dr. Chandra Madramootoo for providing me with the opportunity to deepen my knowledge in the field of water quality modelling with this project as well as for providing funding, valuable guidance and much-needed and unfailing support for this research , despite my slowness to finish this work. My co-supervisor, Dr. Aubert Michaud from the Institut de recherche et de développement en agroenvironnement (IRDA - Research and Development Institute for the Agri-Environment) also played a vital role in facilitating the completion of this thesis by first raising my interest in water quality modelling issues, and second providing advice, great and continuous support along these last years. Thank you for sharing the SWAT-Qc model, the data for its parameterization and calibration, and for your efforts to diffuse the results of this work.

A special thank you goes also to Mme Isabelle Beaudin from the IRDA for her sound technical assistance in hydrological modelling and valuable professional advice. I also thank Isabelle for her generosity in welcoming me at her house during my visit at IRDA. Dr. Mohamed Chikhaoui of the Brace Centre deserves also many thanks for his support. Thank you for your patient guidance and constant availibility when needed. Similarly, Ms. Marie-France Sottile from Ouranos has provided invaluable support and explanation about climate change and climate models. Thank you for your assistance and your time in answering my questions and revising my thesis. Thank you to Mr. Martin Mimmeault from the ministère du Développement durable de l'Environnement et des Parcs (MDDEP) for providing water quality data. Thank you to Georges Dodds, Juliette Blin and Salma Bannouri who helped in correcting and editing this thesis and undoubtedly improved its quality.

Merci à tous ceux qui ont été présent lorsque j'en avais besoin : Johanna Richards, Mélanie Lapointe, Candice Young, Felix Jaria, Ajay Singh, Audrey Wachter, Zehra Rivzi, Felixce N'gwa, Lilya Kenhache et Bano Mehdi ainsi qu'à tous les autres collègues du département qui rendront ces années inoubliables. Merci pour votre écoute et vos conseils. Finalement, merci infiniment Quoc-Hoa Tran pour ta patience, ton support infaillible et tes petits plats réconfortants. De la même façon merci à ma famille **entière** pour leurs chaleureux et réconfortants encouragements ainsi que leur important soutient. Thank you all for your patience, kindness and support.

TABLE OF CONTENTS

LIST OF TABLES

LIST OF FIGURES

LIST OF ABBREVIATIONS

ACU: one climate simulation name

ACZ: one climate simulation name

ADC: one climate simulation name

AE: Absolute error

AFD/AFA: one climate simulation name

ANSWER: Areal Nonpoint Source Watershed Environment Response Simulation

(Ann) AGNPS: (Annualized) Agricultural Non-Point Source

Arpege: one climate simulation name (and French climate model name)

AGCM3: Atmospheric General Circulation Model, 3rd version

AMNO: North-American climate modelling domain

ArcSWAT/ArcView: Interface for SWAT model

BMP: best Management Practices

CGCM: Canadian Global Circulation Model

CRCM4: Canadian Regional Climate Model, 4th version

C_{usle}: USLE cover and management factor

DD: Dynamical Downscaling

DEM: Digital Elevation Model

DJF: December, January, February

DWSM: Dynamic Watershed Simulation Model

ECHAM4: German global climate model of the Max Plant Institute for Meteorology

ERA40: Reanalysis climate data series

EPA: US Environmental Protection Agency

GEF: Global Environment Facility

GIS: Geographic Information System

GHG/GHGE: greenhouse gas emission

HRU: Hydrological Response Unit

HSPF: Hydrological Simulation Program-Fortran

IPCC: Intergovernmental Panel on Climate Change

IRDA: Institut de Recherche et Développement en Agroenvironnement

JJA: June, July, August

LAM: Limited Area Model

MAM: March, April, May

MIKE-SHE: The European Hydrological System Model

MDDEP: Ministry of the environment, Sustainable development, and Parks

MRCC: Model Regional Canadien de Climat (French translation of CRCM)

MUSLE: Modified Universal Soil Loss Equation

NAO: Northern Atlantic Oscillation

N: Nitrogen

NSE: Nash Sutcliffe Efficiency

NPS: Non-Point Source

OBVBM: Organisme de Bassin Versant de la Baie Missisquoi

P: Phosphorus

PAEF: Plan agro-environnemental de fertilisation

PBIAS: Percent Bias

PCP: Precipitation

PS: Point Source

PR_{up}/PR_{dw}/PR_{wq}/PR_{mouth}: Pike River upstream/Pike River downstream/Pike River water quality/Pike River at the outlet

PRMS: Precipitation-Runoff Modelling System

RCM: Regional Climate Model

REA: Règlement sur les Exploitations Agricoles

RnQ : Surface runoff

RUE : Radiation Use Efficiency

SCS CN: Soil Conservation Service Curve Number

SD: Statistical Downscaling

Sed: Sediments

SHETRAN: Système Hydrologique European Transport Model

SON : September, October, November

SRES A2: Special Report on Emission Scenarios (A2 is the name of one scenario).

SubSQ: Subsurface flow

SWAT: Soil and Water Assessment Tool

SWAT-OBS, SWAT-ACZ, SWAT-ACU, SWAT-ADC, SWAT-AFD and SWAT-ARP: Generic names of the simulations run with climate scenarios.

SWCS: Soil and Water Conservation Services

Temp: temperature

TN and TP: Total nitrogen and Total phosphorus

USLE: Universal Soil Loss Equation

WC_{up}/WC_{dw}: Wallbridge Creek upstream/Wallbridge Creek downstream

WMP: Watershed Master Plan

WYLD: Water yield

LIST OF SYMBOLS

$[CO^2]$: Concentration of atmospheric carbon dioxyde

ΔAET: 30-Years mean seasonal changes in evapotranspiration

ΔF-C: Difference between the 30 years mean future and historical simulations

ΔPcp: 30-Years mean seasonal changes in percipitation

ΔRnQ: 30-Years mean seasonal changes in surface runoff

ΔSubSQ: Years mean seasonal changes in subsurface flow

ΔTemp: Years mean seasonal changes in temperature

ΔWyld: Years mean seasonal changes in wateryield

ψ: soil water

K_{sat} : hydraulic conductivity

ψ_{fc} : field capacity

ψ_{sat} soil water saturation

CHAPTER 1: INTRODUCTION

1.1 Problem definition

In recent decades and as a result of the intensification of Québec's agricultural production since the 1970s, agricultural pollution has impaired freshwater ecosystems (Boutin, 2006). More specifically, an increasing number of lakes in the southern portion of the province have become eutrophic due to an overloading of nutrients attributable to intense agricultural activity upstream (Corporation Bassin Versant Baie Missisquoi, 2003; MENV, 2003; MDDEP, 2008). Besides deteriorating water quality and causing the disappearance of ecologically important species, eutrophication also impedes drinking water treatment processes. Worst-case scenarios are characterized by the contamination of waters by toxic blue-green algae blooms (Carpenter et al., 1998).

While this has been an issue for over two decades in Quebec's Missisquoi Bay, located in the northern portion of Lake Champlain (Groupe de travail Québec-Vermont, 2000) the situation became critical province-wide in 2007 when 180 lakes were reported to be contaminated with blue-green algae. In recent years, the number of affected lakes has increased between 108 and 119, with usage restrictions imposed for a dozen affected water bodies (MDDEP, 2009;2011). Between 2004 and 2006, the number of lakes reported to be contaminated more than doubled (Lavoie et al., 2007).

Nutrients originating from a point source can be more easily controlled. Therefore, most recently considerable efforts have been directed towards the abatement of Non-Point Sources (NPS) of pollution in agriculture (MENV, 2003; Boutin, 2006; MAPAQ, 2009a). As such, farmers are encouraged to integrate Best Management Practices (BMP) in their operations. Tools have been developed to identify critical source areas, and support has been provided to apply correctional measures in order to respect Québec regulations (MAPAQ, 2009b; Michaud et al., 2009b). However, with ongoing climate change, concerns are rising about the efficacy of these measures in the long term (SWCS, 2003).

Being extremely dependent on weather, NPS pollution in North America might already be affected by a changing climate and this will most likely continue (SWCS, 2003). In Southern Québec, global and regional climate models predict an increase in temperature and annual precipitation, as well as in the frequency and intensity of storms (Bourque and Simonet, 2008). These climate alterations are expected to accentuate the erosive power of rainfall and runoff and consequently increase the export of sediments and nutrients (SWCS, 2003; Lettenmaier et al., 2008).

The Missisquoi Bay has suffered from the severest cases of eutrophication due to algal blooms recorded in Quebec (Blais, 2002). Flowing directly into the Bay, the Pike River annually receives and delivers a significant amount of nutrients into the Bay. Eighty percent of Phosphorus (P) loads entering the Bay are attributable to NPS pollution from agricultural sources (Troy et al., 2007). As a result, many field, basin and watershed-scale studies have been conducted within the Pike River watershed to understand the dynamics of NPS pollution in this region.

A 2002 agreement between the Province of Québec and the State of Vermont, which share the Bay, sets a 2016 target of 25 µg P L^{-1} reaching the Bay. By identifying and targeting critical areas, important P and Nitrogen (N) transport mechanisms and the BMPs best suited to address the watershed's NPS pollution issues, a number of studies (Deslandes et al., 2002; Madramootoo et al., 2004; Gollamudi, 2006; Deslandes et al., 2007; Eastman, 2007; Michaud et al., 2008) have provided regional stakeholders with information and decision-making tools to effectively address this target. A modelling exercise with the Soil and Water Assessment Tool (SWAT 2000) determined that the Pike River delivered 44 Mg P yr^{-1} into the Bay during the years 2001-2003, with cultivated areas contributing 1.3 kg P ha^{-1} yr^{-1} (Michaud et al., 2007). This was 5 Mg P yr^{-1} above the target load for the Québec side, and recent studies reveal no significant reduction of P loads reaching the Missisquoi Bay during the monitoring period of 1990-2007 (Lake Champlain Basin Program, 2008). It is just within the Pike river watershed that a slight decrease in Total Phosphorus (TP) loadings has been observed. However, overall, P concentration remained at the same high level these recent years- namely 50 µg l^{-1}-a value twice greater than the target cited above (Beck et al., 2012).

Many studies have examined the impact of climate change on hydrological processes in Québec (Minville et al., 2008; Quilbé et al., 2008; Boyer et al., 2010; Sulis et al., 2011) but very few across the world have looked at the implication of climatic and hydrological changes on erosion and both N and P nutrient pollution in a snowmelt basin (Arheimer et al., 2005; Booty et al., 2005; De Jong et al., 2008; Pierson et al., 2010, Dayyani et al., 2012). The magnitude, directions, sensitive time horizons and causes of these changes are therefore not precisely known in Québec. A better assessment and understanding of the impact of climate change on the nutrient delivery by the Pike River watershed, as well as an assessment of BMP efficiencies and a re-evaluation of the location of critical areas caused by more extreme weather conditions could help to maintain and strengthen the ongoing efforts undertaken by the Organisme du Bassin Versant de la Baie Missisquoi (OBVBM) - the local watershed body - to remedy the degradation of water quality in Missisquoi Bay.

This thesis focuses on predicting future trends of nutrient exports within the Pike River watershed under various climate scenarios. It aims more specifically at examining the effect of changes in precipitation and temperature regimes on the principal mechanisms causing soil erosion and NPS pollution within the watershed. This work is the first step in a wider endeavour to investigate the evolution of blue-green algae status under a warmer and wetter climate. The study was conducted in collaboration with the Institut de Recherche et Développement en Agroenvironnement (IRDA) and the Ouranos Consortium, an organization responsible for regional climate modelling and the leader of many studies on the impact of, and adaptation to, climate change in Québec and Canada (Ouranos, 2010b). It was funded by the Natural Sciences and Engineering Research Council of Canada (NSERC) and Ouranos.

For the purposes of the study, a chain of biophysical models was used. The Ouranos Consortium provided a set of climatic projections by the Canadian Global Climate Model

(CGCM) dynamically downscaled by the Canadian Regional Climate Model (CRCM) at a resolution suitable for hydrological modelling processes. These data served as input to a modified version of the Soil and Water Assessment Tool (SWAT) adapted to the agroclimatic conditions of Southern Quebec by IRDA.

1.2 Research objectives

The broad objective of this research was to assess the impacts of future climate scenarios on the quality of water in the Pike River watershed. In order to achieve this objective the following specific objectives were targeted:

1. Calibrate and validate the SWAT model for the Pike River's hydrology, sediment loads and nutrients losses.
2. Integrate the data from four climate change scenarios extracted from two Regional Climate Models (RCM), the Canadian Regional Climate Model (CRCM) and the French Global Climate Model, ARPEGE at variable resolution, into SWAT in order to compare watersheds response between a past (1971-2000) and future (2041-2070) climate.
3. Assess and understand the effect of these scenarios on the hydrology of the Pike River watershed as well as the effect of these hydrological changes on water quality at the outlet of the Pike River.

1.3 Scope

The modelling was conducted on a small watershed (630 km^2) in Southern Québec and results are aggregated at the basin scale. Four climate change scenarios were used, covering a range of possible changes predicted by a set of simulations available for the region. One scenario of future greenhouse gas (GHG) emissions, A2, was used for one time horizon in the near future (2041-2070). Precipitation and temperature changes are variable from one region to another, and hydrologic and nutrients losses are dependent on the watershed's physical characteristics. The results of this study are therefore strictly restricted to the Pike River watershed and Missisquoi Bay for the projected time horizon. Furthermore, land-use was kept constant for all climate scenarios. In reality, land-use could change in the future, and this might affect future nutrient loadings. However, the research is meant to shed light on the impacts of climate change under specific land-use and climate scenarios.

1.4 Thesis outline

This thesis was written as a series of chapters answering the objectives previously cited. Chapter 2 presents a summary of the relevant literature on nutrient NPS pollution; the efforts Québec has expended to reduce such pollution and to address the potential impacts that climate change may have on NPS pollution. Chapter 3 contains the description of the Pike river watershed and the research methodology. Results of the calibration and impact assessment are provided in Chapter 4 and address the quantitative and qualitative aspects of hydrological changes. Chapter 5 summarizes the main findings of this thesis and highlights their utility, while Chapter 6 proposes various future research directions which might serve to complete this assessment.

CHAPTER 2: LITERATURE REVIEW

2.1 Nutrient non-point source pollution

Non-point source pollution affects an increasing number of water bodies throughout the world. Given the severity of its consequences, and the difficulty in controlling or reversing its impacts, this type of pollution has been recognized as a major and rising challenge in water resource conservation (Carpenter et al., 1998; Aladin et al., 2005; Orr et al., 2007; Michaud et al., 2008; Yang and Wang, 2010).

Non-point source pollution encompasses all dispersed pollutants transported into water bodies and occurs mostly through the movement of waters over a wide territory (Carpenter et al., 1998). Highly dependent on a territory's weather, geophysical characteristics and management, NPS pollution is a complex phenomenon, often arising from the interaction of several spatiotemporally variable factors over a wide area. This makes it difficult and costly to measure and regulate (Carpenter et al., 1998; Horan and Ribaudo, 1999). Pollutants generally include sediments, nutrients, pesticides, salt or pathogens (Ribaudo et al., 1999; Aladin et al., 2005; Bos et al., 2005).

Nitrogen and phosphorus become harmful pollutants when their concentration exceeds limits tolerable for aquatic ecosystems, thus causing an acceleration of the water bodies' aging process known as eutrophication (Carpenter et al., 1998; Aladin et al., 2005; Gangbazo et al., 2005). Eutrophication generally occurs on a geological scale, but nutrient over-enrichment accelerates the process to a harmful speed, where it alters the ecological balance of, and services provided by, aquatic ecosystems (Hades, 2003; Chapin et al., 2002).

Indeed, eutrophication results in the proliferation of aquatic weeds and algae, stimulated by a water body's excessive fertility (Sharpley, 1995; Carpenter et al., 1998). Under such conditions of luxury consumption, weeds and undesirable algae gain a competitive edge over typical endemic species, thus restricting their development (Hades, 2003). When these rapidly growing algae and weeds die, micro-organisms start decomposing the increased quantity of decaying biomass and consuming more oxygen, thus depleting oxygen levels in the water to reach anoxic conditions. Under these conditions massive fish kills occur (Carpenter et al., 1998). This alteration in food chain and aquatic habitat may entail the progressive disappearance of fauna. Moreover, eutrophication is often accompanied by outbreaks of toxic algal blooms (Sharpley et al., 1994). In freshwater bodies, these blooms are primarily associated with blue-green algae (a.k.a. cyanobacteria), which can release hepa- and neuro-toxins into the water, thus posing serious health risks to livestock and humans (Sharpley, 1995; Blais, 2002).

Sediments also contribute to eutrophication. In addition to increasing water turbidity and altering the aquatic habitat, they provide a substrate for aquatic weeds to grow in. They also carry adsorbed nutrients to soil particles (particulate phosphorus and nitrogen) and thereby contribute to the loss of a significant proportion of nutrients in waterways (Nearing et al., 2001 in Ritter and Shirmohammadi, 2001).

As a result of near chronic eutrophication, the socio-economic advantages brought about by water bodies' ecosystem goods and services are reduced (Horan and Ribaudo, 1999; Blais, 2002; Lake Champlain Basin Program, 2008). Intoxication hazards, the massive presence of algae, the increase in water turbidity, and the emanation of foul odours from the decomposing biomass decrease water drinkability and hamper the use of water bodies for recreational activities such as swimming or nautical activities. This damage also obstructs and increases the cost of industrial, agricultural and municipal water treatment activities. Furthermore, fish kills and the loss of biodiversity limit food supplies and thus affect fisheries activities and recreational fishing. Finally, tourism and housing values are decreased due to a loss in landscape aesthetics and attractiveness (Sharpley, 1995; Carpenter et al., 1998).

Combined with point source (PS) pollution, NPS nutrient pollution has affected a large number of productive lakes, rivers and estuaries throughout the world. More difficult to control than PS pollution, NPS pollution is frequently the cause of water degradation nowadays, especially in developed countries where financial means are more readily used to address PS pollution (Carpenter et al., 1998; Ribaudo et al., 1999; Bos et al., 2005).

Intensive agricultural activities are often cited as the top source of NPS pollution (Carpenter et al., 1998; Yang and Wang, 2010). They promote the transfer of pollutants from agricultural lands to water bodies by altering local nutrients cycles (massive natural and synthetic nutrient inputs) and local hydrological processes (soil compaction decreasing infiltration rates, rearrangement of drainage channels), the main factors controlling availability and mobility of nutrients (Ritter and Shirmohammadi, 2001).

In a 2004 survey undertaken in the United States, water was found to be unsuitable for human usage in 44 %, 64% and 30% of waterways, lakes and estuaries, respectively. Agricultural activities were, indeed, cited as the top causes of these impairments (EPA, 2009). Horan and Ribaudo, 1999 reported that soil erosion has already cost between 2 and 8 billion dollars per year to American water users. Similarly, in Europe, agricultural NPS pollution is considered as the greatest threat to meeting the requirements of the EU Water Framework Directive goals (Orr et al., 2007; Hesse et al., 2008; Yang and Wang, 2010). In Asia, South America, Africa or Australia, many studies have also reported serious impairment of important lakes and waterways caused by intensive agriculture activities combined with other industrial or urban point sources (Bos et al., 2005; Wang et al., 2006a; Webster et al., 2009; Tian et al., 2010). The most extreme examples of eutrophication documented are the anoxic zone of the Gulf of Mexico, the Chesapeake Bay estuary on the North Atlantic American Coast, the UK’s Mersey River, the Baltic Sea, and the Eurasian portion of the Danube and the Black Sea. The last case is the first example of successful remediation and restoration; however, it required over 15 years, and US$ 3.5 million to restore the Danube as well as US$ 50 million in governance reforms (Global Environment Facility, 2010). The Global Environment Facility (GEF) estimates that the remediation of other important water bodies may cost up to US$ 30 million.

In recent years, billions of dollars have been earmarked to support Québec farms in reducing erosion and nutrient losses through the Prime-Vert Program. Such interventions are important, as, for example, the northern region of Lake Champlain stands to lose several million US$ due to disrupted touristic activities if present conditions persist (Mimeault, 2004).

Both N and P contribute to biomass proliferation, but N is the limiting nutrient in brackish estuarine and coastal waters, while in freshwater ecosystems, such as Lake Champlain, P is the main nutrient controlling biomass proliferation (Sharpley, 1995; Carpenter et al., 1998). However, N presents other dangers as it becomes toxic when NO_3 concentration exceeds 10 mg L^{-1} (Follett, 1995). Much emphasis has nonetheless been placed on P reductions, for two main reasons: (i) blue-green algae have the capacity to fix N from the atmosphere, rendering its availability to the plant difficult to control, and (ii) because field fertilization plans were based for a long time on N requirements, which led to P applications that were much greater than necessary, particularly in the case of manure. Furthermore, because agricultural soils in Québec were poor in P, high quantities of P fertilizers were applied on soils too meet crop requirements. Such excessive P fertilisation led to its gradual accumulation in soils, until levels reached saturation in many agricultural regions of Québec (CRAAQ, 2010). Accordingly, the risk of P loss through runoff increased and P concentrations in many Québec rivers rose well above the tolerable limit of 0.03 mg L^{-1}, a level below which eutrophication seldom occurs (Gangbazo et al., 2005).

2.2 Soil and water conservation efforts in Québec

In 2002, the government of Québec adopted its first Water Policy in order to improve the protection of ecosystems and public health (MDDEP, 2002). Among the policy's five cornerstones, one is the remediation of the quality of impaired waters and the reclaiming of their lost uses by intensifying already implemented efforts to reduce nutrient pollution, especially those related to agricultural NPS pollution.

Thus, a provincial regulation, the “Réglement sur les exploitations agricoles” (REA) was introduced in Québec. The latter legislates farming activities in such a manner as to limit and reduce nutrient losses to waterways through the promotion and application of a better management of nutrients. In addition to prohibiting livestock access to water courses, establishing norms for buffer strips during manure application near wells and waterways, and regulating manure storage, application method, and timing, the REA focuses on the recovery of the soil’s P balance. In order to respect the soil’s carrying capacity and avoid P losses, each farmer is required to develop and follow a fertilization plan (“Plan Agro-environmental de fertilization”, PAEF) based on soil P content and saturation, land availability for manure application, nutrient content in the applied manure and crop nutrient needs. In doing so, field over-fertilization and P accumulation in top soil are prevented, reducing the risk of P transport. Besides controlling nutrient sources, strategies to reduce factors having an impact on nutrient transport are promoted. The policy on protecting river banks, shore lines and floodplains requires farmers to leave an uncultivated strip of a minimum of 3m width near all waterways and lakes to act as a sediment and nutrient filter (Québec, 2012). No-till or reduced tillage, crop residues and several other BMPs are also promoted to reduce runoff transport.

Financial and technical support is achieved through government subsidies (Prime-Vert programme) and by agro-environmental clubs or concerted action agro-networks. As a result, the greatest contributors to nutrient pollution had to comply with all the new regulations by April 2010. In order to hasten the compliance of farms with these regulations, the Prime-Vert programme’s financing of 70% to 100% of necessary upgrades was halved after this date. Besides, most financing programs and agencies authorizing new agricultural projects adopted the principle of environmental cross-compliance. If not in conformity with the REA, financial aids, tax exemptions or new farm projects are not accepted (Financière agricole, 2009).

Finally, in 2009, the policies and efforts undertaken to protect and recover water uses of degraded water bodies were strengthened by a provincial law on water, namely the Act to affirm the collective nature of water resources and provide for increased water resource protection. Under this law, both the government and citizens are legally responsible for water resource protection and must collectively prevent water resource degradation and repair all damages caused to the resource (Assemblée Nationale, 2009).

Guided and coordinated by watershed organisations, the local population and businesses operating within the watershed must therefore develop and follow a Watershed Master Plan (WMP) which delineates the objectives and actions planned for the protection and management of their water resources (Auger and Baudrand, 2004). This plan must then be studied and accepted at the governmental level.

Still, most WMP do not take into account the effects that climate change might have on water quantity and quality. Hence, understanding the potential impact of climate change on hydrological processes and on the export of sediments and nutrients to the bay is an essential first steps for the protection of Missisquoi Bay and its watershed water quality (Stager and Thill, 2010).

2.3 How climate change can affect non-point source pollution

2.3.1 Effect of a change in rainfall regime

As in most other parts of the world, Québec freshwater resources are expected to be negatively impacted in terms of their quantity, quality or both, by climate change (Bates et al., 2008; Bourque and Simonet, 2008). In agricultural watersheds, there are important concerns relative to an increase in NPS pollution, due to the forecast of greater annual precipitation and to an increase in the frequency of intense rainfall events. These would enhance total runoff quantity and intensity, which in turn will increase erosion and nutrient transportation (Bourque and Simonet, 2008; SWCS, 2003).

Nutrients may be transported to surface waters through surface runoff and subsurface runoff in their bioavailable and soluble forms (mostly as phosphate and nitrate) or their insoluble forms (mostly as organic form and/or bounded to sediments). Therefore, the greater the volume of water transiting through these pathways, the greater the risk of transporting nutrients. However, the quantity and specific forms of lost nutrients depend on the pathways taken by rainfall and snowmelt waters before reaching the hydrological networks (SWCS, 2003).

In agricultural watersheds, surface runoff causes the greatest portion of nutrient losses by detaching and carrying soil particles into river networks (Sharpley et al., 1994). Phosphorus is especially sensitive to surface runoff because it is easily adsorbed to soil particles and has a rather low mobility in soil. Therefore, except in the specific conditions under which P may move downward in the soil profile [soil P saturation, preferential flow, acidic organic, sandy or peaty soils (Sharpley et al., 2003)] it generally remains in the first top few millimetres of the soil. Furthermore, eroded sediments tend to carry a higher concentration of nutrients because these sediments, often made up of clay and organic matter, have a higher capacity to attract nutrient ions due to their negative charges (SWCS, 2003; Neitsch et al., 2005). This process is termed sediment nutrient enrichment.

In the Pike river watershed it has been observed that the majority of NPS pollution was generated through surface runoff during snowmelt and fall rainfall events. However, significant amounts of P were also found in the subsurface drainage waters (Jamieson et al., 2003; Deslandes et al., 2007). Therefore, a change in runoff characteristics (amount, timing and intensity) will have a serious impact on the delivery of nutrients to the Bay.

Both rainfall intensity and surface runoff are responsible for water erosion. The erosive power of rainfall is correlated to the 30 minutes at which the storm’s rainfall is at its maximum intensity (Wischmeier and Smith (1978) cited in (SWCS, 2003)). As for surface runoff, its erosive power and pollutants transport capacity depend on its volume, depth and velocity. Again, rainfall amount and intensity determine runoff volume, depth and velocity by influencing soil infiltration. The greater the rainfall intensity, the sooner the precipitation rate exceeds the infiltration rate and the greater the runoff volume, depth and velocity. Similarly, the infiltration rate decreases as soil moisture increases when a large amount of precipitation occurs through a greater number of wet days, or through higher rainfall rates remaining below infiltration rates (SWCS, 2003).

Pruski and Nearing (2002b) found that all other factors being equal, an increase in annual precipitation by 1% (increase of the number of wet days only) triggered an average increase in surface runoff and erosion of 1.28% and 0.85%, respectively across different soil, slope, crop and weather regimes. If the intensity of precipitation was to simultaneously increase (increase of wet days and rainfall amount per day), surface runoff and erosion would further increase by 1.97% and 1.66%, respectively, on average. In similar studies in semi-arid (Arizona and Mediterranean) and humid (Belgium) watersheds, Nearing et al. (2004) and Nunes et al. (2008) found that an increase in rainfall intensity has a greater effect than an increase in wet days. They also all noted that both changes would likely trigger greater changes in runoff and erosion than a simple increase in rainfall depth. The SWCS (2003) concluded that an increase in wet days would be less erosive than an increase in intensity but is likely to increase the transport of nutrients, especially soluble nutrients, to surface and ground waters through subsurface transport and leaching.

It is also important to note that in winter greater precipitation events will occur as rainfall due to warmer temperatures. However, soils may remain frozen which will considerably reduce water infiltration and trigger runoff, erosion and nutrient transport (Michaud, 2010).

Slope of the terrain, the soil structure and permeability, soil chemistry, land-use, and land-use management also affect surface runoff and infiltration. Some of these variables may change in the future depending on how climate change will affect biomass growth, and how farmers will adopt new practices to reduce NPS pollution and adapt to climate change effects (Nearing et al., 2005; Jeppesen et al., 2009). However, these aspects are outside the scope of this project and will not be reviewed here because of time constraints.

2.3.2 Effect of a change in temperature regime

In addition to rainfall amount and intensity, changes in temperature should also strongly affect several components of the water cycle such as runoff and therefore NPS pollution, indirectly. Over the last three decades, significant changes within snowmelt river basins were observed and mainly attributed to the past decades' warmer temperatures (Bates et al., 2008). In Canada, mean stream flow discharge seems to have increased during winter, but decreased in summer, while the onset of spring floods occurs earlier (Whitfield and Cannon, 2000). Similar changes have been observed in the American Northeast, with snowmelt and the resulting spring flood recorded one to two weeks earlier than usually (Hodgkins et al., 2003; Hodgkins and Dudley, 2006). Furthermore, the depth and duration of snow cover in this region has tended to decline with greater snowmelt and rainfall events during the winter explaining the greater winter discharge (Huntington et al., 2004; Burakowski et al., 2008; Campbell et al., 2010).

Boyer et al. (2010) pointed out that these observed changes were partly related to positive anomalies in the North Atlantic Oscillation (NAO), a natural warming occurring periodically, part of the natural variability of the climate. Although the results of the past warming were not all attributed to climate change, they give an insight into the potential consequences of a change in climate towards higher temperatures.

As mentioned above, temperature changes are also indicative of possible increase or change in soil degradation and nutrient losses. Changes in seasonal runoff and stream-flow directly affect the timing of nutrient delivery. Moreover, the decrease in snowpack reduces soil protection during winter, increasing soil vulnerability to increased rainfalls and runoff episodes (Jeppesen et al., 2009). Similarly, if more precipitation events occur during vulnerable periods, as predicted for the spring and autumn (see section 2.4.2) when crops offer little protection to the soil and manure has been spread, erosion and nutrient loss risks are heightened (SWCS, 2003). This could be magnified by higher temperatures which would prompt earlier harvests and leave soil unprotected for a longer period (Jeppesen et al., 2009). Conversely, an increase in temperature may also accelerate crop growth and nutrient uptakes, reducing the risk of erosion and nutrient losses by protecting the soil earlier in spring and subtracting nutrients to runoff or leaching (Bouraoui et al., 2002). This last response, contrary to the direct effect of precipitation and temperature on water balance, is categorized as an indirect effect of climate change.

Finally plant residue decomposition rate and microbial activity involved in the mineralisation and chemical transformation of nutrients may also be stimulated under a warmer climate. This may increase the availability of nutrients and their mobility (Bouraoui et al., 2002; Jeppesen et al., 2009).

2.3.3 Indirect effects of climate change

Indirect effects include the impact of CO_2, solar radiation, temperature and soil water availability on biomass growth (Pruski and Nearing, 2002a). A stress in water and in temperature during the summer is likely to decrease soil protection provided by the biomass, resulting in increased erosion and nutrient losses if heavy rainfalls occur. On the other hand, a CO_2 increase may have the inverse effect on plant growth and biomass as higher CO_2 concentration might increase the photosynthesis processes and decrease evapotranspiration rates of crops by reducing the stomatal apertures of the leaves through which water evaporates. As a result, both crop water use efficiency and crop cover increase. This may result, in turn, in improved soil protection (Bunce, 2004; Leipprand and Gerten, 2006).

The response of soil erosion and nutrient losses to a change in climate is therefore complex and will result from the combined response of plant biomass and runoff to climate change (SWCS, 2003). Pruski and Nearing (2002a) found, however, that an increase in rainfall would likely lead to an increase in erosion in most cases. Inversely, a decrease in rainfall could lead to either a decrease or increase in erosion and nutrient transport depending on the stress exerted on the plants. Increase in plant biomass may therefore protect the soil under more extreme conditions and mitigate the impacts of rainfall increase and intensity, without entirely negating them. These results were confirmed by Nearing et al. (2004) and Ficklin et al. (2010) who found, respectively, that agricultural runoff was much more sensitive to rainfall than vegetation cover, or CO_2 and temperature.

2.4 Climate change in southern Québec

2.4.1 Regional observations

Yagouti et al. (2008) analysed changes in several temperatures and precipitation indices for southern Québec (south of 52°N, roughly corresponding to the latitude of Sept-Îles on the North shore) between 1960 and 2005. They found that changes were not always significant but nonetheless tended towards an increase in surface temperatures, with more pronounced warming for the western and southern regions of the province. This increase was greater during winter, with daily maximum and minimum increases ranging from 1.5°C to 2.5°C. In summer too increases in temperatures were significant but they were less important (1.0°C to 1.5°C). Accordingly, the number of days when frost and thaw occurred within the same day increased in winter, but decreased in spring and fall. As a result, the frost season decreased to the benefit of the growing season. As for precipitation, increasing trends were noted for total annual rainfall but summers became drier. The number of rainfall days increased while snowfall days and snow cover decreased, confirming the decrease in the ratio of snowfall/rainfall observed in similar studies across Canada (Zhang et al., 2000).

2.4.2 Regional projections

Hydro-climatic changes observed in the past are expected to be accentuated with further increase in CO_2 levels in the atmosphere. Table 2.1 shows the changes in precipitation and temperature predicted for the period 2041-2070 relative to the period 1961-1990 for southern Québec (South to Saguenay Fiord). These changes were predicted with a set of global and regional climate models and future Greenhouse Gas Emission (GHGE) scenarios of the Special Report on Emission Scenarios (SRES) developed by the Intergovernmental Panel on Climate Change (IPCC) (Nakicenovic et al., 2000).

Table 2.1: Climate norms and summary of climate model projections for Southern Québec (Bourque and Simonet, 2007)

Season		1961-1990 Norms	Average changes for 2041-2070 horizon	Average changes for 2071-2100 horizon
Winter	Temperature Precipitation	-7.5°C to -11°C 270-330 mm	+2°C to +5°C + 0% to +32%	+3.5°C to +8°C +1% to +43 %
Spring	Temperature Precipitation	3.5°C to 6°C 240-280 mm	+2°C to +5°C +2% to +25%	+2.5°C to +8°C +4% to +39%
Summer	Temperature Precipitation	18°C to 20°C 280 -350 mm	+2.5°C to +4°C -7% to +13%	+2.5°C to +6°C -11% to +15%
Fall	Temperature Precipitation	6.5°C to 9°C 270-330 mm	+2°C to +4°C -8% to +16%	+2.5°C to +5.5°C -7% to +18%

In addition to change in the rainfall depths, the frequency of heavy rainfalls is expected to increase (Bourque and Simonet, 2008). Recently, several authors have examined this variable in Southern Québec. Mailhot et al. (2007), using CRCM simulations, found that maximum rainfall events of 2 and 6 hours would double, while maximum events of 12 and 24 hours would decrease by one third. With the same model, Dayyani et al. (2012) observed that for summer and fall, extreme rainfall events and peak flow for a given return period increased by the end of the century.

Few studies have investigated water quality vulnerability to climate change in Québec. Using a projection of the CRCM4 into the water quality model DRAIN-WARMF, Dayyani et al. (2012) found a significant increase in annual and seasonal NO_3-N loadings in a South-western watershed and that the contribution of subsurface flow to nitrate loadings would increase by 14% to 39% by 2100. Changes in N losses were described greater than changes in flows, which led them to suggest that a progressive saturation of soils in N would occur.

In snowmelt basins in Ireland (Jennings et al., 2009), and Denmark (Jeppesen et al., 2009), studies using regional temperature and precipitation predictions along with water quality statistical models showed that P loads would increase in winter and early summer, but decrease during summer months.

2.4.3 Regional climate models

Downscaling

Regional Climate Models (RCM) are increasingly used for impact assessment and as a means to downscale large-scale climate patterns predicted by global climate models (GCM) whose resolution is too coarse for regional impact studies. Two main types of downscaling approaches were developed in the last decade: the statistical and dynamical approaches (Fowler et al., 2007). Statistical Downscaling (SD) methods are based on empirical relationships which linked large-scale atmospheric predictors to local climate variables needed for impact assessment. These methods are appreciated for their rather rapid execution, which allows the downscaling of large sets of global simulations. Yet, because of their empirical basis, they are susceptible to miss important aspects of the future climate system. In contrast, a dynamical downscaling (DD) method uses physically-based models, known as RCM, which, because of their physical basis, may be more accurate than the SD (Boe et al., 2009).

Because they are computationally expensive, RCM can only operate on one restricted region at a time. They are therefore nested in a GCM to obtain atmospheric boundaries conditions simulated at a larger scale. In that case, we can say that the RCM is driven by the GCM. Hence the RCM simulates climate in consistent ways with other large scale global changes occurring within the rest of the globe (ESCER, 2009). RCM have also demonstrated that they are able to improve the prediction of extreme events and climate variability thanks to their refinement and complexity in describing local processes (Fowler et al., 2007). Therefore, these advantages make them stand out as the best tools that can be used to simulate the impact of climate change on erosion, sediment and nutrient losses.

<u>Description of the Canadian climate models</u>

The Canadian Global Circulation Model (CGCM) and its homologue the Canadian Regional Climate Model (CRCM) are two Canadian models under continuous evaluation and development and are broadly used for impact assessment (UCAR, 2007; Ouranos, 2010a).

Developed at the Canadian Centre for Climate Modelling and Analysis (CCCma) of Environment Canada, the third version of CGCM (CGCM3) results from the coupling of the Atmospheric General Circulation Model (AGCM3) to a three-dimensional dynamic ocean model which includes a thermodynamic sea-ice component (Rahman et al., 2010). The models are described in McFarlane et al. (2005) and Flato and Boer (2001), respectively. Energy and water exchanges between the land surface and the atmosphere were governed in both Canadian models by the Canadian LAnd Surface Scheme (CLASS) (Verseghy, 1991; Verseghy et al., 1993).

The CRCM is a Limited Area Model (LAM) developed by the “centre pour l’Étude et la Simulation du Climat à l’Échelle Régional” (ESCER center) of the Université du Québec à

Montréal (UQAM). The 4th version of CRCM (CRCM4) has a horizontal resolution of 45 km, true at 60° N following a uniform grid in a stereographic projection, and a variable vertical resolution. Basically, it uses the same physical parameterization package as its homologue and driver CGCM3 (Scinocca and McFarlane, 2004; McFarlane et al., 2005). It resolves its climate with the fully elastic Euler's equations allowing climate variables to be generated at reduced spatial resolution (Plummer et al., 2006; Laprise, 2008).

These models thereby satisfy the minimum criteria of quality established by the Task Group CI, TGCI, and IPCC to be used in impact assessment. Despite their improved resolution, almost all RCMs continue to have an important bias, partly inherited from their GCM driver (Leung et al., 2003; Fowler et al., 2007; Boe et al., 2009). Biases due to the CRCM4 alone were investigated by Gagnon et al. (2009) for two watersheds close to the Pike River. They concluded that the predictions were reliable, but that they also display significant biases for all seasons, especially for runoff predictions. Bias corrections were therefore recommended before the use of the regional predicted climate. However, correction methods like the SD may not remain valid for future climate (Boe et al., 2009; Gagnon et al., 2009).

Dealing with uncertainties

Although models and scenarios are the best representations of the Earth system that we currently have, they remain imperfect and are tainted by many uncertainties which are difficult to assess due to the complexity of the modelled system and the computational resources that this assessment would require (de Elia and Cote, 2009). Whenever possible, modellers use several GHGE scenarios and "multi-model sets or multi-parameter sets based on a single model" to account for all possible results rising from these uncertainties (Fowler et al., 2007; de Elia and Cote, 2009).

The GHGE SRES scenarios were developed based on storylines describing possibilities of world developments where scenarios of the "A" family focus primarily on economic development, whereas those of the "B" family are more environmentally and economically balanced. These scenarios also bear, besides the letter, the label 1 or 2 which stand for global or regionally-oriented, respectively. The two most alarmist scenarios are depicted by A1F (Global economy driven by intensive fossil fuel consumption) and A2 (Fragmented world, regionally-oriented economic growth) scenarios. Both predict that CO_2 emissions will be increasing by 30 Pg yr^{-1} by 2100, compared with the actual rate of 6 Pg yr^{-1} (Cohen and Waddell, 2009). Formal probabilistic assessments are still rare (Bates et al., 2008).

2.5 Hydrological and water quality modelling under climate change

Although climate models simulate all components of the hydrological cycle, their resolution and level of accuracy in simulating local interactions within the soil-vegetation-atmosphere system is too crude to provide precise estimates of changes in the local water cycle or to simulate the nutrient cycle. Therefore, downscaled outputs of regional or global climate models are used with diverse impact models to investigate future changes in freshwater resources and the fates of pollutants.

Among impact assessments previously performed, two main approaches were identified:

i. Those based on empirical relationships between runoff, sediment and nutrient loadings (Arheimer et al., 2005; Andersen et al., 2006; Jeppesen et al., 2009; Pierson et al., 2010). They all predict future changes in stream flow and runoff with physically-based hydrological models. Then, these changes are applied to loading functions or regression analysis of runoff and nutrient loads data

and,

ii. those using complex processes models allowing prediction of the behaviour of the watershed in more comprehensive ways. The choice of these approaches depends on the ultimate purpose of the project and available resources (time, data, computing capacity).

Regression analyses are often more straightforward and accurate than physically-based models, but they are based on statistical analysis and therefore require a long history of observed data (Ritter and Shirmohammadi, 2001). Within the Pike River watershed, such relationships have been developed several times (Simoneau, 2007; Adhikari et al., 2010). However, the amount of recorded data may be too limited to apply such relationships to climate change study. As shown in Simoneau (2007), relationships have changed with time due to different hydrological conditions but also due to the effect of pollution abatement measures. Statistical methods provide quick and useful insight into future loadings. However, similarly to statistical downscaling and bias correction, their predictive ability is limited in future changing conditions since they are based on observed records. Contrary to a model that is completely physically-based, they do not simulate the effect of temperature on the nutrient cycle and other biogeochemical processes such as plant nutrient intake and residue decomposition rates which may change under a warmer climate (Campbell et al., 2011).

A wide variety of such models (ANSWERS, (Ann) AGNPS, DWSM, MIKE-SHE, PRMS, SHETRAN, HSPF, SWAT) are commonly used to assess P and N NPS pollution, and, in some cases, to test land management scenarios in order to develop abatement pollution strategies. These models often explicitly account for inputs of fertilizer and manure to agricultural lands, and maintain a soil nutrient balance by simulating plant uptake, microbial decomposition, and P loss to surface and sub-surface flow (Pierson et al., 2010). The next section presents a short review of the most commonly used watershed-scale models, and focuses on those able to handle climate change impacts.

2.5.1 Review of water quality models

The Aeral Non-point Source Watershed Environment Response Simulation (ANSWERS-2000) (Beasley et al., 1980) has shown a good performance, but is often cited in literature reviews for its inability to simulate snowmelt processes. It is therefore not suited for snowmelt basins (Booty and Benoy, 2009; Yang and Wang, 2010).

A second well-known model is the Agricultural Non-Point Source pollution model (AGNPS/AnnAGNPS) developed by USDA-ARS (Young et al., 1989). It was designed first for single storm events and then updated to simulate continuous long-term periods of time (Annualized AGNPS). It is a distributed parameter model which accounts for watershed heterogeneity. It was used by Parker et al. (2008) in climate change impact studies in eastern Ontario to evaluate the efficiency of BMPs under several climate change scenarios. The model includes in its calculation: i) surface runoff computed by the SCS Curve Number (CN) method, ii) erosion computed by the USLE method and iii) sediment-bound/soluble nutrient losses in runoff. However, its equations used to simulate nutrient cycles are based mainly on empirical data, as it uses a correlation relationship between sediment, runoff and nutrient concentration (Jeppesen et al., 2009; Yang and Wang, 2010).

Since the frequency of heavy rainfall will increase with climate change, a model such as AGNPS, which is capable of simulating damage caused by intense precipitation events, is a good candidate for such studies. Similarly, the Dynamic Watershed Simulation Model (DWSM) (Borah et al., 2002) is deemed to be a very promising tool for simulating extreme events and resulting pollution in agricultural watersheds. It was judged to have a robust physical basis and to simulate accurate results. However, it does not simulate long-term periods and is therefore not suitable for this study (Borah and Bera, 2003, 2004). On the other hand, both the European Hydrological System Model or MIKE-SHE (Refsgaard et al., 1995) and the Precipitation-Runoff Modelling System (PRMS) (Leavesley et al., 1983) have the capacity to handle long-term and single storm simulations. However, the PRMS long-term model only simulates hydrological processes and will therefore not be further discussed. MIKE-SHE is a comprehensive, distributed and physically-based model describing processes at small time step and at a high level of detail. However, it is not efficient for long-term simulation and large watersheds, and is judged more applicable to small watersheds and studies requiring results of high precision because of its intensive computational requirements (Borah and Bera, 2003). The Système Hydrologique Européen TRAnsport Model (SHETRAN) (Ewen et al., 2000) is a relatively new model based on MIKE-SHE. Though promising, it remains very complex and little assessed (Pierson et al., 2010; Yang and Wang, 2010).

Finally, the Hydrological Simulation Program–Fortran (HSPF) (Donigian et al., 1995) and the Soil and Water Assessment Tool (SWAT) (Arnold et al., 1998) are two popular comprehensive GIS-based physical models which have received very positive reviews for their accuracy and modelling efficiency (Borah and Bera, 2004; Singh et al., 2005). Both supported by the US Environmental Protection Agency (EPA), these models have undergone thorough assessments which focus on climate and the impacts of land-use change on hydrology and water quality of twenty major drainage basins in the US (Aqua Terra Consultants, 2010). Both were designed to simulate the impact of climate and watershed management practices on the long-term. However, SWAT was judged to be more accurate than HSPF when it comes to intensive agricultural watersheds because of its greater ability to discriminate landscape heterogeneity. Whereas, HSPF was judged better suited to urban or mixed agricultural watersheds (Borah and Bera, 2004). Furthermore, although HSPF can simulate storm events thanks to sub-daily time step processes, it lacks tile drainage and plant growth components which in the latter case may play an important role in climate change studies. Similarly, plant diversity and soil moisture influencing evapotranspiration are lumped into one parameter, and evapotranspiration is calculated based on user input records (Van Liew et al., 2003; Singh et al., 2005) which may not remain valid in a warming world.

In a comparative study Van Liew et al. (2003) found that HSPF (vs. SWAT) provided better hydrological results for the calibration period and Yang et al. (2008) reported in their review that two other studies had confirmed this. However, these two studies disagreed on which model better predicted nutrient loadings. Van Liew et al. (2003) observed, nonetheless, that SWAT gave better results for their validation period and when parameters were transferred to similar watersheds. This suggests that this model may be more robust and capable of handling variables climatic conditions. Although SWAT has shown little capacity to simulate intense rainfall events and their resulting effects on erosion and nutrient losses, it has still been widely used for assessments of climate change impacts on NPS pollution (Bouraoui et al., 2002; Marshall and Randhir, 2008; Nunes et al., 2008; Ficklin et al., 2010).

2.5.2 Model selection: SWAT

SWAT (Arnold et al., 1998) was chosen for its ability to simulate large, heterogeneous, and agriculturally-intensive watersheds over a long period, based on sound conceptual and physical foundations (Borah and Bera, 2003, 2004; Deslandes et al., 2007). It was also successfully applied several times within the Pike river watershed from the field scale (Eastman, 2007; Gollamudi et al., 2007) to the subwatersheds and whole watershed scales (Deslandes et al., 2007). An increasing number of studies have used SWAT for climate changes studies (Douglas-Mankin et al., 2010). Lastly, its superior ability in simulating BMPs makes it a first-choice candidate if climate change adaptation strategies need to be developed (Borah and Bera, 2004).

SWAT 2000 (Soil and Water Assessment Tool ; Arnold et al., 1998) has demonstrated a good ability to reproduce the hydrological and P loss behaviours of the Pike River watershed (Deslandes et al., 2007). It is however a modified version of SWAT 2005 (Michaud et al., 2008) which was used in this study.

The version of SWAT 2005 allows more accurate predictions of nitrate fluxes (Neitsch, 2005) and is believed to correct some flaws linked to subsurface and surface flow partitioning noted during the preceding applications of SWAT 2000 within the watershed (Madramootoo et al., 2004; Gollamudi, 2006; Deslandes et al., 2007). However, the version of SWAT 2005, did not entirely succeed in resolving this issue within the Pike river watershed, and Michaud et al. (2008) customized algorithms related to soil water transfer in SWAT 2005 to improve tile flow predictions. Given its utility in predicting nitrate loads and improving hydrological predictions for our study, it is this customized version which was adopted for this project. The description of the model given in the next section is mostly based on the theoretical documentation of Neitsch et al. (2005).

2.6 SWAT description

2.6.1 SWAT general operation

Based on a Digital Elevation Model (DEM), SWAT first delineates the contours of the entire watershed and a collection of subwatersheds connected through the hydrological network. The outlet of the subwatersheds may be entered by the user or defined along the subwatersheds' borders during the delineation process. Each subwatershed is further divided into Hydrological Response Units (HRU). HRUs are lumped areas representing the dominant biophysical characteristics prevailing within the subwatershed. They are obtained by overlaying soil and land-use maps and represent a unique combination of land-use, soil and management practices. They are the basic calculation units for each physical processes occurring within the watershed. All results computed at the HRU scale are then aggregated at the subwatershed scale, transferred into the reach and routed through the hydrological network.

Once all landscapes attributes which define the HRUs have been entered in the model, climate and field operations management data can be entered.

All processes in SWAT are modelled on a daily basis. Being an important factor in erosion and nutrient losses, hydrological processes must be well reproduced to simulate water quality. Each day the following daily soil water balance is updated in SWAT.

$$SW_t = SW_0 + \sum_{i=1}^{i=t}(R_{day} - Q_{surf} - E - W_{seep} - Q_{gw}) \quad [2.1]$$

Where,

E	is the evapotranspiration on day *i* (mm),
Q_{gw},	is the return flow to the stream on day *i* (mm),
Q_{surf}	is the depth of surface runoff on day *i* (mm),
R_{day}	is the depth of precipitation on day *i*(mm),
SW_t	is the final soil water content (mm),
SW_0	is the initial soil water content (mm, initialized to 0 or 100% for the first day of the simulation), and
W_{seep},	is the water leaving the soil profile for the vadose zone on day *i* (mm), the vadose zone being an unsaturated zone located between the last layer of the soil profile and the shallow aquifer. No processes were simulated within this zone.

The detailed pathways of water movement simulated in SWAT are represented in figure 2.1.

Climate variables are important inputs since they provide the moisture and energy that govern the components of the hydrologic cycle. Precipitation, air temperatures (minimum and maximum), solar radiation, speed of the wind and the relative humidity are required on a daily basis. A weather generator can fill in missing information based on US historical weather statistics (Neitsch et al., 2005). However, it only produces representative weather for the region and its data may lack in precision. It is therefore strongly recommended to reduce the use of the weather generator whenever possible. Data from local weather gauges along with their location can be entered into SWAT, which then distributes the daily data over the land belonging to the closest subwatersheds (Di Luzio et al., 2002; Neitsch et al., 2005).

Three methods are available for calculating evapotranspiration: the Penman-Monteith (Monteith, 1965), Priestley-Taylor (Priestley and Taylor, 1972) and Hargreaves (Hargreaves et al., 1985) methods. The Penman-Monteith method is widely used but requires a greater number of inputs (solar radiation, relative humidity, wind speed and temperature) and may lead to significant errors when mean daily inputs are used.

Furthermore, when only temperatures and precipitation are available, weather generators used to estimate the other parameters may add considerable uncertainty (Benaman et al., 2005). The Hargreaves method, on the other hand requires only the input of temperatures.

After calculating evapotranspiration, the model evacuates the surplus of water through tile flow, lateral flow and percolation. Lateral flow is calculated for each soil layer according to soil water content (ψ), slope, and differences of hydraulic conductivity (K_{sat}), while percolation is simulated when water content of the soil exceeds field capacity (ψ_{fc}). Groundwater flow is governed by threshold parameters set by the user during the calibration. These control the amount of water reaching shallow aquifer. All parameters are described in Appendix I.

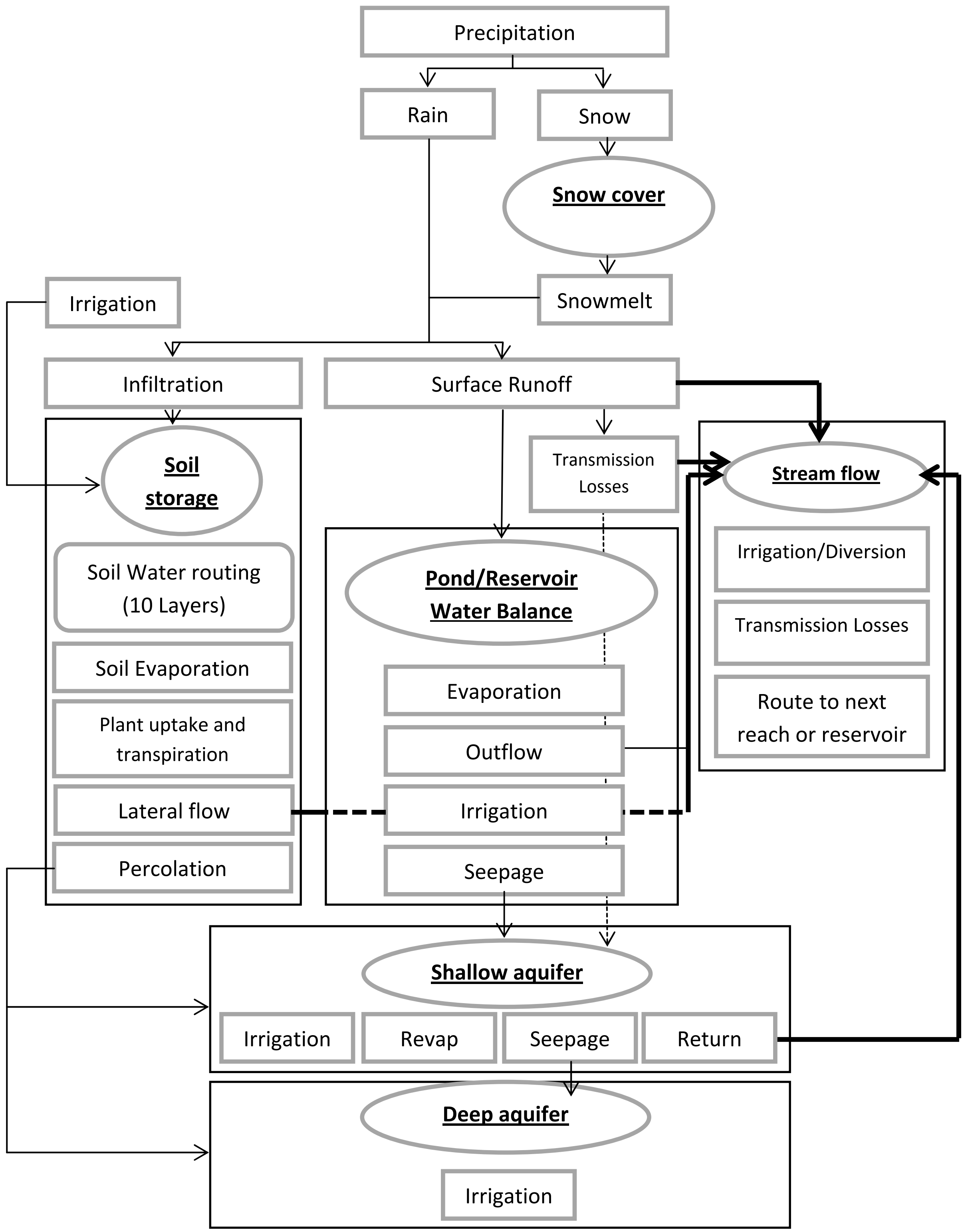

Figure2.1: Possible water movements in SWAT (Neitsch et al., 2005)

2.6.2 Surface runoff and snowmelt

As previously mentioned, surface runoff is the major hydrological factor contributing to sediment and phosphorus transport. Once estimated, it is entered into the sediment losses algorithm, whose estimates are in turn used to predict particulate nutrient losses. As P is the limiting nutrient for eutrophication and the one that is mostly lost under particulate form, runoff predictions needs to be as accurate as possible.

SWAT includes two options to calculate runoff: the Green and Ampt infiltration method (1911) and the US Soil Conservation Service (SCS) Curve Number (CN) procedure (USDA Soil Conservation Service, 1972). The first method is more physically-based and infiltration is modelled over time, based on soil physical properties [*e.g.*, K_{sat}, soil water saturation (ψ_{sat}), and ψ_{fc}]. However, it requires sub-daily rainfall data that are rarely available; therefore, this method is not commonly used. Comparatively, the empirically-based SCS CN method has been found to be reliable and is widely used (Gollamudi, 2006).

$$Q_{surf} = \frac{(R_{day} - 0.2S)^2}{(R_{day} + 0.8S)} \qquad [2.2]$$

where,

Q_{surf}	is the accumulated surface runoff arising from rainfall excess (mm),
R_{day}	is the amount of rainfall for the day (mm), and,
S	is a retention parameter (mm).

The retention parameter accounts for soil infiltration prior to the onset of runoff as well as for initial abstractions such as surface storage and canopy interception. It also accounts for variations in land-use, soils, antecedent soil moisture conditions, field management and slope effects on runoff and infiltration. It is calculated using CN developed empirically by the SCS Engineering Division. The CN takes on different values according to the above variations. Their initial values are entered by the users, and then, daily updated by SWAT according to soil moisture changes.

These CN values available in SWAT theoretical documentation (Neitsch et al., 2005) consistently over-predicted runoff under Québec hydroclimatic conditions and under-predicted tile and groundwater flow. To remedy this situation, CN values applied under such conditions were lowered in Deslandes et al. (2007) and in several other studies (Perrone and Madramootoo, 1998; Tolson and Shoemaker, 2004). In addition, Michaud et al. (2008) modified the above equation to increase surface retention vs. runoff to 50:50, instead of the initial 20:80 (the 0.2 and 0.8 coefficients associated with the S retention parameter in equation 2.2). This is believed to prevent too much water from running off, and foster its infiltration. These modifications were based on the argument that runoff conditions in Québec were rather caused by soil saturation than, as might be the case in the US where the model was developed, by episodes of intense rainfall which exceed the infiltration rate.

When snowmelt occurs it replaces or is added to R_{day} in equation 2.2. Snowmelt depends on air and snow pack temperatures, maximum and minimum melting rate factors and the areal coverage of snow. The melting rate factors (SMFMIN and SMFMX) may be changed during the calibration by the user. Areal coverage of snow depends on a mass balance equation accounting for snowfall, snowmelt, and sublimation, where snowfall is controlled by a snowfall threshold temperature (SFTMP). If the average daily temperature is under SFTMP, SWAT classifies precipitation as snow, otherwise, as rainfall. Similarly, snowmelt depends also upon a snowmelt threshold temperature (SMTMP). Both thresholds may be defined during the calibration of the model.

No infiltration occurs, if soil temperature is under 0°C.

2.6.3 Changes in SWAT2005 to improve drainage predictions in Québec

Michaud et al. (2008) modified three sets of algorithms within SWAT 2005 in order to build a model adapted to surface runoff and tile drainage conditions in Québec. These changes affect: 1) soil water flow towards tile drains and preferential flow, and 2) the distribution of precipitation between surface runoff and infiltration. Furthermore, SWAT 2005 does not account for subirrigation nor controlled drainage.

Concerning the first modified algorithm in SWAT 2005, tile drainage was not easily or accurately predicted, because the water table was initialized at six meters below the first soil layer, which was too deep for the water table to reach the tile drains. For tile drainage to occur, the water table must be above the tile lines. This limitation was not present in SWAT 2000, since tile flow was calculated based on soil water saturation of the layer where the tile drains are located. Moreover, contrary to the 2005 version, SWAT 2000 considered flow towards the tile drains first, before evacuating water through lateral flow and percolation. Therefore SWAT 2000 equations were brought back into SWAT 2005 to properly simulate tile flow.

The second algorithm modification allowed for the addition of preferential flow directly to tile flow, instead of first directing the water towards the shallow aquifer. Finally, the third algorithm modification changed the precipitation distribution between surface runoff and surface retention within the SCS-CN (equation 2.2). In this equation, 80% of the precipitation was attributed to surface runoff and 20% to surface retention. This method was developed based on field measurements in parts of the United States. In order to better represent Québec conditions, this ratio of 80/20 was set at 50/50, to decrease runoff and increase water retained on the soil surface. The latter phenomenon increases infiltration of water through the soil profile.

2.6.4 Erosion calculation

Erosion and sediment yields are simulated with the Modified Universal Soil Loss Equation (MUSLE) (Williams, 1975) presented below. It uses surface runoff energy instead of rainfall intensity to detach and transport soil particles. The improvement comes from the fact that soil moisture antecedent conditions are taken into account and there is no need to calculate the sediment delivery ratio.

$$Sed = 11.8\ (Q_{\text{surf}} * Q_{\text{peack}} * area_{\text{HRU}}) * 0.56 * K_{\text{usle}} * C_{\text{usle}} * P_{\text{usle}} * LS_{\text{usle}} * CFRG \qquad [2.3]$$

where,

Sed	is the sediment yield on a given day (Mg),
Q_{surf}	is the volume of surface runoff (mm ha^{-1}) from equation [2.2],
Q_{peak}	is the peak runoff rate ($m^3\ s^{-1}$),
K_{usle}	is the USLE soil erodibility factor (0.013 Mg m^2 hr m^{-3} Mg^{-1} cm^{-1}),
C_{usle}	is the USLE cover and management factor (unitless),
P_{usle}	is the USLE support factor (unitless),
LS_{usle}	is the USLE topographic factor (unitless),
$CRFG$	is the coarse fragment factor (unitless).

The peak runoff rate is the maximum runoff rate during a rainfall event. It is an indicator of the erosive power of a storm and is calculated by SWAT according to the time of water concentration within the subwatershed (automatically calculated by SWAT according to the watershed properties entered during the model set-up) and the maximum half-hour rainfalls. The time of concentration is the time necessary for the runoff within the entire basin to contribute to the flow outlet. The maximum half-hour rainfall is also calculated by SWAT based on recorded data provided by the user or on statistics of the past 40 years in the SWAT weather generator. When runoff comes from snowmelt, this maximum half-hour rainfall equals one where the rainfall energy effect on the peak runoff rate is cancelled, and assumes a uniform snowmelt for a 24hour period.

The erodibility of a soil depends on its physical properties. This factor can be obtained from inventory or calculated using the equation of Wischmeier *et al.* (1971) which integrates soil properties such as percent organic matter (% OM), as well as codes for soil structure and permeability, particles sizes, and percentages of particle type.

The cover and management factor account for canopy and residue protection of the soil. Its minimum value is colligated in SWAT crop database for each plant and is updated during the year to simulate the impact of plant growth on erosion.

The support practice factor reproduces the effect of anti-erosion measures implemented in the field (*e.g.*, contour tillage, strip-cropping). It is a calibration parameter whose value is given in the SWAT manual based on land slope and type of cultivation practices.

The topographic factor accounts for the effect of the length and slope of the field on erosion (the longer and steeper, the greater the erosivity of runoff) (Neitsch *et al.*, 2005). The coarse fragment factor represents the percentage of rock within the first soil layer.

SWAT also takes into account the presence of snow on the ground and the way it protects the soil from erosion by reducing the amount of estimated sediments lost (calculated with equation 2.3). The reduction is determined based on the water content of snow cover.

2.6.5 SWAT phosphorus and nitrogen cycles

<u>Soils nutrients equilibrium</u>

SWAT organizes the different organic and mineral forms of nutrients present in soils into 5 pools for N and 6 pools for P (Figures 2.2 and 2.3, respectively). Organic forms of N and P are associated with humus or fresh material, with humic substances divided into active and stable pools. The mineral forms of ammonium (NH_4^+) and NO_3^- constitute the two other pools of N. The mineral P forms are organized in active, stable and solution pools. Phosphorus bound to sediments is represented within the active and stable pool.

Nutrient contents of each pool are initialized in SWAT either by the user, based on the knowledge they have of the chemical characteristics of their soil, or with SWAT default values and equations derived from general soil characteristics. When common characteristics do not exist, the pool is set at 0 and is initialized during the warm-up period of the simulations.

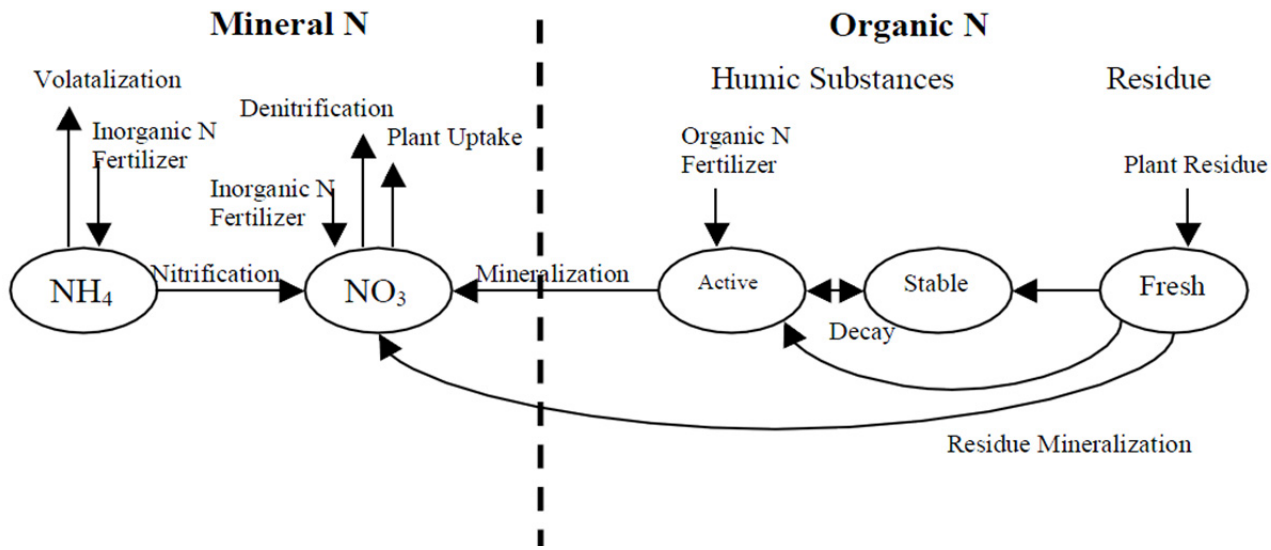

Figure2.2: Soil nitrogen pools in SWAT (Neitsch et al., 2005)

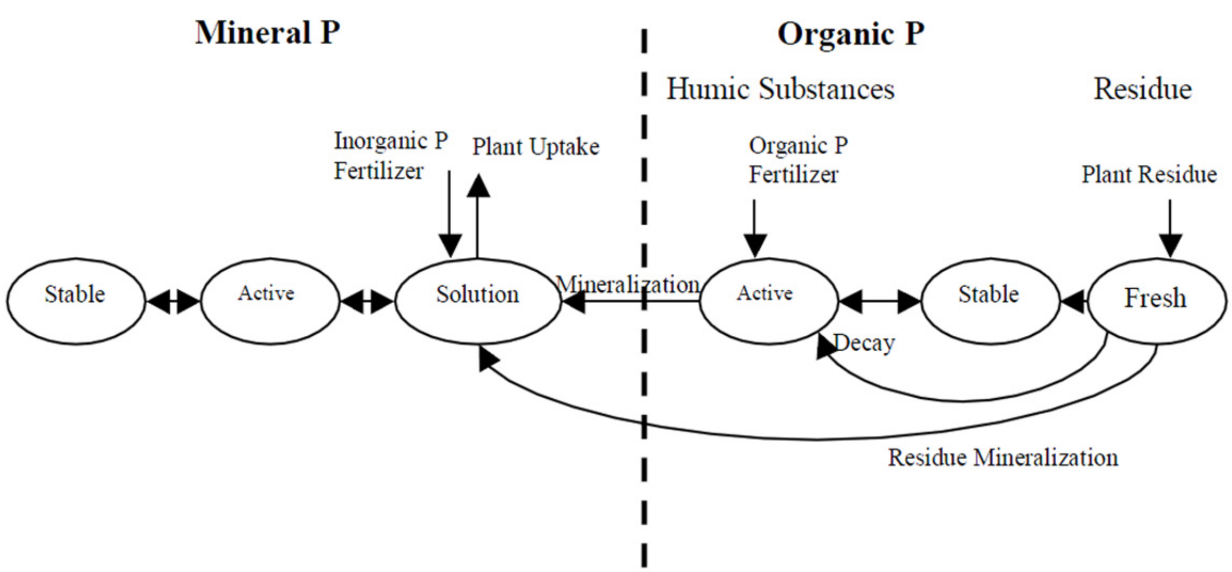

Figure 2.3: Soil phosphorus pools in SWAT (Neitsch et al., 2005)

For P, the solution concentration is initialized at 5 mg kg^{-1} for each layer. It is assumed this concentration is representative of unmanaged land under native vegetation. Deslandes et al. (2007) has already calculated these concentrations for the Pike River watershed. These are the values that will therefore be used. Then, calculation of the mineral active pool content is achieved using the Phosphorus Availability Index (PAI) (also called the P sorption coefficient). The PAI determines the amount of P remaining in solution versus the amount transferred to the active mineral pool. This is done using the equation of Jones et al. (1984).

$$minP_{act,ly} = P_{\text{solution, ly}} \times \frac{1-PAI}{PAI} \qquad [2.4]$$

where,

$minP_{act,ly}$ is the amount of P in the active mineral pool (mg kg^{-1}), and
$P_{solution,\,ly,}$ is the amount of P in the solution pool (mg kg^{-1})

The PAI can be defined by the user through the calibration parameter 'psp' or remain at its default value 0.4 (*i.e.*, 40% of P will remain in solution) (Vadas and White, 2010).

The amount of P in the stable pool is assumed to be 4 times the amount in the active pool. Organic P and N levels are calculated according to common C:N and N:P ratios found in humic substances, and the fresh pools according to the percent of N (0.15%) and P (0.3%) in fresh materials of the residue pool for the top 10 mm of soil. The amount of fresh material may be entered by the user through a calibration parameter: rsd_{surf} in kg ha^{-1} or set to default values.

During the simulation, users may add organic and mineral fertilizers several times per year through the management operation options of SWAT.

The pools are in slow or rapid equilibrium with each other to satisfy the state of equilibrium when a change in the soil environment occurs (addition or removal of nutrients). SWAT maintains this equilibrium using algorithms which simulate the processes that are reproduced in figures 2.2 and 2.3.

Changes in the soil environment may occur naturally through plant uptake, runoff, and increase in temperature which accelerates the decay and mineralization processes, or artificially, through the additions of organic and mineral fertilizers. Inputs of N may also occur with rainfall and bacterial atmospheric fixation and removals, through leaching, volatilization and denitrification. SWAT calculates rainfall N inputs by multiplying the quantity of rainfall during the day by its concentration in N. This concentration is established with the calibration parameter RCN. Nitrogen fixation is simulated with plant nutrient uptake processes.

Plant uptake follows a supply and demand approach. A daily comparison of the optimal and actual nutrient concentration in the plant allows a computation of nutrient uptake. The optimal concentration varies with the growth stage of the plant.

Decomposition and mineralization of organic material as well as the other nitrogen-related processes such as nitrification/denitrification are simulated according to the ratios C:N and C:P of the residues which allow the diverse processes to occur. The users can also define during the calibration diverse coefficient rates and other important factors related to temperature and water availability which influence these processes. The coefficient rates correspond respectively to the parameters CMN (mineralization of active pool humus) and RSDCO (residue), CDN (denitrification rate) and SDNCO, a threshold for the nutrient cycling factor above which denitrification can occur. Exchanges between the three P mineral pools representing sorption and desorption processes are governed by algorithms involving the PAI index (see Eq. 2.4).

Nutrient transport

SWAT simulates N processes within each layer of the soil profile and the shallow aquifer. Nitrogen is transported through surface runoff and lateral subsurface flow. Phosphorus is considered less mobile due to its capacity to be adsorbed to soil particulates or precipitated when the soil solution is saturated. It is only simulated within the first soil layer, and removed from the HRU through surface runoff. However, tile and groundwater may transport soluble and particulate P due to preferential flow in clay soils or soil P saturation (Enright and Madramootoo, 2004; Neitsch et al., 2005; Michaud et al., 2009a). To account for the presence of P in subsurface flow, SWAT allows the user to enter a concentration of soluble P that will remain constant throughout the simulation. Particulate P is not taken into account in subsurface flow.

Amount of N in solution leaving the HRU through surface runoff, lateral flow, and percolation:

The portion of N leaving the HRUs in soluble form is generally NO_3^- and can be removed from each soil layer through surface runoff, lateral flow and percolation. For each of these pathways, the amount of removed soluble nutrients is calculated according to the volume of water transiting through them and the averaged concentration of NO_3^- in this volume of water. Equations are:

$$NO_{3surf}^{-} = \beta_{NO_3^-} \times [NO_3^-] \times Q_{surf} \qquad [2.5]$$

$$NO_{3\ lat10}^{-} = \beta_{NO_3^-} \times [NO_3^-] \times Q_{lat,ly10} \qquad [2.6]$$

$$NO_{3\ lat}^{-} = [NO_3^-] \times Q_{lat,ly} \qquad [2.7]$$

$$NO_{3\ perc,ly}^{-} = [NO_3^-] \times w_{perc,ly} \qquad [2.8]$$

where

$\mathbf{NO_{3\,surf}^-}$, $\mathbf{NO_{3\,lat10}^-}$, $\mathbf{NO_{3\,lat}^-}$, **and** $\mathbf{NO_{3\,perc,ly}^-}$, are respectively nitrates removed in surface runoff, lost through lateral percolation in the top 10 mm of the soil, lost through lateral percolation in each subsequently deeper layer of the soil, and nitrates reaching the underlying layer by percolation, all in kg N ha^{-1}

$\boldsymbol{\beta_{NO_3^-}}$ is the nitrate percolation coefficient. It is a calibration parameter (NPERCO) which controls the relative amount of nitrate leaving the top 10 mm through surface runoff *vs.* percolation. When NPERCO tends towards 1, runoff and percolation are equivalent, while when it tends towards 0.01, nitrate leaves the layer uniquely by percolation and its concentration in runoff is considered null.

$[\mathbf{NO_3^-}]$ is the average concentration of nitrate in the total volume of water leaving each soil layer through surface runoff (for the top 10 mm), or lateral flow or percolation (kg N mm^{-1}). This concentration depends of the amount of mobile water within the soil layer, the amount of NO_3^- and the saturated water content of the layer, and, a factor linked to the repulsion of anions such as NO_3^- around soil minerals. The amount of nitrate in each layer depends on initial concentration updated by the biochemical (mineralization, nitrification, plant uptake, etc.) and physical processes (fertilization, outflow currently described, etc.) of the nitrogen cycle.

$\mathbf{Q_{surf}}$ is the quantity of surface runoff on a given day (mm) and,

$\mathbf{Q_{lat,ly10}}$ and $\mathbf{Q_{lat,ly}}$ are, respectively, the amount of water discharged by lateral flow (mm) from the top 10 mm of soil and from each of the other layers.

Along the same lines, the amount of P in solution leaving the HRU through surface runoff would be:

$$P_{surf} = \frac{P_{\text{solution,surf}} \times Q_{\text{surf}}}{\rho_{\text{b}} \times depth_{\text{surf}} \times k_{\text{d,surf}}} \qquad [2.9]$$

where,

$P_{solution,surf}$	is the amount of phosphorus in solution in the top 10 mm of the soil (kg P ha^{-1})
Q_{surf}	is the quantity of surface runoff on a given day (mm).
ρ_b	is the bulk density of the top 10 mm of soil (Mg m^{-3})
$depth_{surf}$	is the depth of the first surface layer of soil, namely 10 mm
$k_{d,surf}$	is the phosphorus soil partitioning coefficient (m^3Mg^{-1}) and,
Q_{surf}	is the amount of surface runoff on a given day (mm H_2O).

The P soil partitioning coefficient represents the ratio between the soluble P concentration in the 10 mm of topsoil and the concentration of soluble P in runoff. It corresponds to the calibration parameter PHOSKD.

Amount of nutrient transported with sediments by surface runoff:

The amount of organic N and organic and mineral P leaving the HRUs in particulate form sorbed to sediments is calculated using the loading function developed by McElroy et al. (1976) and modified by Williams and Hann (1978).

$$sedNutr_{surf} = 0.001 * conc_{sed,Nutr} * \frac{sed}{area_{hru}} * \varepsilon_{Nutr:sed} \quad [2.10]$$

where:

$SedNutr_{surf}$ is the amount of nutrient (N or P, organic and mineral) transported with sediments to the main channel in surface runoff (kg N ha^{-1} or kg P ha^{-1}),

$conc_{sed,Nutr}$ is the concentration of nutrients (N or P) sorbed to sediment in the first 10 mm of the soil (P or N as g Mg^{-1} of soil). This concentration is calculated according to ρ_b (Eq. 2.9) and the amounts of P in the active and stable mineral pools and humic and fresh organic pools of P, or the N in the active, fresh, and stable organic pools of N,

sed is the sediment yield on a given day (Mg),

$area_{hru}$ is the area of the HRU (ha), and

$\varepsilon_{Nutr:sed}$ is the nutrient enrichment ratio, which is the ratio of the concentration of the nutrient transported with sediments to the concentration of the nutrient in the topsoil. SWAT calculated this value for each storm. The user can also enter their values as a calibration parameter (ERORGP or ERORGN).

This last equation is applied separately to particulate N and P loss.

2.6.6 SWAT and climate change

Besides integrating future projections of climate variables, SWAT can simulate the effect of an increase in CO_2 concentration on plant growth and evapotranspiration. Both of the latter might have an effect on surface runoff, erosion and nutrient losses.

To begin with, a higher level of CO_2 leads to an increase in biomass. In turn, an increase in biomass and therefore in Leaf Area Index (LAI) of the plant would better soil protection and reduce the risk of erosion. An increase in CO_2 would therefore reduce the risk of erosion and nutrient losses.

In SWAT, projected crop growth is calculated according to the increase in biomass. This increase is itself dependent on the Radiation Use Efficiency (RUE) of the plant and solar radiation that its leaves intercept. Indeed, to calculate biomass, the crop RUE has to be adjusted by SWAT according to the level of CO_2 entered by the user Hence, SWAT establishes a direct link between CO_2 and biomass. The link it establishes between CO_2 and erosion, however, is an indirect one.

Indeed, according to SWAT equations, the increase of CO_2 does not have an effect on erosion because the amount of biomass and the leaf area index (LAI) are not taken into account when calculating erosion. In fact, the protection of the soil by the plant coverage is simulated through the C_{usle} factor (2.6.3). The latter is disconnected from biomass production and varies uniquely according to the amount of plant residue present on the soil. This amount is established by the users when harvests are simulated.

Other effects of CO_2 increase include: effects on nutrient uptakes as nutrient uptakes calculation depends on plant biomass (Neitsch et al., 2005) and an increase of crop water use efficiency caused by the reduction of plant evapotranspiration itself caused by a diminishing of stomatal apertures. To simulate this reduction in evapotranspiration SWAT diminishes the leaf conductance terms of the Penman-

Monteith equation by 40% for a doubling concentration in CO_2 (660 vs 330 ppm). The leaf conductance is a measure related to the rate of water vapour exiting the plant and of the CO_2 entering.

Very few studies have incorporated these two options to account for changes in CO_2 concentration. Eckhardt and Ulbrich (2003) found that the latter method underestimated evapotranspiration, while Ficklin et al. (2010) used it in the context of sensitivity analysis, rather than as a precise impact assessment with climate model predictions.

2.7 Summary

This literature review has provided the context relevant to this project and set the basis for its realization. This review began by showing that NPS source pollution is an important issue in agricultural areas, where it severely degrades water bodies to the point of affecting their biodiversity, reducing ecosystem services and impeding their use. In Missisquoi Bay, as for other water bodies, this causes great economic and health concerns because of the contamination of drinking and recreational waters. This issue is especially worrisome because NPS pollution is difficult to control and to limit due to its complex and variable nature in space and time. However, considerable efforts have been made at every scale (field, basin, and watershed, regional and national) to restore the water quality of impaired freshwater resources and protect them from further degradation. Climate change constitutes a threat to these efforts since its impacts might increase erosion and nutrient losses, impeding or slowing down the achievements of the P reduction target set to improve Missisquoi Bay water quality. Assessing these impacts on future nutrient exports is identified by water managers as a necessity to adapt present water management plans and strategies (Stager and Thill, 2010).

The use of regional climate model outputs as inputs to a physically-based water quality model is a common practice to predict future exports of sediment and nutrient losses to water bodies. Therefore, for the realization of this study were used a version of SWAT 2005 adapted for Québec's conditions and several climate change scenarios produced by the CRCM4. Changes in temperature and precipitation regimes, as well as solar radiation, CO_2 level in the atmosphere and solar radiation, have been found in several studies to have direct and indirect effects on nutrient exports. The direct effects of temperature and precipitation amounts and intensity have the greatest impact.

CHAPTER 3: MATERIALS AND METHODS

3.1 Description of the Pike river watershed

The Pike River watershed spans the Québec/Vermont border and drains towards the Missisquoi Bay, located in the northern portion of Lake Champlain (Figure 3.1). Of the watershed's 630 km^2 area, 84% lies within southern Québec's Eastern Townships/Montérégie region. Its main town, Bedford, is located at its center, near the shore of the Pike river, 60 km south-east of Montréal. The town of Bedford marks the separation between the geophysically distinct upstream (390km^2) and downstream (240 km^2) portions of the watershed.

Considered as a critical contributor to recurrent contaminations of Missisquoi Bay by toxic cyanobacteria, the Pike river watershed has been characterized in several multi-scale hydrological studies (Beaudin et al., 2006; Deslandes et al., 2007; Michaud et al., 2007).

The upstream portion of the watershed is characterized by a hilly Appalachian Piedmond landscape, with a mean slope of 5°. Steeper slopes, within the range of 35-38° are primarily forested, though there is some farming on such slopes. The dominant soils are sandy and shale loams. The downstream section is flatter with a mean slope of 0.6°, and its dominant soils are clay in low-lying areas. At higher elevations calcareous and shaly tills are predominant. Agriculture is the most intensive economic activity thanks to the fertile soils and flatter topography. Overall, 75% of the watershed is under cultivation, 50% of which is devoted to annual crops. These have been identified as the main sources of soil and water degradation.

The hydrological regime of the 65 km Pike River is characteristic of snowmelt basins, with one major peak flow during the snowmelt season in April, and a lower discharge during the summer. The climate is temperate. Summers are short and humid with hot days (mean daily maximum temperature of 20°C) while winters are long, cold (mean daily maximum temperature of -10°C) and dry, with a considerable amount of snow

(20% of annual precipitation). Climate normals (1971-2000) for annual rain and snowfall range between 1 095 mm and 1 272 mm and 204 and 281 cm at Farnham and Sutton weather stations respectively (see Figure 3.1 for station location). Half of the precipitation falls during the growing season extending from May to September (Environment Canada, 2008).

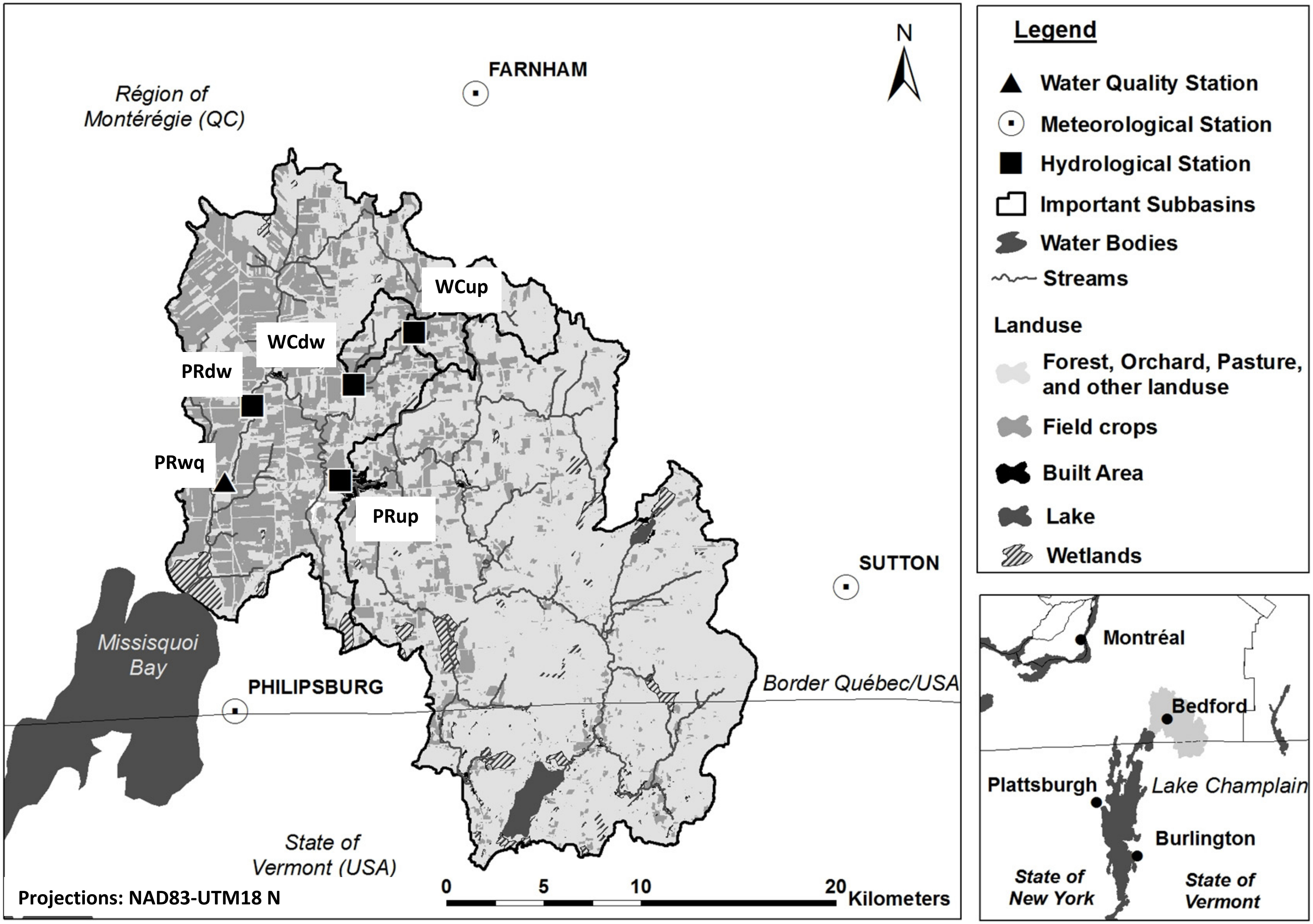

Figure 3.1: Maps of the Pike river watershed indicating the location of meteorological and hydrological stations. The land-use data are derived from a Landsat imagery taken in July 1999 (Cattaï, 2003).

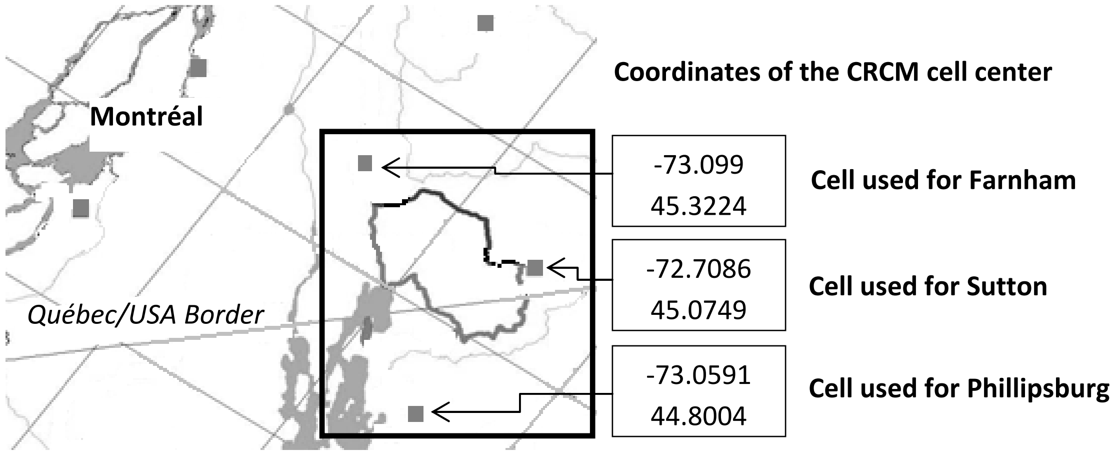

Figure 3.2: Map of the CRCM grid cells providing the simulated climate data

3.2 Hydrological and water quality modelling

3.2.1 SWAT input data

As SWAT has been previously applied on the Pike River watershed, data for the spatial parameterization of the model were retrieved from the study of Deslandes et al. (2007) and transferred from SWAT2000 to a SWAT2005 platform (Arnold et al, 1998; http://swatmodel.tamu.edu/contact/). Spatial data were entered into SWAT through a graphical interface ArcSWAT linked to Arcview 3.3 (ESRI, Redlands CA, http://www.esri.com/). The data consisted of a Digital Elevation Model (DEM) with a spatial resolution of 30 m ± 1.3 m as developed by Deslandes et al. (2002), a digital hydrographic network with 99 subwatershed outlets, a land-use layer derived from the classification of Landsat 7 ETM+ imagery obtained in July 1999 (Cattaï, 2004), a digital soil layer and soil physical properties extracted or estimated from different soil surveys and studies of the region (Thériault et al., 1943; Cann et al., 1948; Bernard, 1996; USDA-NRCS, 1999; USDA-SCS, 2006), and a soil degradation inventory, (Tabi et al., 1990). Details can be found in Deslandes et al. (2007).

Daily precipitation and temperatures from 1970 to 2006 were extracted from the National Climate Archives Database (Environment Canada, 2007) for the three meteorological stations closest to the watershed: Farnham, Phillipsburg, and Sutton, at respective elevations of 68m, 53m and 390m (Figure 3.1 a) and were also entered into SWAT through ArcSWAT. Missing values were interpolated by monthly regression with a nearby station giving the highest coefficient of regression (≥0.6). Wind speed, relative humidity (ratio of the air pressure at a certain humidity level to its pressure at saturated humidity), and solar radiation were estimated by SWAT with its Weather Generator. SWAT calculated these climatic parameters based on statistics from the Plattsburg NY State Meteorological Station, located 50 km southeast of the Pike River outlet.

SWAT uses management files to account for field operations management (tillage, sowing, fertilizing, and harvest). The dates of field operations were estimated annually for each crop between 1998 and 2006, based on reports of the State of the Crops from La Financière agricole (2008). These reports contained general information about the evolution/state of field work, and crop growth in the fields throughout the year. As in Deslandes et al. (2007) probable schedules of field management were determined for each year by overlaying information from the reports, rainfall events and observed management practices. No reports were available before 1998. Therefore 1998-2006 schedules were applied to years between 1971 and 1998. A table of this management schedule and fertilizer amounts is provided in Appendix Ia as well as the decision criteria used in setting the dates.

Initial soil nutrient content and fertilizer applications were kept as originally set in Deslandes et al. (2007) and Michaud et al. (2006). They calculated organic N and P concentrations (mg kg^{-1}) of each soil, according to SWAT manual estimates (Neitch et al., 2005), i.e., based on the percentage of organic matter found in the region's inventory of soil degradation (Tabi et al., 1990) and the C/N and N/P ratios usually found in organic matter (see 2.6.4). Labile N concentrations were set to SWAT default values, but labile P was calculated based on the richness of the soil determined by in situ measurements collected within the watershed between 1995 and 2001 (Deslandes et al., 2004; Michaud et al., 2006). Fertilizer applications were determined according to annual expenditures for inorganic fertilizer, livestock composition (for manure) and crop types listed on governmental farm registration records for 2000. Details in the composition of manure and distribution of the annual fertilizer load by crops, soils and through the years can be found in Michaud et al. (2006, 2008) and Levesques (2003).

Similarly, specific information about management practices (tillage type, best management practices already implemented) and changes brought to the crop database can also be found in Deslandes et al. (2007) and Michaud et al. (2006).

3.2.2 SWAT Set-up and calibration

As explained in 2.6.1, the SWAT calculation unit is the HRU. SWAT first delineated 99 subwatersheds from the entered DEM and digital hydrological network. The overlay of the land-use and soil digital maps resulted in 1, 872 HRUs. During the process of creating the HRUs, the threshold controlling the HRUs' distribution in ArcSWAT was set at 10% for the soils map in order to lump minor contributing areas (soils occupying less than 10% of a subbasin) into more dominant HRUs. This allowed the reduction of the 2, 250 HRUs of the SWAT2000 modelling version (Deslandes et al., 2007) down to 1, 872, but required model recalibration. This process mainly affected the multi-segmented small rural, urban and road areas. This enabled the focus to remain on the main pollutant-contributing agricultural areas.

The calibration procedure remained the same as in Deslandes et al. (2007), but the periods used to test the results changed slightly due to the greater data available and the need to test the model over a longer period of time. As such, while earlier studies focused on the years 2000-2003, in this study, the model was run continuously for the periods of 2000-2006 and 1971-2000. The first period supported the calibration and validation of the model and was divided into three sets: (i) from January 1^{st}, 2000 to November 1^{st}, 2001 for model warm-up, (ii) from November 1^{st}, 2001 to May 21^{st}, 2003 for calibration, and (iii) from November 1^{st}, 2001 to May 21^{st}, 2003 for validation. The second period (1971-2000) was also used for a second validation meant to test the robustness of the calibration parameters to varied climate conditions over a longer term, in order to take into account natural climatic variability. For this run, the model was 'warmed up' from 1971 to 1980 and the validation was performed from 1980 to 2000. The divisions of the two periods resulted from the availability of water quality data used to guide the adjustments of the model calibration parameters.

For the period 1971-2000, water quality data were available only from 1980 onwards. However climate data were available as of 1971. Since climate change scenarios are run over 30 years, and we had 20 years of observed data, it was decided to use 10 years for the warm-up period. However, there is no rule about the duration of the warm up period and it could have been reduced.

The calibration parameters used to adjust the model were those highlighted during previous modelling exercises within the region (Gollamudi, 2006; Deslandes et al., 2007; Michaud et al., 2007) and are given in Appendix Ib. Several simulations were made to adjust the model by varying the calibration parameters one at a time. The auto-calibration in SWAT gave poor results. Therefore all parameters were adjusted manually. The performance of the model was judged based on the visual inspection of the hydrographs and three frequently used statistical indices of goodness of fit (see 3.2.3). Runoff was estimated by the SCS Curve Number method (USDA-SCS, 2006), evapotranspiration by the Hargreaves method (Hargreaves et al., 1985) and the routing of flow through the hydrological network by the Muskingum method (Overton, 1966) (see 2.6.1 and 2.6.2).

First, the calibration focused on adjusting components of the annual water cycle for the upstream and downstream sections of the watershed defined by the hydrological stations 'Pike River upstream' and 'Pike River downstream' (PR_{up} and PR_{dwn}), located on the main section of the river (Figure 3.1). Daily stream flows were then adjusted against measured data at the two hydrological stations. Once hydrology was set, sediments, TP and TN were calibrated in this order. Calibration was performed from the upstream to the downstream sections.

No accurate data of total P and N were available for the calibration of the Pike River loadings. However, two experimental subwatersheds, namely the 'Wallbridge Creek upstream' (WC_{up}) and 'Wallbridge Creek downstream' (WC_{dw}) watersheds, were instrumented to collect sound hydrological and water quality data at their outlets (Michaud et al., 2004). Hydrological and water quality stations, WC_{up} and $WC_{dw,}$ are located on figure 3.1. These subwatersheds were chosen in previous studies for their representative characteristics of the upstream and downstream portions of the entire watershed (Deslandes et al., 2007). Therefore, a second set-up, similar to the first one but only representing the two experimental subwatersheds was created. Hydrology of these two subwatersheds was first calibrated with their own parameters using the same method as for the main watershed. Then monthly sediment, total P and N predictions have been calibrated against data collected by Michaud et al. (2004).

The four hydrological stations were operated by the Centre d'Expertise Hydrique du Québec (CEHQ) of the ministère du Développement durable (MDDEP). The MDDEP codes for these stations are 030420 (PRup), 030424 (PRdw), 030427 (WCup), and 030428 (WCdw).

Once entirely calibrated, the model was validated at all recording stations for the period 2004-2006 (for hydrology only in set-up 1, representing the entire watershed, and for hydrology and water quality in set-up 2, representing the experimental subwatersheds). Then the water quality parameters simulated for each of the two subwatersheds were transferred to the respective upstream and downstream sections of the entire watershed. At this point, the model was validated over the longer 20-year period for the entire watershed with set-up 1. Hydrological data from the downstream gauging station (PR_{dw}) did not cover such a long term period. Stream flow was therefore validated at the outlet of the upstream portion of the watershed (PR_{up}) which receives water from 75% of the watershed. This 75% encompasses areas highly representative of the whole watershed (intensive farmland, forest, steep slopes, etc.). Water quality data came from a fifth station PRwq (for water quality), also referred to with the code 03040015 of the MDDEP. These data had been recorded by the MDDEP since 1979.

This station receives nutrient loadings from three-quarters of the whole watershed and should therefore provide a rather good overview of the loads received by the entire watershed. However, sediments and total N and P were sporadically sampled once a month (or even sometimes only 3 or 4 times a year) without the corresponding stream flow. The derived monthly loadings may therefore not be very accurate and were only used for a rough comparison with the model predictions.

To estimate monthly loadings, the stream flow recorded at PR_{up} was first adjusted to reflect stream flow of the PR_{wq} station by multiplying daily stream flow by 1.4, which is the ratio between the two drainage areas upstream of the PR stations. Then daily stream flow and water quality data were sent to IRDA, which had developed experimental rating curves linking sediments and nutrient loadings samples to stream flow discharge using the U.S. Army Corps of Engineer program Flux5.0 (Walker, 1998). The procedure is detailed in Michaud et al. (2004.) This program was already used to estimate P loadings to Lake Champlain several times (Smeltzer et al., 2009).

3.2.3 Assessment of the model performance

The performance of the model was determined using three statistical indices often used in hydrological studies: the coefficient of regression R^2, the Nash-Sutcliffe model efficiency coefficient (NSE) and the percent deviation (PBIAS) (Moriasi et al., 2007).

The coefficient R^2 evaluates how the predicted variable is correlated to the corresponding measured data, but does not assess "additive or proportional divergence" between the series and therefore does not provide complete information about the fit between them (Moriasi et al., 2007). On the other hand, the NSE coefficient is deemed to be the best objective function for this last purpose and complements the R^2 assessment. NSE cannot be used for cumulative data, since it would compound errors. Values of 1 represent a perfect fit. NSE values between 0 and 1 are generally acceptable but modellers usually aim for a minimum value of 0.5. The PBIAS simply evaluates the over- or under-estimation of the model.

The NSE and PBIAS are calculated as follows (Moriasi et al., 2007):

$$\text{NSE} = 1 - \left[\frac{\sum_{i=1}^{n}(Y_i^{\text{obs}} - Y_i^{\text{sim}})^2}{\sum_{i=1}^{n}(Y_i^{\text{obs}} - \bar{Y})^2}\right] \quad [3.1]$$

$$\text{PBIAS} = \left[\frac{\sum_{i=1}^{n}(Y_i^{\text{obs}} - Y_i^{\text{sim}}) * 100}{\sum_{i=1}^{n}(Y_i^{\text{obs}})}\right] \quad [3.2]$$

where

Y_i^{obs} is the i^{th} observation of the evaluated variable,
Y_i^{sim} is the i^{th} simulated value of the evaluated variable,
$\bar{Y}$ is the mean of the observed data for the evaluated variable, and
n is the total number of observations.

3.3 Climate projections and impact assessment

The validated SWAT was run with four climate projections provided by the Ouranos Consortium of Québec. The climate datasets differed according to the climate model, the version of the model, and the initial (starting date) and lateral boundary conditions (domain and driver, see 2.4.2) used for their creation. They were purposely chosen in order to account for a variety of uncertainties related to climate modelling and to encompass a wide range of possible futures. The climate models used and attendant datasets are presented below in greater detail.

3.3.1 Climate datasets and impact assessment

Mean changes in the watershed hydrology and nutrient losses for the horizon 2050 were predicted by comparing the future period (2041-2070) with the historical or control period (1971-2000). Ouranos produced the climate datasets relative to these two periods with the Arpege and the CRCM4 climate models driven at the boundary of its domain by the CGCM3. The domain of a model is the area it covers. The three models were presented in the Literature Review in section 2.4.2.

Climate for the historical period was simulated for each of the four projections (table 3.1), with the purpose of reconstituting current watershed hydrology using SWAT and the climate models. This allowed the combined GCM-RCM-SWAT models to be assessed when used together, by comparing the reconstructed hydrology they generated over the historical period to SWAT predictions generated with observed climate data. Also, assuming model biases for control and future periods to be more or less similar, a comparison of the two synthetic hydrological series (historical and future) would cancel out biases included in climate projections and hydrological modelling (Pan et al., 2001). This approach is convenient since it can provide a quantitative assessment of changes while reducing systematic bias included in models used in cascade.

Figure 3 shows the climate input datasets to the various formulations of SWAT. To interpret the results more accurately, a supplemental dataset (ERA40 (Uppala et al. (1999)), created through re-analysis of observed data (as a driver of the CRCM) was employed to validate the use of SWAT with CRCM data, and potentially highlight sources of error in the resulting SWAT and CRCM predictions. The output of the model was defined as SWAT 2 (Figure 3). Table 3.1 provides key characteristics of each climate dataset.

Paired *t*-tests, (or the non-parametric Wilcoxon test when data were non-normal) were applied to stream flow, water yield, sediments, TP and TN to determine if changes in the means spanning 30 years between the 2041-2070 horizon and the control period were significant. The threshold of significance was 5%. If not significant, we considered the changes to be part of the natural 30-year variability in climate.

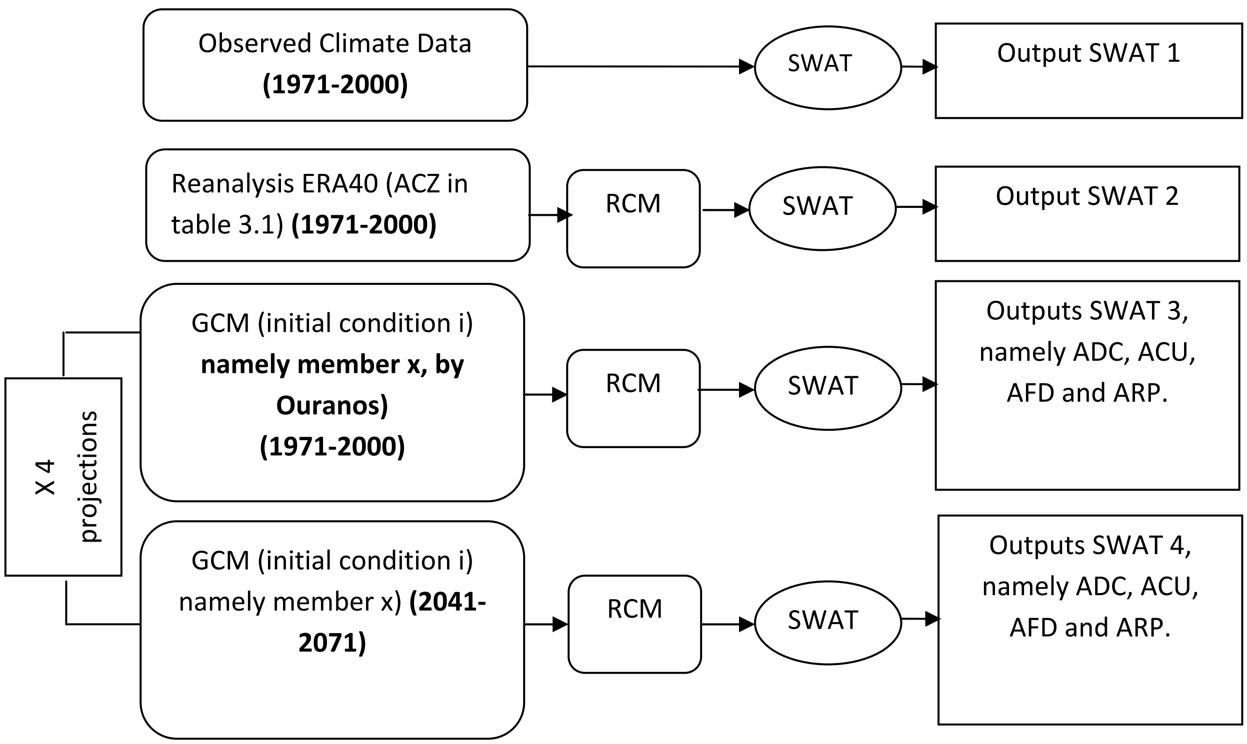

Figure 3.3: Schematic diagram of the performed simulations (adapted from Jha et al., 2004)

Initial condition i refers to the starting date and the parameterization of the CGCM, and member x is a name given by Ouranos to GCM simulations with a certain initial conditions. Members used for this project are described in Scinocca and McFarlane (2004).

Table 3.1: Characteristics of the climate datasets driving SWAT

Name of the climate simulation	Time Window	Regional Climate Model (RCM)	Driver of the RCMs	GCM Member (Expressing Initial Conditions)	RCM Domain (cells*cells)	GHG Emissions Scenario	Utility
ACZ	1971-2000	CRCM 4.1.1	Reanalysis ERA40	None since driven with reanalysis	Québec (112*88)	Current	RCM Limitation and RCM-SWAT Validation
ADC	1971-2000 And 2041-2070 (The 4 climate projections have equal probability of occurrence)	CRCM 4.1.1	CGCM3 3.7.1	1	Québec (112*88)	A2	GCM limitation, GCM-RCM-SWAT Validation AND, Climate Change Impact Assessment
ACU		CRCM 4.1.1	CGCM3 3.7.1	4	Québec (112*88)	A2	
AFA/AFD		CRCM 4.2.3	CGCM3 3.7.1	5	AMNO (182 * 174)	A2	
Arpège (ARP)		Arpège 4.4	No Driver Arpège. Variable Grid Mesh	1	T 159 (182 * 174)	A2	

Daily precipitation, maximum and minimum temperatures at 2-m above ground, and the maximum half hour rainfall were directly transferred from three RCM grid points into SWAT for the control and future periods. The points were chosen so that their centres fell as close as possible to the meteorological stations used to calibrate the hydrological model. Cells were centred over the geographical coordinates (-73.099, 45.3224, for Farnham; -72.7086, 45.0749 for Sutton; and -73.0591, 44.8004 for Phillipsburg) (Figure 3.1 b).

RCMs are subject to systematic errors transferred from the GCMs driving them (Déqué and Piedelievre, 1995), or due to RCM uncertainties themselves (Jha et al., 2004; Gagnon et al., 2009). Conventionally a bias correction is applied to resolve this issue (Graham et al., 2007; Boe et al., 2009; Prudhomme and Davies, 2009). However, unbiased data series preserving both a physical coherence between the climate variables and changes in the distribution and intensity of rainfall events were not available at the time of the study. Corrections of bias were therefore omitted, assuming any bias would be reduced through a comparison between the control and the future period.

For the future climate simulations, climate models were supplied with the IPCC SRES A2 (Nakicenovic et al., 2000) while for the control period, measured concentrations of greenhouse gas emissions were used. The A2 scenario represents a world development scenario that produces one of the highest continual increase in GHG emissions (see 2.4.2 for more details). Other SRES scenarios present few differences in the global surface warming for the time horizon chosen in this study (Fig 10.4, IPCC, 2007- WGI). Therefore, using more than one scenario to capture uncertainties resulting from predictions of greenhouse gases emissions was not deemed of primary importance for this horizon.

On the other hand, numerous studies have recorded that a great deal of variability and uncertainty in climate projections arise from GCMs and the downscaling method (Abbaspour et al., 2009; Boyer et al., 2010). Figure 3.2 shows scatterplots of temperature and precipitation changes for 128 simulations produced with 20 recognized GCMs and 12 simulations with Ouranos CRCM including the four chosen simulations of this project. GCMs and the CRCM were run with different parameterizations and GHG emission scenarios. The 12 CRCM simulations from Ouranos typically fell within the cloud of all future projections indicating that they represented future changes in climate fairly well. The four projections ADC, ACU, AFA-AFD and ARP (Table 3.1) used in this project were chosen to cover the widest spectrum of simulated changes, especially for winter, since during this season the effects of climate change due to temperature variations are expected to be greater (Boyer et al., 2010).

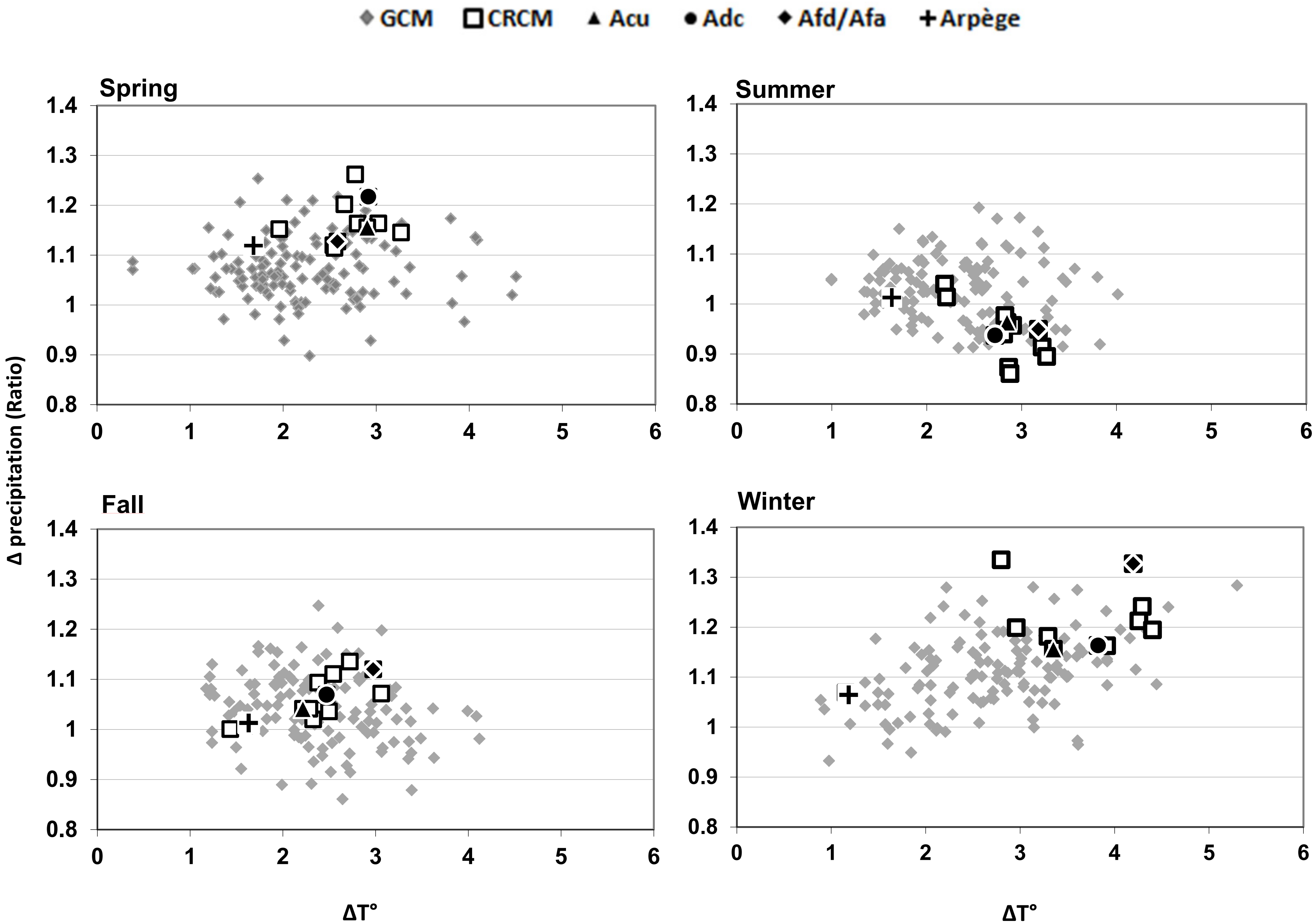

Figure 3.4: Changes in temperatures and precipitation in Missisquoi Bay between 1971-2000 and 2041-2070

CHAPTER 4: RESULTS AND DISCUSSION

4.1 SWAT performance in simulating hydrology

4.1.1 SWAT performance with observed climate data: calibration and validation

Initial simulation

In SWAT, each subwatershed utilizes the precipitation and temperature conditions from the nearest weather station entered into the model. Accordingly, half of the watershed (southern part of the upstream and downstream sections) was under the influence of Philispburg's weather while 29% (the downstream north) was under the influence of Farnham's weather and 21% (the upstream north), under Sutton's. The wettest section of the watershed is the upstream due to its proximity to Sutton which received in average 1,272 mm of precipitation during the last 30 years versus 1,156 mm for Farnham and 1,096 mm for Philispburg. During 2001-2006, the upstream section of the watershed received about 75 mm more precipitation than the downstream section.

In Southern Québec, annual evapotranspiration was roughly estimated to account for 55% of annual precipitation (Atmospheric Environment Service, 1975). Moreover on a global scale 5% to 10% of the water is lost through percolation within the deep aquifer (Oki and Kanae, 2006). For the 2001-2006 period, predicted annual evapotranspiration was 462 mm and the recharge of the deep aquifer was 17 mm, prior to SWAT calibration. This corresponds to 42% and 2% of annual precipitation respectively. Therefore, SWAT underestimated evapotranspiration by 15% and deep aquifer recharge by 8 %. Because of this, the water yield, which is the sum of surface runoff and subsurface flow (ground water, lateral and tile flow) was overestimated. Indeed, with 618 mm, the water yield accounted for 55 % of annual precipitation. According to values presented above and the water budget equation [2.1]: $SW_{\mathrm{t}} = SW_0 + \sum_{i=1}^{i=t}(R_{\mathrm{day}} - Q_{\mathrm{surf}} - E - W_{\mathrm{seep}} - Q_{\mathrm{gw}})$, the water yield ($Q_{\mathrm{gw}}+Q_{\mathrm{surf}}$) should be approximately 35-40% of precipitation. Δ Soil (SW_{t} - SW_0) is the change in soil moisture during the time step. This variable is difficult to estimate at a yearly step and can be very small. SWAT does not provide this value. Values of the complete water budget predicted by SWAT are presented in table B1.

Although the upstream section receives more precipitation than the downstream section, predicted surface runoff was greater in the downstream section and the downstream subwatershed. This agrees with field observations made in the Wallbridge subwatersheds by Michaud et al. (2004). They explained that because downstream areas are in a lower position within the watershed, the water table is more likely to rise near the soil surface due to soil water saturation. Soils in the downstream sections are less permeable and have higher water holding capacity (Figure A3). These two factors therefore promote greater runoff. In addition, the upstream section has greater forest cover which might have reduced runoff due to greater rainfall interception by the canopy, greater soil roughness and infiltration, and greater evapotranspiration.

Furthermore, Michaud et al. (2008) determined that surface runoff contributed for 30% of the water yield within the upstream subwatershed Wallbridge and 26% of the water yield within the downstream Wallbridge during the period of November 2004 –May 2006. Prior to calibration, annual surface runoff for the entire watershed was 279 mm and subsurface flow 339 mm. This corresponds to 45% and 55% of an already overestimated water yield. Similarly, surface runoff predictions were 331 mm and 340 mm for the upstream and downstream subwatersheds. This corresponds to 51% and 55% of annual water yield, which confirms SWAT allocates too much water to surface runoff *vs* infiltration. Runoff is therefore overestimated due to a high water yield and deficient distribution of rainfall between surface runoff and infiltration.

On a daily scale, the predictions of runoff events needed some adjustments. Indeed, many inexistent peak flows had been predicted to occur over the whole winter, while in reality most snowmelt events only occurred in March/beginning of April. This was due to inaccurate predictions of snowmelt events (Figure B2). Actually, in SWAT, at near zero temperatures, predictions of snowfall or snowmelt occurrences are not accurate because it bases its predictions on the average of daily temperature and temperature threshold parameters (Deslandes et al., 2007). By only considering this average, SWAT misses the daily temperature variations and over- or underestimates snowmelt (or snowfall) if the snowmelt and snowfall temperature threshold are not well adjusted. This explains why in warmer winter periods that occurred during the calibration and validation (January-February 2002; December-March 2002-03; December-March 2005-06) SWAT simulated inexistent peak flows and reduced snow cover. It also shifted spring floods towards winter.

Also summer and fall events were overpredicted or simulated slightly too early. Lastly, base flow (or groundwater flow) seemed too high especially during the growing season and, recessions of the hydrograph were too sudden.

Balancing the annual water budget

A sensitivity analysis of calibration parameters performed within the watershed showed that the SCS CN method, coefficients of evapotranspiration compensation ESCO and EPCO, landslope, soil physical parameters and, factors controlling water movements within the soil profile and between the aquifers and stream flow (GWQMN, REVAPMN, GW_REVAP and RCHRG_DP) were the most sensitive to hydrology calibration (Gollamudi, 2006; Deslandes et al 2007). Values assigned to the calibration parameters, their allowed range of values and their definitions are given in table A2.

Parameters were changed manually one at a time. After each change, the average annual water balance for the upstream and downstream sections of the watershed and daily stream flows were analysed. According to the results, further adjustments were made as follows.

As surface runoff plays a major role in soil and water degradation, runoff adjustment was a major aspect of the calibration. Under Canadian climate conditions, it is known that initial CN values overestimate runoff (Gollamudi et al., 2006; Perrone and Madramootoo, 1998). Despite modifying SWAT code to reduce surface runoff and to increase tile flow (section 2.6.2) initial simulations presented above showed CN needed to be lowered to correct runoff predictions. Then, RCHRG_DP was increased to allow more percolation towards the deep aquifer as well as the threshold depth of water for base flow to occur (GWQMN) in order to reduce base flow. Similarly, coefficient GW_REVAP which controls the rate of water transferred from the shallow aquifer to overlaying soils was increased to allow more evapotranspiration to occur. Concurrently, threshold REVAPMN which represents the minimum depth of water allowing revap to occur was decreased.

At this stage, evapotranspiration was already higher, likely due to the increase of soil water availability, satisfying better the plant and soil evapotranspiration demand. The soil evaporation compensation factor ESCO and the plant uptake compensation factor EPCO helped finalize the balance of the water budget. Although parameters related to soil properties were often cited as useful for underground and soil water movement adjustment, we used field measurements from survey reports to remain close to physical reality (Benaman et al., 2005; Deslandes et al., 2007; Gollamudi et al., 2007).

After calibration, SWAT reproduced accurately each component of the water budget (Table B1). On average and as recorded by meteorological stations of the region (Environment Canada, 2011), 20% of the annual precipitation occurred in the form of snow. Fifty percent of precipitation left the watershed through evapotranspiration, while surface runoff accounted for 30% of the water yield. Only the downstream Wallbridge Creek WC_{dw} subwatershed continued to have higher runoff depth than wished with values accounting for 40% of the water yield instead of 30%. On the long term validation period, predictions were similar (column SWAT.OBS of table 4.2) which proves SWAT capacity to perform under varied climate conditions.

<u>Hydrograph adjustments</u>

The calibration of stream flow on a daily basis required the adjustment of further parameters controlling snowfall, snowpack depth and its rate of melting, lag time of runoff to reach the outlet and, some aspects related to the magnitude of stream flow peaks and to the recessions of the hydrographs. SNOCOV50 and SNOCOVMX were manually adjusted by trial and error, and the snowmelt and snowfall temperature thresholds were decreased to force snowfall and avoid snowmelt events during winter months. Maximum and minimum melting rate factors as well as the snow pack temperature lag factor were also manually adjusted by trial and error. The runoff lag time factor, length of slope and coefficients of manning were increased to delay runoff events. Finally, the ground water delay period (GW_DELAY) and base flow recession (ALPHA_BF) were also increased to correct the sharp peak recessions due to high stream flow response to the shallow aquifer recharge (Neitsch et al., 2005).

After calibration, the model reproduced stream flow at each station adequately. Winter flow, snowmelt and summer peak flow were clearly improved. The majority of events are well simulated time-wise with recessions of peak flows comparing rather well to observed conditions for both calibration and validation periods (Figure B2). Stream flow calibration was performed at a daily scale to be more precise and achieve better results. However, the impact of climate change is studied on an annual, seasonal or monthly scale; therefore the three coefficients of performance R^2, NS and the PBIAS were computed on a monthly basis.

Graphs illustrating the goodness of fit between daily predicted and measured stream flow can be found in appendix B. Monthly hydrographs are given concurrently with water quality results. For the calibration period of November 2001-May 2003, the coefficients of performance for each of the four hydrological stations fell within the ''satisfactory'' to "very satisfactory" range of Moriasi et al. (2007). In fact, on a monthly basis, R^2 values exceeded 0.7; NSE values exceeded 0.5, and the absolute deviation remained below 25% (Table B3 for 2001-2006 period and table 4.1 for 1971-2000 period).

On the other hand, for the validation period (November 2004-May 2006) the model performed rather poorly, with statistical indices sometimes close to, but nonetheless remaining under acceptable values (e.g., $R^2 < 0.5$, NSE < 0.5, PBIAS > 15%). This poor performance is mainly attributable to intense rainfalls in the spring of 2006. The model could not reproduce the resulting high discharges and the statistical indices are very sensitive to extreme values (Moriasi et al., 2007). By removing the problematical period (March-May 2006) values of R^2 improved from 0.5 to 0.6 for WC_{up} and from 0.6 to 0.7 for WC_{dw} and values of NSE improved from 0.28 to 0.43 for WC_{up} and from 0.47 to 0.58 for WC_{dw}.

The calibration period (2001-2003) was about 50 mm wetter than the validation period (2004-2006). During the calibration period, the amount of precipitation recorded for each year was normal (within 2 standard deviations from the average) whereas the validation period suffered from dry and wet years (outside 2 standard deviations). Indeed, the years 2004 and 2005 received at least 30% less precipitation than the 30-year average at Philipsburg and Farnham stations. As for the year 2006, Sutton received 30% more precipitation than the 30-year average. Philipsburg and Farnham precipitation values were respectively 17% and 10% above the average. This is wet but remains within the two standard deviations. The calibration was therefore performed for a period of normal weather, whereas the validation of the model was undertaken under very variable and sometimes extreme weather events which may explain the lower performance.

SWAT's long term performance is acceptable as demonstrated by the annual water budget results over the control period (1971-2000) and stream flow prediction over the last 20 years (1980-2000). Values of R^2, NSE and bias remained within satisfactory ranges ($R^2 > 0.5$; $0.50 < NSE < 0.65$; $\pm 15 < PBIAS < \pm 25$) (Table 4.1).

Table 4.1 : SWAT performance statistics for stream flow prediction for the long term validation

Climate Input	R^2		NSE		PBIAS (%)	Diff (mm)
	Monthly	Yearly	Monthly	Yearly	Computed on cumulative stream flow for the period	
Observed	0.61	0.86	0.55	0.52	-14	-1 566
Rean-CRCM	0.44	0.32	*0.26*	*0.22*	-10	-1 083

Predicted and measured stream flows for this period are illustrated, concurrently with simulations performed with climate model inputs, in figure 4.1 (annual time step) and figure 4.3 (monthly basis).

4.1.2 SWAT Performance with climate model inputs

<u>Average annual water cycle</u>

Table 4.2 shows average annual values for the main components of the water cycle simulated with the different climate datasets over the reference period. The names of the simulations are constructed from the name of the simulated climate ADC, ACU, AFA-AFD and ARP. Thus, each simulation refers to SWAT outputs obtained with the specific climate inputs from regional climate modelling described in table 3.1.

Table 4.2: Simulation of the water cycle over the entire Pike River watershed between 1971 and 2000 for the different climate datasets; thirty annual averages in mm yr^{-1}.

	SWAT-OBS	SWAT-ACZ	SWAT-ADC	SWAT-ACU	SWAT-AFD	SWAT-ARP
Precipitation	1147	1239	1239	1227	1267	1476
Snowfall	256	257	202	211	300	310
% of pcp	**22%**	**21%**	**16%**	**17%**	**24%**	**21%**
Snowmelt	241	245	192	202	283	295
% of pcp	**21%**	**20%**	**15%**	**16%**	**22%**	**20%**
Wateryield	522	550	520	516	820	834
% of pcp	**46%**	**44%**	**42%**	**42%**	**65%**	**57%**
Evapotr.	597	647	662	660	417	594
% of pcp	**52%**	**52%**	**53%**	**54%**	**33%**	**40%**
Deep Aquifer	68	68	79	76	112	123
% of pcp	**6%**	**5%**	**6%**	**6%**	**9%**	**8%**
Surface Runoff	167	212	145	155	218	206
% of WYLD	**32%**	**39%**	**28%**	**30%**	**27%**	**25%**
Subsurf. flow	354	336	375	362	502	628
% of WYLD	**68%**	**61%**	**72%**	**70%**	**61%**	**75%**

Explanation of the abbreviations in the table:

- SWAT-OBS, SWAT-ACZ, SWAT-ADC, SWAT-ACU, SWAT-AFD, and SWAT-ARP are the outputs of the model SWAT run with observed climate and climate scenarios described in 3.3.
- Pcp stands for precipitation, Evapotr., for Evapotranspiration and WYLD, for water yield (which is total runoff).

SWAT.OBS (or SWAT1) is the reference simulation used to validate SWAT performance without the influence of climate model biases. SWAT-ADC, SWAT-ACU, SWAT-AFD and SWAT-ARP (SWAT3) are the historical simulations with which respective future simulations (SWAT4) will be compared. SWAT-ACZ is used to assess CRCM alone without the influence of CGCM. As expected, the watershed received between 80 mm (SWAT-ACU) and 329 mm (SWAT-ARP) more precipitation when driven the predicted climate for the period 1971-2000. This is likely due to the systematic bias within climate model outputs (Gagnon et al., 2009; Minville et al., 2009). These biases affect absolute values of the water cycle components, but not necessarily the overall hydrological processes. In fact, the proportional distribution of the watershed moisture through the water cycle is rather well simulated with SWAT-ACZ, SWAT-ADC and SWAT-ACU, since the proportions obtained compare relatively well to those obtained from SWAT-OBS. Annual runoff was slightly overestimated (7%) by SWAT-ACZ, with nearly 40% of the water yield leaving the watershed as surface runoff. Since other components of the water cycle are satisfactorily reproduced, this may be caused by differences in the distribution of precipitation events affecting soil moisture and water infiltration.

On the other hand, SWAT-AFA and SWAT-ARP presented a relatively high water yield (60%) and low evapotranspiration (40%). This imperfect allocation of precipitation to the water cycle components may be attributed to i) a negatively biased temperature – especially in the summer since snowfall appears to be correctly reproduced and/or to ii) positively biased summer precipitation with insufficiently high temperatures to evaporate the resulting surplus of moisture. The comparison of CRCM precipitations and temperatures to observed data shown in figure C1 validates this explanation.

These results show that biases in the regional climate model are transferred to hydrological results, through the model's high sensitivity to climate. However, the contribution to bias of the CRCM alone (SWAT-ACZ) does not affect hydrological processes on a yearly basis, confirming the capacity of the model to produce climate data suitable for hydrological studies over the region. On the other hand, as seen with simulations SWAT-AFA and SWAT-ARP, the GCM driving the regional climate model may sometimes negatively affect hydrological simulations because both temperature and precipitation data are very different from observed conditions.

Annual stream flow

Figure 4.1 compares annual flows from the SWAT-ACZ (Reanalysis) simulation to those predicted with the observed weather as well as to the longest available observed flow series recorded at PR_{up}. The major bias in both simulations is introduced by SWAT because of difficulty in reproducing the wettest years. This lowered the three coefficients of performance. Stream flow series predicted with SWAT were therefore compared to each other instead of to observed flows.

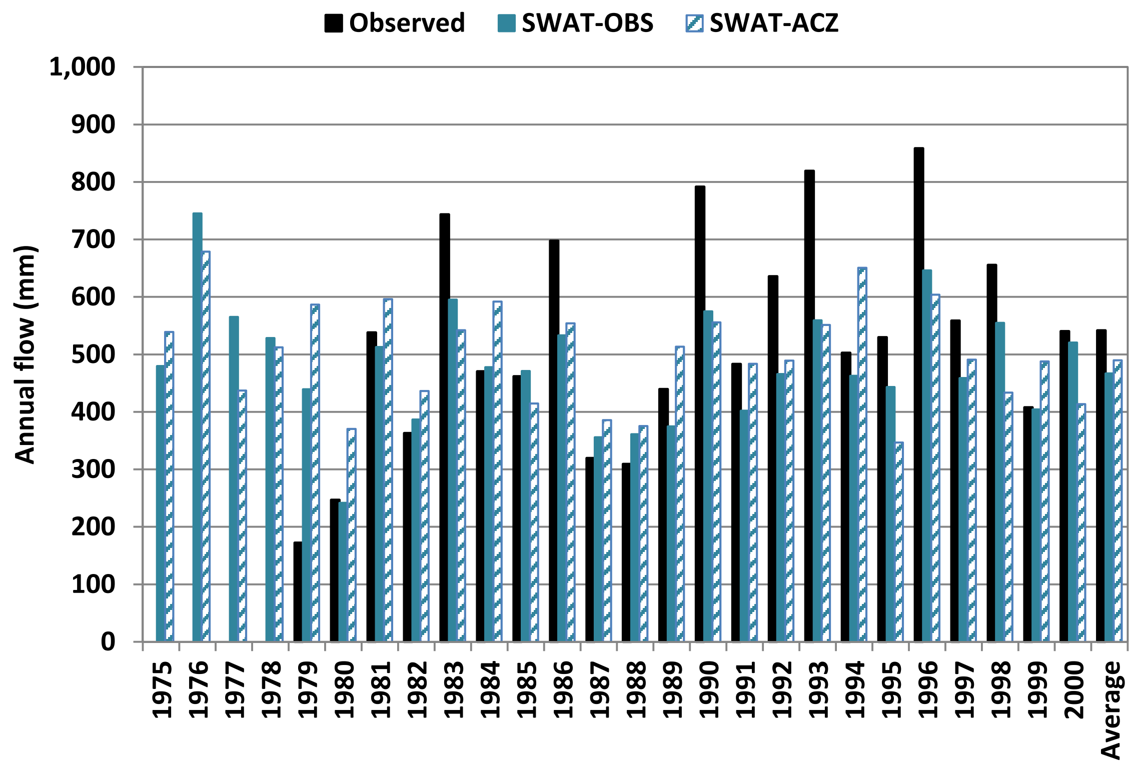

Figure 4.1: Long -term comparison of observed and simulated annual stream flow at the hydrological station PR_{up}

Annual flows predicted by the CRCM weather module (CRCM with reanalysis) do not necessarily match observed flows or those predicted with observed data on a month-to-month and year-to-year basis. This temporal mismatch occurs because spatial resolution of regional climate models does not sufficiently capture local climatic events. There are discrepancies between station-measured rainfall and temperatures and 45km^2 simulated rainfall and temperatures. Therefore, when SWAT-ACZ is compared to observed flows, R^2 and NSE values fall under thresholds of confidence (R^2 and NSE < 0.5) (Table 4.1) because as previously mentioned these two statistical indices are very sensitive to the magnitude and the order in which events occur (Moriasi et al., 2007).

Visual inspection of the hydrographs suggests that SWAT-ACZ and SWAT-OBS produced similar annual flow averages and inter-annual variability for the past 30 years. To validate this last point, return periods for annual and highest monthly spring flows were analyzed for each simulation using the Gumbel probability function developed for extreme values (Bedient et al., 2008). Akhtar et al. (2008) used this probability function on future hydrological outputs to study future peak discharge magnitudes and return period while Wang et al. (2006b) also used a similar function (Generalised Extreme Value) on maximum daily discharge to validate predicted stream flow, using RCM input against observed flows.

The analysis focused on high flows because they are of primary importance for NPS pollution transport. As shown in figure 4.2, the two simulations predicted total annual flow of a given magnitude with similar frequency, and the difference in magnitude for each return period between the simulations is within ±10% (Table D2). As for the four historical simulations, SWAT-ADC and SWAT-ACU show a fairly close agreement with SWAT-OBS, but for most return periods SWAT-AFA and SWAT-ARP systematically overestimate by about 50% the magnitude of annual flows. These results are consistent with those of the water budget, showing similar trends in the overestimation of precipitation and water yield. Results for the spring flood are presented within the section below.

For the four historical simulations, temporal mismatch is also due to global climate models internal variability. They do not simulate sequences of weather events as recorded by meteorological stations (Laprise, 2008; de Elia and Cote, 2009). Rather they simulate their own meteorology with statistics similar to observed climate which brings other discrepancies between the observed and simulated climate.

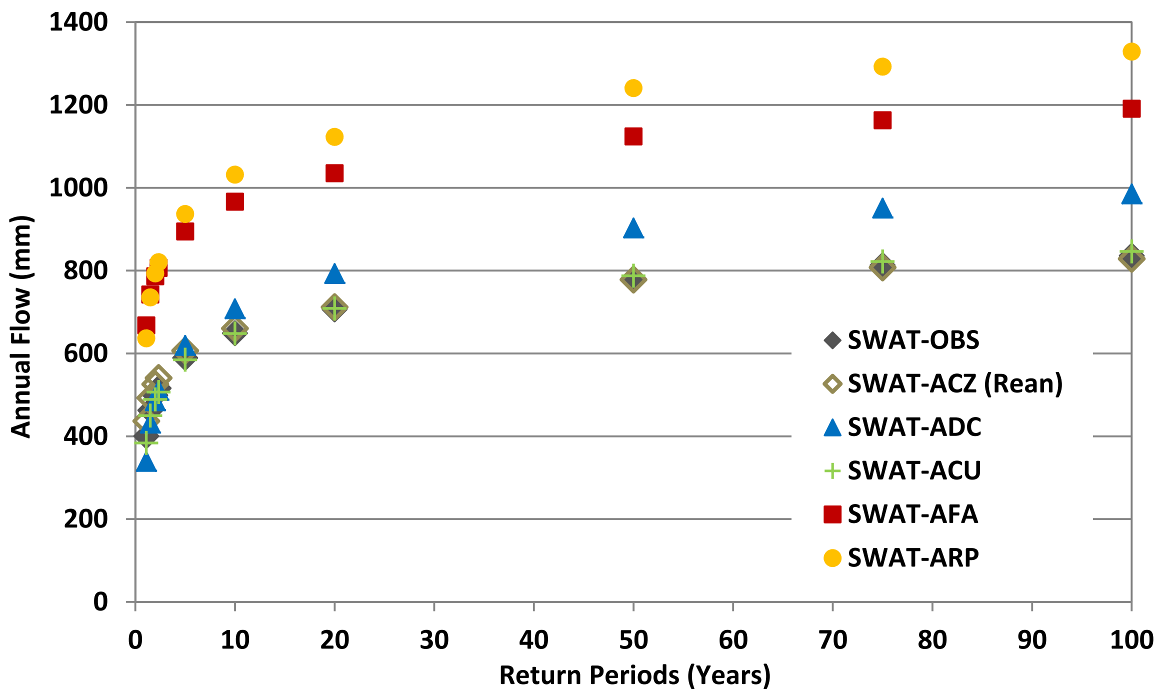

Figure 4.2: Return periods for annual flows predicted for the Period 1971-2000 for each historical simulation, as calculated with the Gumbel Probability Theory.

Seasonal and monthly stream flow

Other studies on the impact of climate change on snowmelt showed significant changes in the seasonal flow regimes (Minville et al., 2008; Quilbé et al., 2008; Minville et al., 2009; Boyer et al., 2010; Sulis et al., 2011). This could have implications for the future management of freshwater resources and runoff control (Bourque and Simonet, 2008). Moreover, Deslandes et al. (2007) found that 80% of sediment losses in the study subwatersheds occurred during the short, but very hydrologically-active periods of the spring and fall. Therefore, validation with the CRCM was also done on a monthly basis. Once again, the first results presented focused on the validation simulations SWAT-OBS and SWAT-ACZ, and then on the control simulations SWAT-ADC, SWAT-ACU, SWAT-AFA and SWAT-ARP reconstructed for the detection of hydrological change in the future.

A plot of average monthly stream flow at PR_{up} and at the outlet of the river for the period 1971-2000 (Figure 4.3) shows that SWAT-ACZ performs in similar manner to SWAT-OBS. And as the distance between PR_{up} and the outlet of the river is 18 km (24%

of the river length), it is reasonable to assume that SWAT-ACZ can also be used to simulate the hydrology of the entire basin. However, SWAT-ACZ did not match SWAT.OBS during the months of spring snowmelt months of March, April and May. SWAT-ACZ simulated shortened and delayed, but larger spring flood peaks. This is explained as follows. March mean daily temperatures produced by the CRCM were too low compared to the snowmelt temperature threshold established during the calibration of SWAT (Figure C2). Therefore, SWAT-ACZ underestimated snowmelt during March, shifting the snowmelt runoff to April and May, and simulated the overestimation of stream flows seen in April and May. Once again temperature biases of the climate model, and their effect on SWAT hydrology may be due to the spatial resolution of the CRCM.

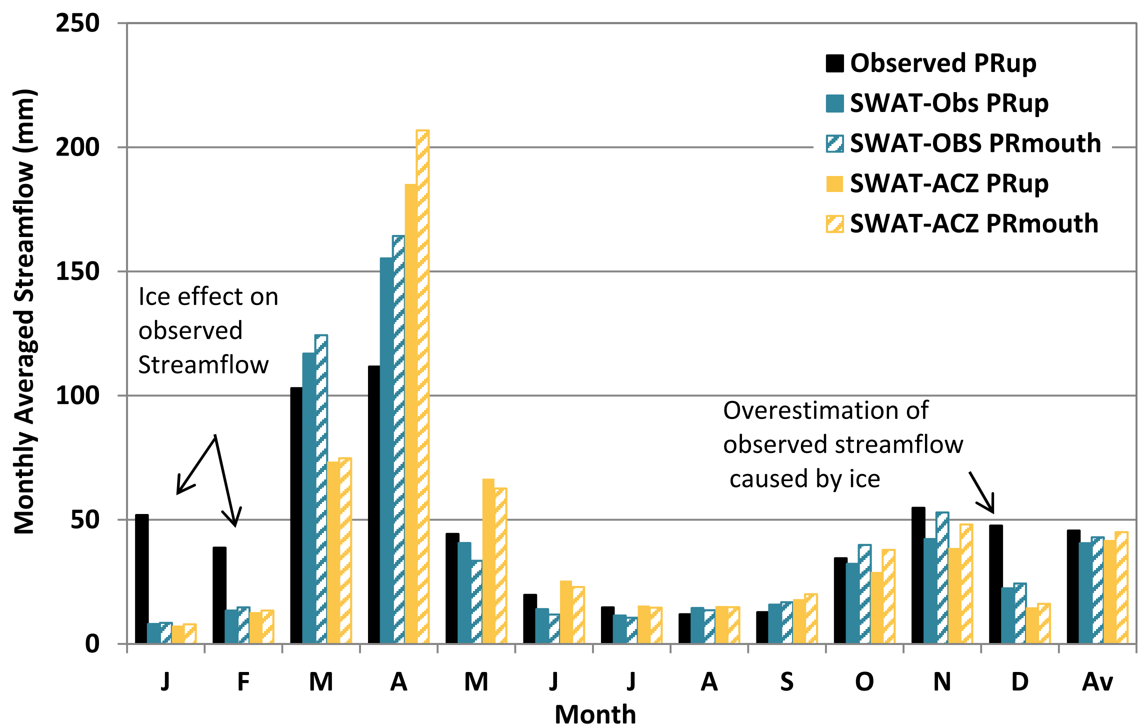

Figure 4.3: Long-term comparison of monthly observed and simulated averaged stream flow for the period 1971-2000, at the PR_{up} hydrological station and the Pike river outlet

These discrepancies also occurred in the three CRCM-historical simulations (SWAT-ADC, SWAT-ACU and SWAT-AFA of SWAT3) with some differences being attributable to biases introduced by the CGCM (Figure 4.11). Similarly, GCMs' systematic bias affected the four historical simulations by overestimating winter and summer flows. The comparison between observed and predicted temperature and precipitation series showed that all climate simulations used in the study overpredicted monthly precipitation in the summer (Figure C1). In the winter, precipitation values were underpredicted except for the SWAT-ARP simulation. Monthly mean temperatures were almost always underestimated except, again, for SWAT-ARP.

Biases of CRCM and CRCM nested in the CGCM have also been observed for other basins in Québec. Gagnon et al. (2009) compared observed temperature and precipitation to predictions from the CRCM4 driven by the same ERA 40 reanalysis over the Châteauguay and Chaudière watersheds (2530 and 6682 km^2, respectively). They found that bias for maximum temperature was not very strong for temperatures less than 1°C, but minimum temperatures were clearly underestimated by 2°C in winter and spring. Total precipitation was overestimated in winter, spring and summer by 11%, 35% and 30%, respectively.

Similarly, Minville et al. (2009), working on the 27 000 km^2 Peribonka watershed, found that the same combination of models (CGCM-CRCM) underestimated monthly maximum temperatures by up to 6°C in April and underestimated temperatures by up to 4°C in the summer and fall, and overestimated precipitation in the spring, summer and fall by 25%. These findings correspond roughly with the delayed and amplified occurrence of spring flow and summer flow overestimations, found in the present study.

In their studies, Minville et al. (2008; 2009) corrected bias before using the climate predictions for hydrological modelling. However in our case, changes in intensity and distribution of meteorological events were important for future assessment of NPS pollution and no available correction method existed at the time to capture these changes. Therefore results are interpreted by looking at differences rather than absolute values.

Despite the biases described above, the four reconstructed mean monthly stream flow (Figure 4.11) represent current conditions fairly well. Return periods for highest monthly flow in the spring are shown in figure 4.4. As with total annual flow, peak flows simulated by SWAT-ACZ match closely those simulated by SWAT-OBS. Differences between the simulations for each return period do not exceed ± 10% (Table D4). On the other hand, the four historical simulations either over- or under-estimated peak flows for all return periods (Figure 4.4). This is again related to systematic bias introduced by the GCMs.

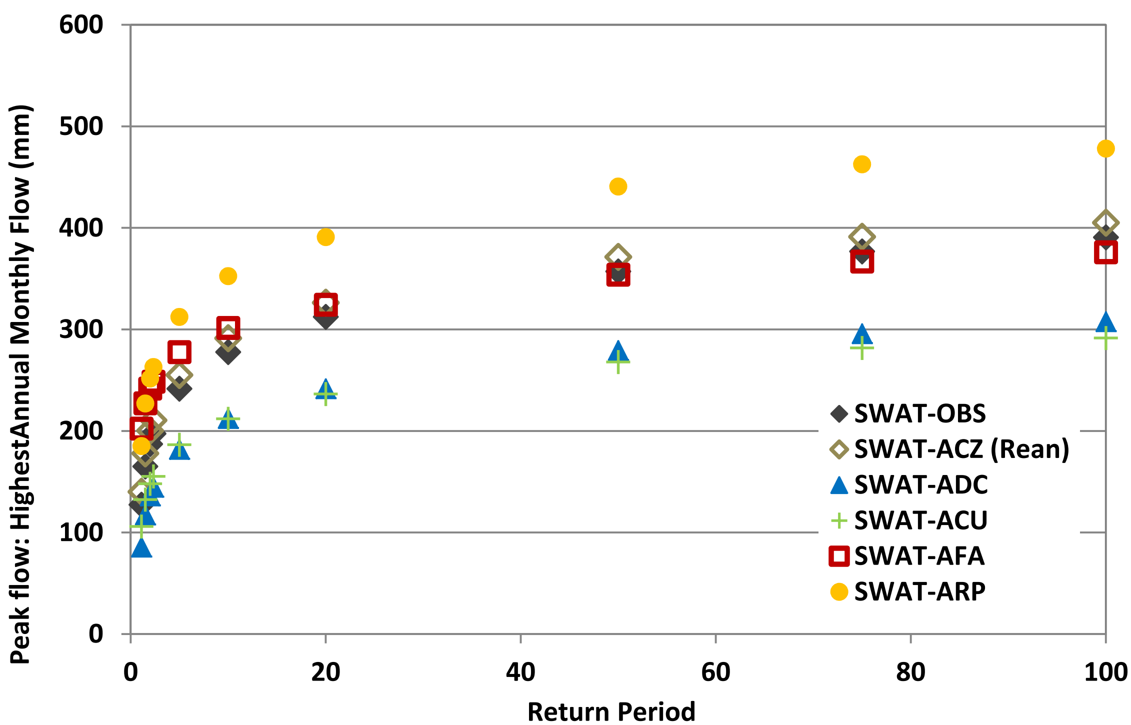

Figure 4.4: Return periods for highest monthly flow in spring for the period 1971-2000 for each historical simulation, as calculated with the Gumbel Probability Theory.

To summarize, SWAT and the CRCM reasonably reproduced inter-annual stream flow variability, flood frequency and average stream flows over 30 years. Therefore it is considered as a good tool for reproducing the current hydrological conditions of the basin. The historical simulations (SWAT3) of future predictions (SWAT4) did not differ much from current condition except for two simulations (SWAT-AFA, SWAT-ARP), which did not reproduce the annual water cycle very well. Likewise, interpretation of the results should be carried out cautiously for spring months as bias is introduced by the CRCM and GCM, due to the sensitivity of snowmelt to temperature (Jha et al., 2004). Moreover, the apparently good performance of seasonal and annual simulations is partly due to smoothing out of monthly results.

4.2 SWAT performance in simulating water quality

This section presents results on the calibration and validation of SWAT for sediment, total P and total N.

SWAT outputs for the three variables were first extracted from the model at the outlet of the two experimental watersheds, Wallbridge Creek upstream (WC_{up}) and Wallbridge Creek downstream (WB_{dw}) and were compared on a monthly basis to water quality data collected by IRDA between November 2001 and April 2003 (calibration period) and November 2004 and April 2006 (validation period). The calibration parameters were then transferred to the respective upstream and downstream sections of the entire watershed. Predicted sediments and P loads were compared to estimated loads from the Pike River water quality station, as described in section 3.2.2.

As for the calibration of hydrology, because the present study focuses primarily on climate change, only a sample of the graphical results is presented; specifically those for the downstream subwatershed (closer to the outlet of the river). Results for the upstream subwatershed can be found in Appendix B.

4.2.1 Hydrology of the two experimental subwatersheds

As previously mentioned, the two experimental subwatersheds were calibrated and validated for hydrology parameters in order to provide a basis for water quality calibration. Calibration results were deemed satisfactory to very satisfactory, but the model performed somewhat poorly during the validation process, probably due to the very different climate conditions that prevailed during this period (Section 4.1.1). Nonetheless, the annual water cycles were well reproduced for both subwatersheds, as well as the timing of events on a daily basis (Appendix B). Similar to the case with predicted stream flow, the magnitude of some particularly high flows was difficult to reproduce. For an appreciation of the goodness of fit between predicted and measured stream flow on a monthly basis, observed and predicted flows are displayed along with water quality data (downstream: Figures 4.5, 4.6 and 4.7; upstream: Figure B4).

4.2.2 Sediments

Table 4.3 presents measured and predicted sediment loads before and after calibration for the two evaluation periods and for each of the experimental subwatersheds. Table 4.4 presents the three coefficients of performance and absolute errors (AE) for the same. Calibration improved total sediment load predictions for WC_{up} from 0.01 Mg ha^{-1} to 0.22 Mg ha^{-1} over the calibration period and from 0.01 Mg ha^{-1} to 0.45 Mg ha^{-1} over the validation period, reducing errors from -96% (-0.21 Mg ha^{-1}) to -3% (-7.0 kg ha^{-1}) and from -96% (-0.32 Mg ha^{-1}) to 38 % (0.12 Mg ha^{-1}), respectively. Similar results were obtained for WC_{dw} with final predicted loads of 0.44 Mg ha^{-1} over the calibration period and 0.54 Mg ha^{-1} during the validation periods reducing the percentage errors from -98% (-0.52 Mg ha^{-1}) to -18% (-0.09 Mg ha^{-1}) and from -98% (-0.63 Mg ha^{-1}) to -16 % (-0.11 Mg ha^{-1}).

Table 4.3: Comparison of measured and predicted sediment loadings (Mg ha^{-1}) for the calibration and validation period

	Period of calibration - 2001-2003			Period of validation - 2004-2006		
Water quality station	Measured data	Before calibration	After calibration	Measured data	Before calibration	After calibration
WC_{up}	0.22	0.01	0.22	0.33	0.01	0.45
WC_{dw}	0.53	0.01	0.44	0.64	0.01	0.54

These percentage errors indicate the average tendency of the model to over or underestimate measured data. According to Moriasi et al. (2007) and Engel et al. (2007) these values lie within an acceptable range, with a performance rating ranging from good (15% ≤|PBIAS| ≤ 30%) for WC_{up} during the validation period to very good for all others(|PBIAS| ≤ 15%).

Table 4.4: Coefficients of performance for SWAT predicted sediment loadings

		Period of calibration		Period of validation	
Water Quality Station	Performance statistic	Before calibration	After calibration	Before calibration	After calibration
WC_{up}	R^2	0.59	0.70	0.16	0.48
	NSE	-0.5	0.64	-0.8	-0.31
	PBIAS (%)	-96	-3	-96	38
	AE*	-157.7 (-0.21)	-5.1 (-0.007)	-233.1 (-0.32)	91.3 (0.12)
WC_{dw}	R^2	0.54	0.59	0.09	0.46
	NSE	-1.19	0.44	-0.74	0.43
	PBIAS (%)	-98	-18	-98	-16
	AE*	-390 (-0.52)	-70.8 (-0.09)	-473.5 (-0.63)	- 79.1 (-0.11)

*AE: Absolute error in Mg or (Mg ha^{-1})

Engel et al. (2007) deemed an R^2≥0.6 to be acceptable, while Moriasi et al. (2007) set the threshold at 0.5. After calibration, R^2 values improved substantially, but for the validation period they remained close to, but below 0.5 for both subwatersheds.

Typically, NSE values superior to zero are viewed as acceptable (Moriasi et al., 2007). However Engel et al. (2007) and Moriasi et al. (2007) set their acceptability threshold at 0.6 and 0.5, respectively. Similar to R^2, all values of NSE improved substantially. Nonetheless, only the predicted loadings at WC_{up} presented a good fit (NS = 0.64) for the calibration period. The performance for the validation dropped substantially to $^-$0.31. On the other hand, the NS values of 0.44 and 0.43 for WC_{dw} corresponded to an acceptable if not strong fit for both calibration and validation periods, respectively (Eastman, 2007).

Goodness of fit between predicted and observed sediment loads for the calibration and validation of the WC_{dw} subwatershed can be viewed graphically (Figures 4.5 a, b, respectively) while that for the WC_{up} subwatershed is shown in figure B4. Typically predictions underestimated loadings during the spring snowmelt season and overestimated them in the winter.

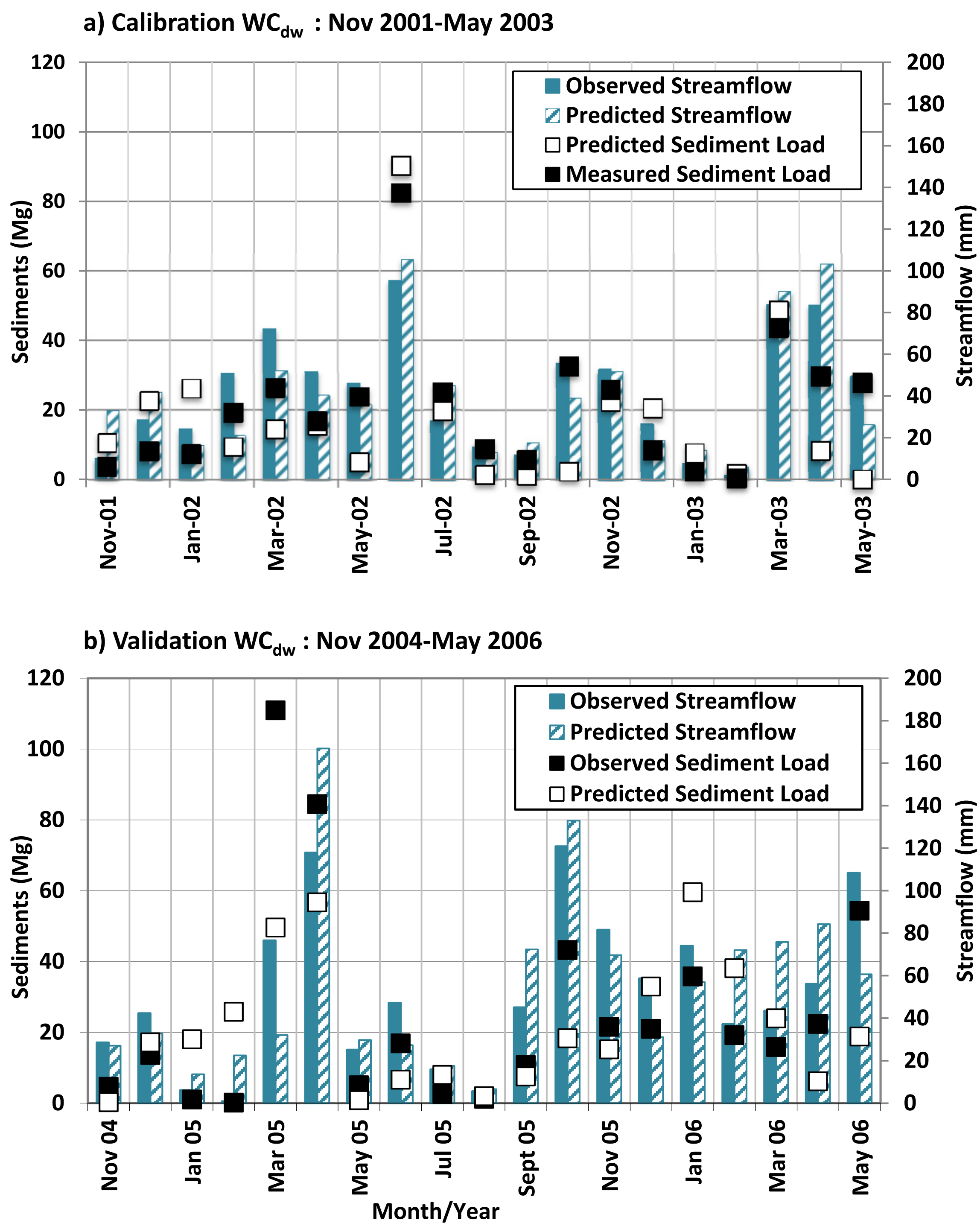

Figure 4.5 : Comparison of observed and predicted sediment yield at the outlet of the downstream Wallbridge creek (WC_{dw}) subwatershed for the model (a) calibration and (b) validation.

With the exception of a few months (April 2003; October 2005; December, January and April 2006) predicted sediment loads generally followed measured trends and also mimicked stream flow with minor over- and under-estimations for both subwatersheds and evaluation periods.

Figure 4.6 shows how sediment loads measured near the river outlet compare with SWAT predicted loads in the long term. As already mentioned the original data were very sparse (four grab samples per year, sometimes none) and stream flow was not simultaneously monitored. These data are therefore of rather poor accuracy and are used here only to provide a rough overview of historical sediment loads. The R^2 and NS values do not satisfy criteria of acceptability. However, the deviation (PBIAS) indicates the model overestimates long term sediment prediction by 55%. This lies at the extreme lower limit of the satisfactory range of Moriasi et al. (2005).

The overestimation of sediment loads mainly occurred in March. Figure 4.6 shows that predicted and estimated sediment loads differ substantially for this month. This is at the beginning of the snowmelt season, when sediment and nutrient losses are at their highest in the region (Jamieson et al., 2003; Deslandes et al., 2007). Two facts may explain this phenomenon: (i) between 1980 and 2000, grab samples were rarely taken during the snowmelt season, leading to a possible important underestimation of loads, and (ii) SWAT overpredicts its loads because land-use and field operations management used for the entire period were set to those of the year 2000, reflecting intensive agricultural practices not in place during the beginning of the simulation.

Nonetheless, sediment load predictions follow seasonal and annual variability as well as stream flow predictions, indicating that the model reproduces erosion processes reasonably.

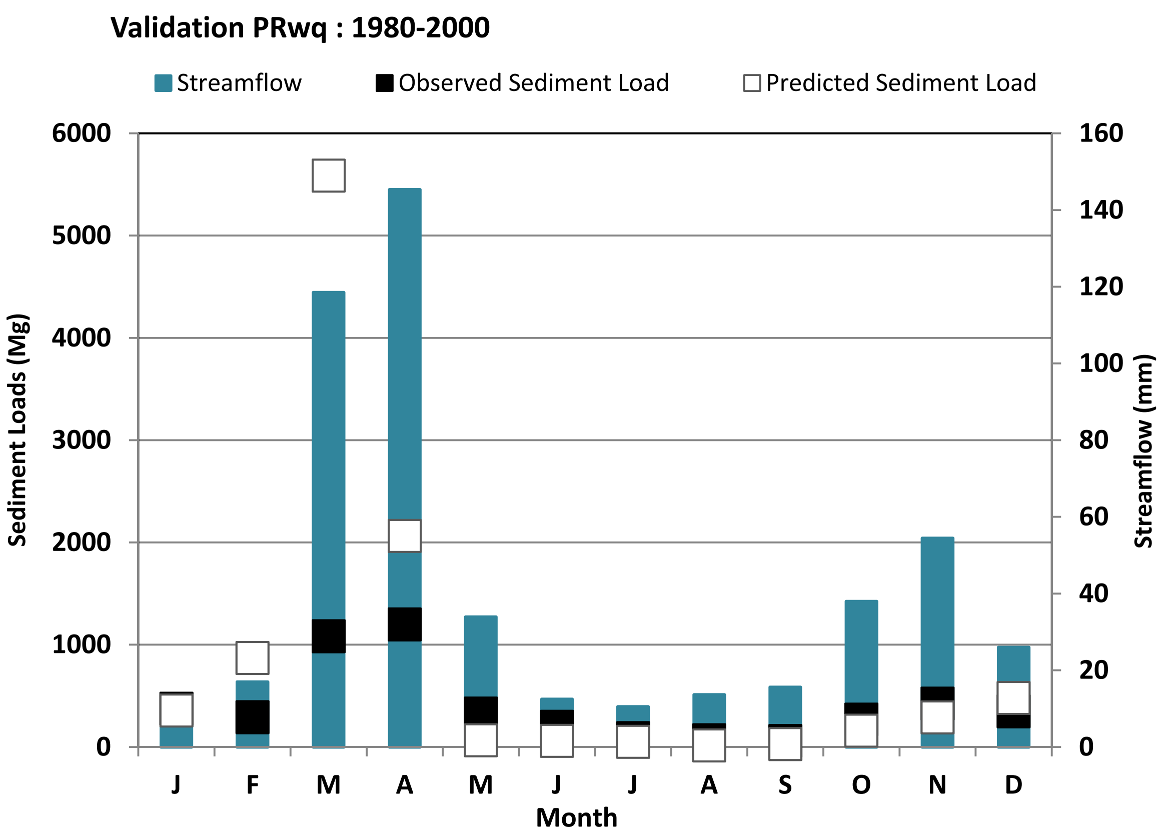

Figure 4.6: Comparison of observed and predicted sediment yield at the downstream water quality (PR_{wq}) station on the Pike river for the long term validation

Table 4.5: SWAT coefficients of performance for the long term validation (1980-2000) of sediment and total P loadings.

	Station: PRwq			
	R^2	NSE	PBIAS	Absolute Error
Sediments	0.44	-2.8	55	1.35 (Mg ha^{-1}) or 0.18 (Mg ha^{-1}yr^{-1})
Total P	0.52	-0.67	42	4.99 (kgha^{-1}) or 0.81 (kgha^{-1}yr^{-1})

4.2.3 Phosphorus

SWAT P outputs in the streams consisted of ORGP_OUT (organic phosphorus transported with water out of the reach in kg) and MINP_OUT (mineral phosphorus transported out of the reach in kg). After calibration, P load predictions were also significantly improved for both evaluation periods (Tables 4.6, 4.7). However, similar to sediment loadings only predictions during the calibration period met the acceptability criteria proposed within the literature (Engel et al., 2007 and Moriasi et al., 2007). With, values of $R^2 \geq 0.53$, NSE ≥ 0.6 and $|PBIAS| \leq 15\%$, model performance during calibration can be considered as good to very good. Despite the fact that for the validation phase R^2 and NSE values indicate a rather poor fit between measured and predicted P loads, mean loads over the period of evaluation remain within the acceptable limits of prediction ($|PBIAS| \leq 25$ %).

SWAT provides also P outputs at the HRU level. These are ORGP (Organic P contributed by HRU to reach), SEDP (Mineral P attached to sediments contributed by HRU to reach), SOLP (Soluble P contributed by HRU in surface runoff) and P_GW (Soluble P contributed by HRU in groundwater). During the period 2001 to 2003, Michaud et al. (2008) measured that 25% of total P losses occurred in the soluble form for the downstream Wallbridge subwatershed. For the upstream subwatershed, this percentage was 42%. Predictions at the HRU levels were summed for subwatersheds. For the upstream subwatershed, the partition between particulate (SEDP and ORGP) and soluble forms (SOLP and P_GW) was generally well reproduced as SOLP and P_GW accounted for 38% of the total (SOLP+P_GW+ORGP+SEDP) for the period 2001-2003 and for 45% for 2004-2006. However, predictions for the downstream subwatershed were overestimated as soluble P forms accounted for 39% of total P for 2001-2003 and 45% for 2004-2006.

Difference between TP (ORGP_OUT+MINP_OUT) and SOLP+P_GW+ORGP+SEDP is that TP is values at the outlet of the river or the reach, while the other is P coming from

HRU. Processes occurring within the reach are therefore not included in the sum SOLP+P_GW+ORGP+SEDP.

Table 4.6: Comparison of measured and predicted total P loadings (kg ha^{-1}) for the calibration and validation period

	Period of calibration - 2001-2003			Period of validation - 2004-2006		
Water Quality Station	Measured data	Before calibration	After calibration	Measured data	Before calibration	After calibration
WC_{up}	1.05	8.84	0.89	1.30	8.78	1.59
WC_{dw}	1.32	10.58	1.34	1.75	10.71	1.9

Table 4.7: Coefficients of performance for SWAT predicted P loadings

		Period of calibration		Period of validation	
Station	Indices	Before calibration	After calibration	Before calibration	After calibration
WC_{up}	R^2	0.58	0.75	0.24	0.14
	NS	-73	0.71	-59	-0.26
	Dev (%)	741	-16	573	22
	AE*	5 728 (7.78)	-121 (-0.16)	5 497 (7.47)	210 (0.29)
WC_{dw}	R^2	0.53	0.67	0.1	0.35
	NS	-1.19	0.61	-45	0.32
	Dev (%)	6.98	1	513	9
	AE*	6 963 (9.25)	9.79 (0.01)	6 745 (8.97)	118 (0.16)

*AE: Absolute error in kg or (hg ha^{-1}).

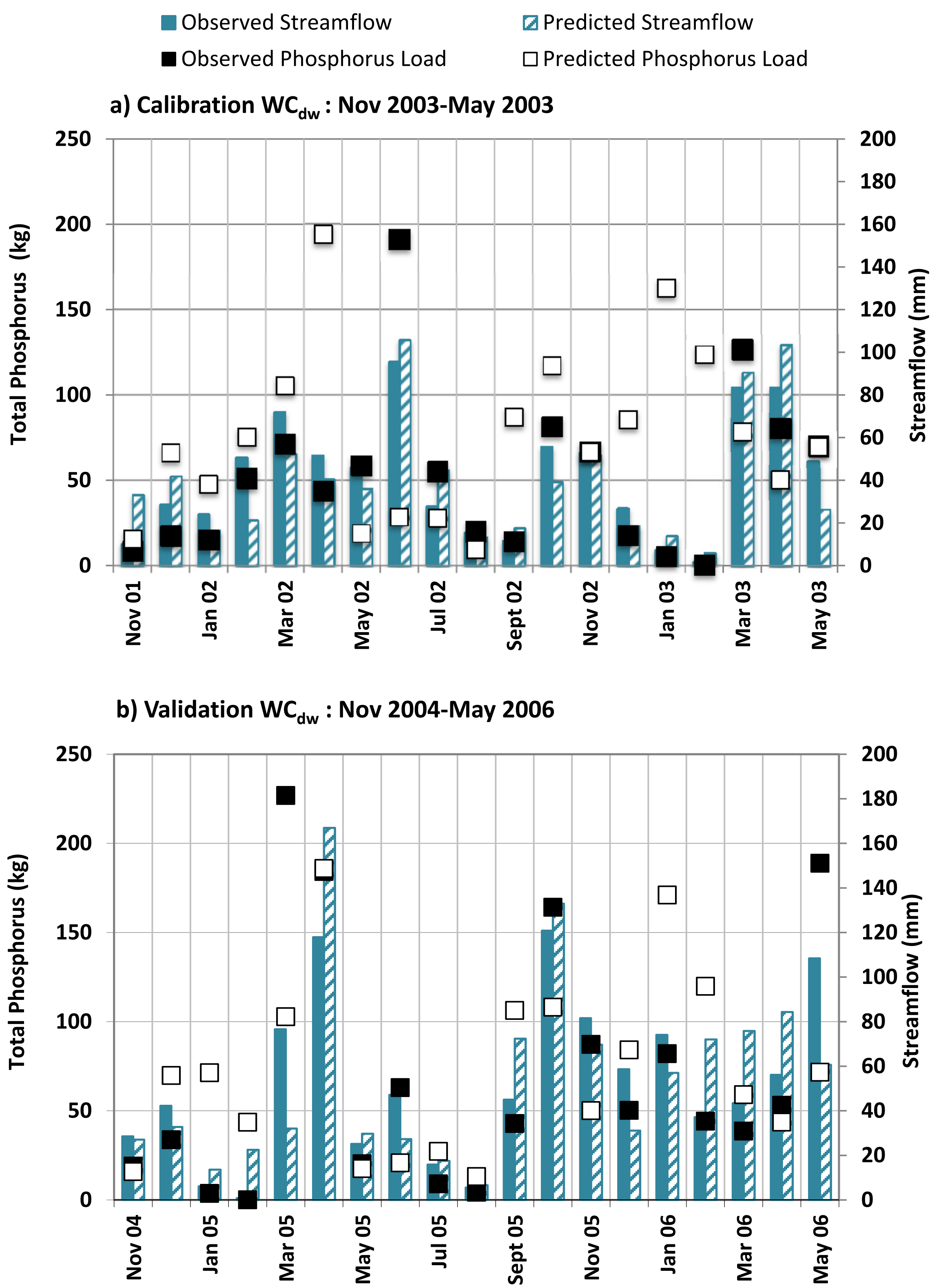

Figure 4.7: Comparison of observed and predicted phosphorus loadings at the outlet of the downstream Wallbridge creek subwatershed (WC_{dw}) for the (a) calibration and (b) validation periods.

The overestimation of predicted P loads during January-March is probably due to the overestimation of soluble P since stream flow and sediments are for their part better predicted. This might be due to the attribution of too high a value to the parameter GW_P which set a concentration of soluble P in groundwater for the entire year.

For the long term evaluation, results similar to those for sediment loads were obtained. While seasonal cycles and inter-annual variability were rather well reproduced (Figure 4.8), P was overestimated in March, thus lowering the overall R^2 and NSE values to less than acceptable values (Table 4.7). Once again, this overestimation might come from the inaccuracy of measured data and from fertilizer applications being much higher during the first decade of the simulations. Statistiques Canada (2008) presented tables from the agricultural census of 2001 and 2006 showing an increase in cattle and poultry production in the region. These increases suggest that manure application on fields increased between these two periods as probably also during the preceding and subsequent years. Although tillage and fertilization are generally done in late May, March loads can be explained by applications in the previous fall being stored in the topsoil over the winter, or P-saturated soils being eroded during snowmelt.

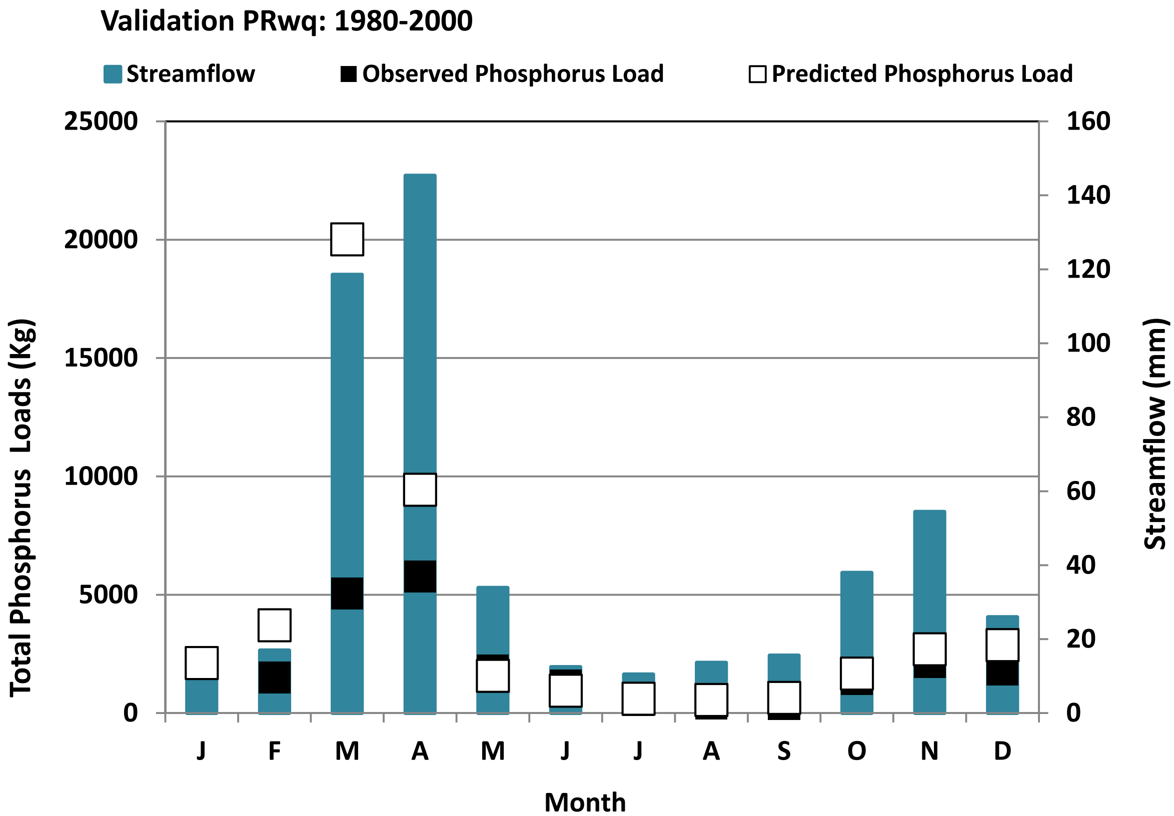

Figure 4.8: Comparison of observed and predicted phosphorus loadings at the downstream water quality (PR_{wq}) station on the Pike river for the long term validation.

4.2.4 Nitrogen

SWAT nitrogen output consists of ORGN_OUT (organic nitrogen transported with water out of the reach in kg), NO3_OUT (nitrate), NH4_OUT (ammonium), and NO2_OUT (nitrite). Measured and predicted loads of total N for the two experimental subwatersheds are presented in table 4.8. Once again predictions after calibration were much more accurate for both subwatersheds, with an excellent performance rating during the calibration period but a poor one for the validation period because of poor fit between measured and predicted loads (Table 4.9).

Figure 4.9 and figure B6 illustrate the goodness of fit between measured and predicted loads. Total N predictions were closely linked to stream flow, with common deviations from measured data.

Table 4.8: Comparison of measured and predicted total nitrogen loadings (kg ha^{-1}) for the calibration and validation periods

	Period of calibration -2001-2003			Period of validation-2004-2006		
Water Quality Station	Measured data	Before calibration	After calibration	Measured data	Before calibration	After calibration
WC_{up}	62.35	69.51	58.86	62.44	73.75	71
WC_{dw}	51.25	84.32	46.19	45.43	93.58	59.17

Table 4.9: Coefficients of performance for SWAT predicted total nitrogen loadings

TN (Total nitrate)		Period of calibration		Period of validation	
Water Quality Station		Before Calibration	After Calibration	Before Calibration	After Calibration
WC_{up}	R^2	0.26	0.78	0.04	0.68
	NSE	-0.64	0.69	-0.43	-0.42
	PBIAS (%)	11	-6	18	14
	AE*	5 265 (7.15)	-2 530 (-3.49)	8 321 (11.31)	6 302 (8.57)
WC_{dw}	R^2	0.34	0.74	0.09	0.37
	NSE	-2.58	0.68	-2.73	-0.53
	PBIAS (%)	65	-10	1	30
	AE*	24 885 (33)	-3 820 (-5.08)	8 321 (48.15)	10 343 (13.15)

*AE: Absolute error in kg or (kg ha^{-1}).

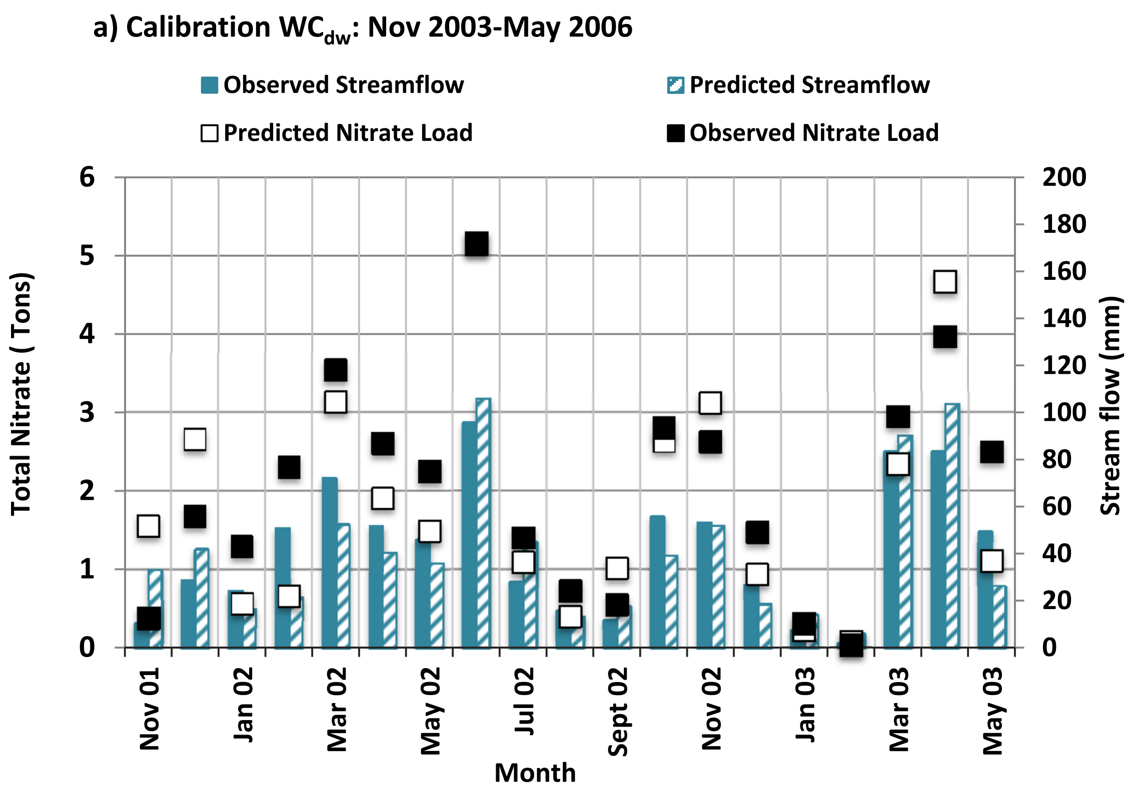

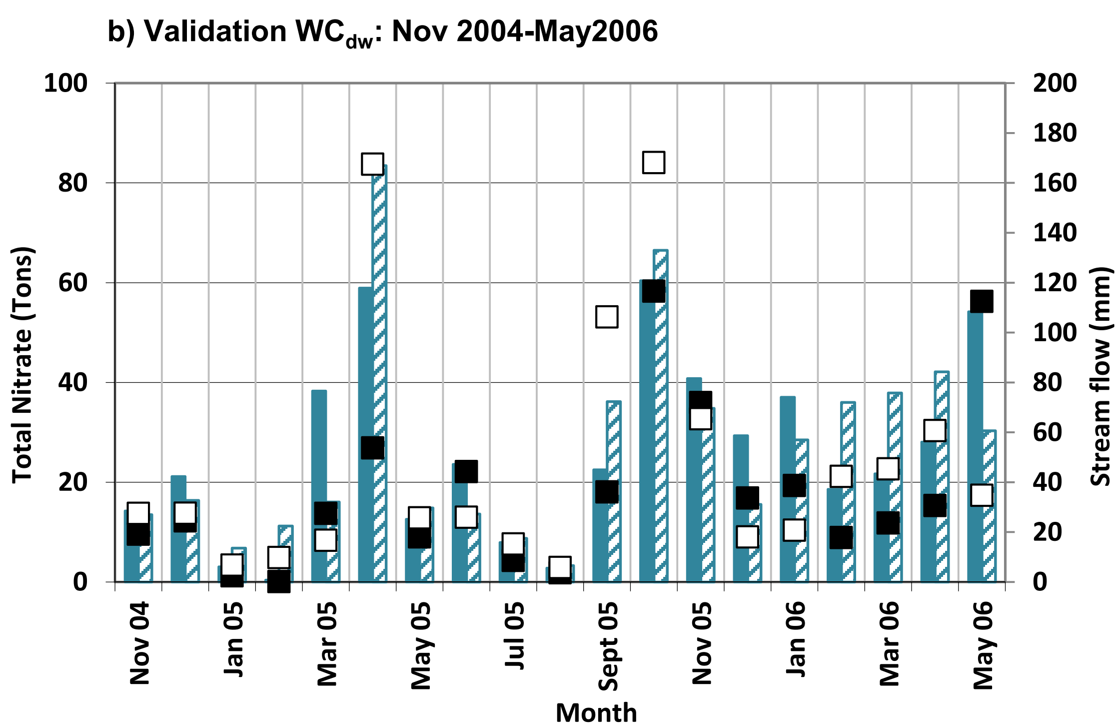

Figure 4.9 : Comparison of observed and predicted N loadings at the outlet of the downstream Wallbridge creek subwatershed (WCdw) for the (a) calibration and (b) validation.

4.2.5 SWAT performance with climate data from the CRCM

Figure 4.10 a, b and c shows how bias from climate models, resulting from natural variability and spatial resolution, influence predictions in sediment and nutrient loads. Previous results were presented in absolute terms to get an idea of the magnitude of nutrient loads generated by the subwatersheds or the whole watershed. However further results will be presented as a specific load (mass/ha) because this measure is more commonly used and therefore better understood.

As previous sections indicate, historical long-term loading predictions are uncertain. Therefore, validating the predicted sediment, P and N obtained with SWAT and the climate projections would not allow a more accurate interpretation of the final simulations. However, as shown in graphs 4.10, biases resulting from both the CRCM and GCM projections significantly influence SWAT projections, especially during the spring season. Large uncertainties are therefore present.

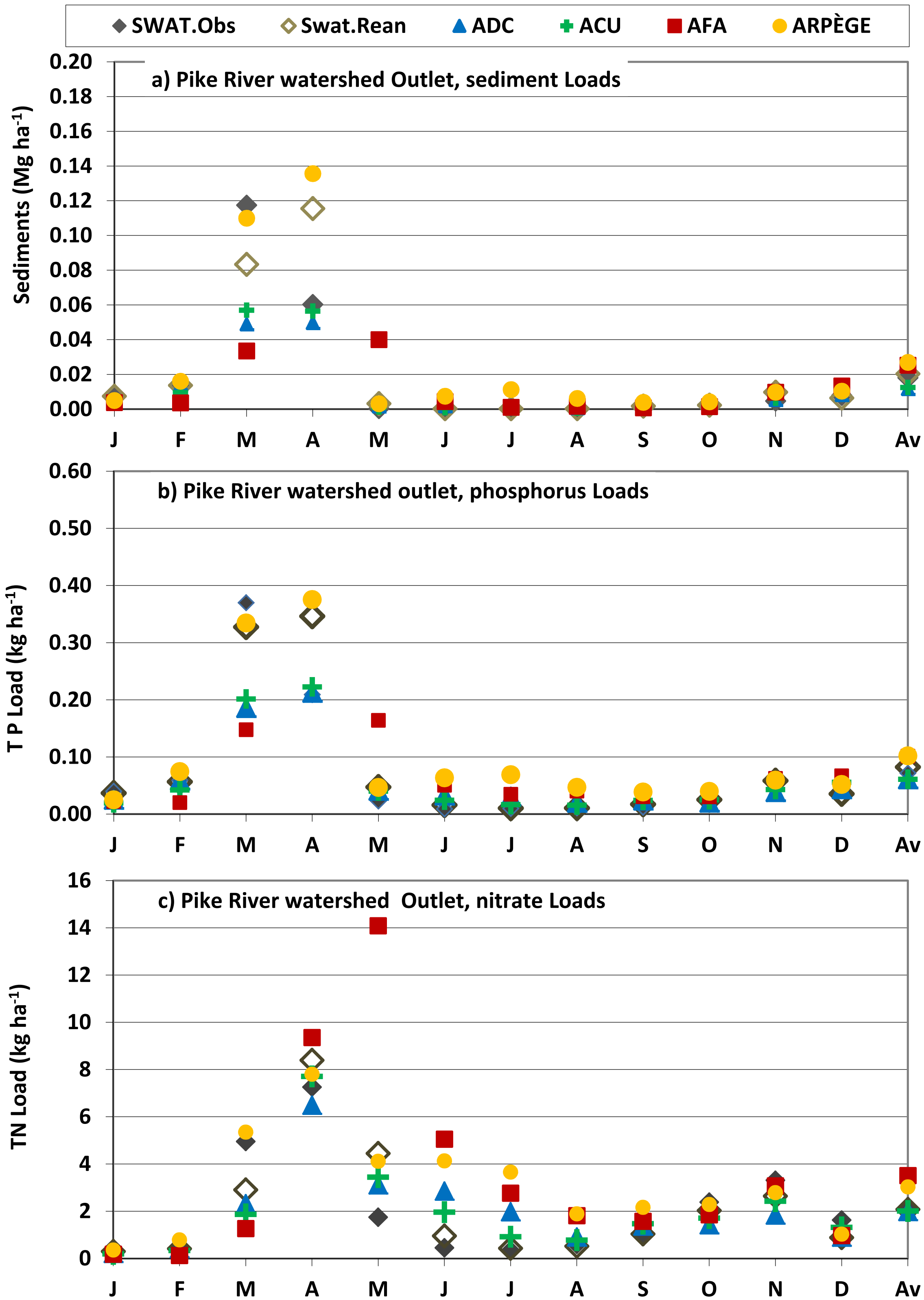

Figure 4.10: Comparison of specific loads predicted over the historical period (1971-2000) with observed and simulated climate at the outlet of the watershed (63 360 ha)

4.3 Potential hydrologic changes caused by a warming climate

4.3.1 Annual changes in the hydrologic cycle

Table 4.10 presents annual changes for the main components of the hydrologic cycle simulated between 2041-2070 and the historical period 1971-2000. Changes in mean annual values remained below 12% for all components, except snowfall and surface runoff. Snowfall, because of its high sensitivity to the increase in temperature, shows marked decreases of -8%, -12%, -14% and -25% (SWAT.ARP, SWAT.AFD, SWAT.ADC, SWAT.ACU, respectively) which corresponded to decreases of between 25 mm and 54 mm in snow-water equivalent. Increase in precipitation led to an increase in annual stream flow of between 37 mm and 98 mm (7 and 11%) but only one simulation was significantly different (SWAT.AFD).

Water yield represents the total runoff (surface and subsurface flow contributing to the river) and is therefore almost equivalent to stream flow. The small differences can be attributed to river evaporation or transmission losses of water through the bed of the river (Neitsch et al., 2004). Overall, an increase in evapotranspiration partly compensates for the increase in precipitation, which explains the absence of significant changes in stream flow or water yield. The four simulations generally agreed with each other, except in terms of the allocation of water to surface runoff versus groundwater. Two simulations (SWAT.ADC and SWAT.ARP) indicated that almost no change occurred in mean surface runoff, whereas one (SWAT.ACU) predicted a decrease of 17% (27 mm), and another (SWAT.AFD) predicted an increase of 8% (17 mm).

The components of the water cycle remained in the same proportions as in the historical historical simulations: 30% to 55% of precipitation still left the watershed by evapotranspiration, while water yield accounted for 42% to 65% of the hydrologic budget (Table 4.10 vs table 4.2 for historical simulations). These results demonstrate that more water is circulating through the hydrological cycle components as also simulated also by Jha et al. (2004). According to these authors, this testifies to the intensification of hydrological processes as Huntington (2006) has begun to notice on the global scale for the 20th and 21st century.

Our results coincide also with those of Boyer et al. (2010) who analyzed the future impact of climate change on the hydrological regime of the main Saint-Lawrence River tributaries by examining how several “hydroclimatic” indices such as the ratio between snowfall and precipitation (S/P) might evolve in the future. They predicted the winter-spring S/P ratio to decrease from 35% before 1980, to 20% between 2040 and 2070, over the Richelieu River watershed. The Richelieu River is an important tributary which flows from Lake Champlain to the southern shore of the Saint-Lawrence. It is located relatively close to the Pike River watershed, and therefore provides a good comparison. Within the Pike River watershed this ratio decreased also by about 15% for all simulations (Table 4.11). Boyer et al. (2010) also found that mean annual changes in stream flow were lesser than 15%, with most simulations predicting an increase, except one driven by the German GCM ECHAM4, which predicted a decrease of 12% for the Richelieu River.

Minville et al. (2008; 2009) and Quilbé et al. (2008), who analysed the impact of climate change further north, in the Peribonka and Chaudière watersheds, also found similar results. Mean annual inflows predicted with several downscaled GCMs (including CGCM3) were statistically significant for three time horizons 2020, 2050 and 2080, and for both SRES scenarios A2 and B2. Minville et al. (2008) showed the increases to be between 5% and 15% for the 2050 horizon depending on the GCM used. Only ECHAM4 showed a decrease which was not always significant in either study.

Table 4.10 : Mean annual changes in the main components of the hydrologic cycle in absolute (future – historical period : ΔF-C) and percentage (Δ%) values compared to the historical period (C). Greyed cases indicate statistically significant changes for stream flow (paired t-test, $P \leq 0.05$). Δ% = 100× [(F-C)/C]

	Simulations	Stream flow (mm)			PCP (mm)			ET (mm)			WYLD (mm)			RnQ (mm)			Snowfall (mm)		
		F	ΔF-C	Δ%	F	ΔF-C	Δ%	F	ΔF-C	Δ%	F	ΔF-C	Δ%	F	ΔF-C	Δ%	F	ΔF-C	Δ%
Mean **Annual** Values for 30 years	ADC	571	61	**12**	1350	111	**9**	728	66	**10**	583	63	**12**	141	-4	**-3**	174	-28	**-14**
	(% of pcp or *Wyld)							(54%)			(43%)			*(24%)			(13%)		
	ACU	543	37	**7**	1316	89	**7**	723	63	**9.5**	554	38	**7**	128	-27	**-17**	157	-54	**-26**
	(% of pcp or *Wyld)							(55%)			(42%)			*(23%)			(12%)		
	AFA/AFD	894	89	**11**	1399	132	**10**	467	50	**12**	909	89	**11**	235	17	**8**	263	-37	**-12**
	(% of pcp or *Wyld)							(33%)			(65%)			*(26%)			(19%)		
	ARP	893	74	**9**	1569	93	**6**	621	27	**4.5**	909	75	**9**	208	2	**1**	285	-25	**-8**
	(% of pcp or *Wyld)							(40%)			(58%)			*(23%)			(18%)		

Explanation of abbreviations in the table: Pcp: Precipitation; Wyld: Wateryield ; ET: Evapotranspiration ; RnQ: Surface runoff .

Table 4.11: Spring winter snowfall/precipitation ratio for historical and future simulations

Simulations	Current and historical simulations: 2071-2000			Future simulations: 2041-2070			
	Snowfall (mm)	Winter/Spring precipitation (mm)	Ratio (mm)	Snowfall (mm)	Winter/Spring precipitation (mm)	Ratio (mm)	Ratio difference (%)
ADC	202	467	0.43	174	580	0.3	-13 %
ACU	211	476	0.44	157	557	0.28	-16 %
AFA/AFD	300	533	0.56	263	645	0.41	-15 %
ARP	310	620	0.50	285	708	0.40	-10%

4.3.2 Seasonal changes in stream flow

Figure 4.11 compares predicted hydrographs of future monthly stream flow to their corresponding historical ones, while figure 4.12 illustrates how the components of the hydrologic cycle can change on a seasonal scale. The impact of the four climate projections on hydrological processes varies. Differences and similarities between the results are seasonal.

Figure 4.11 shows that all projections predicted significantly more pronounced changes in stream flow during the winter and at the beginning of the spring than on an annual basis, or for the fall or summer. Spring flooding rose faster in March and lasted longer for all projections, but results were mixed with regard to the direction of changes in peak flow in April. Two projections predicted a decrease in the peak flow, with only one being significant, while the two other projections did not predict any changes. Similarly, the recession of peak flow in May was faster for two projections with stream flow falling well below current conditions (ACU and AFA), whereas spring peak recession of the two other projections (ADC and ARP) appears to remain constant between the future and historical periods.

For summer, results were mixed; two projections predicted a significant decrease in stream flow for the months of June and July (ADC) or August (AFA) whereas the two other projections did not predict any change. Fall did not seem to experience significant changes except for one simulation in November at the end of the season.

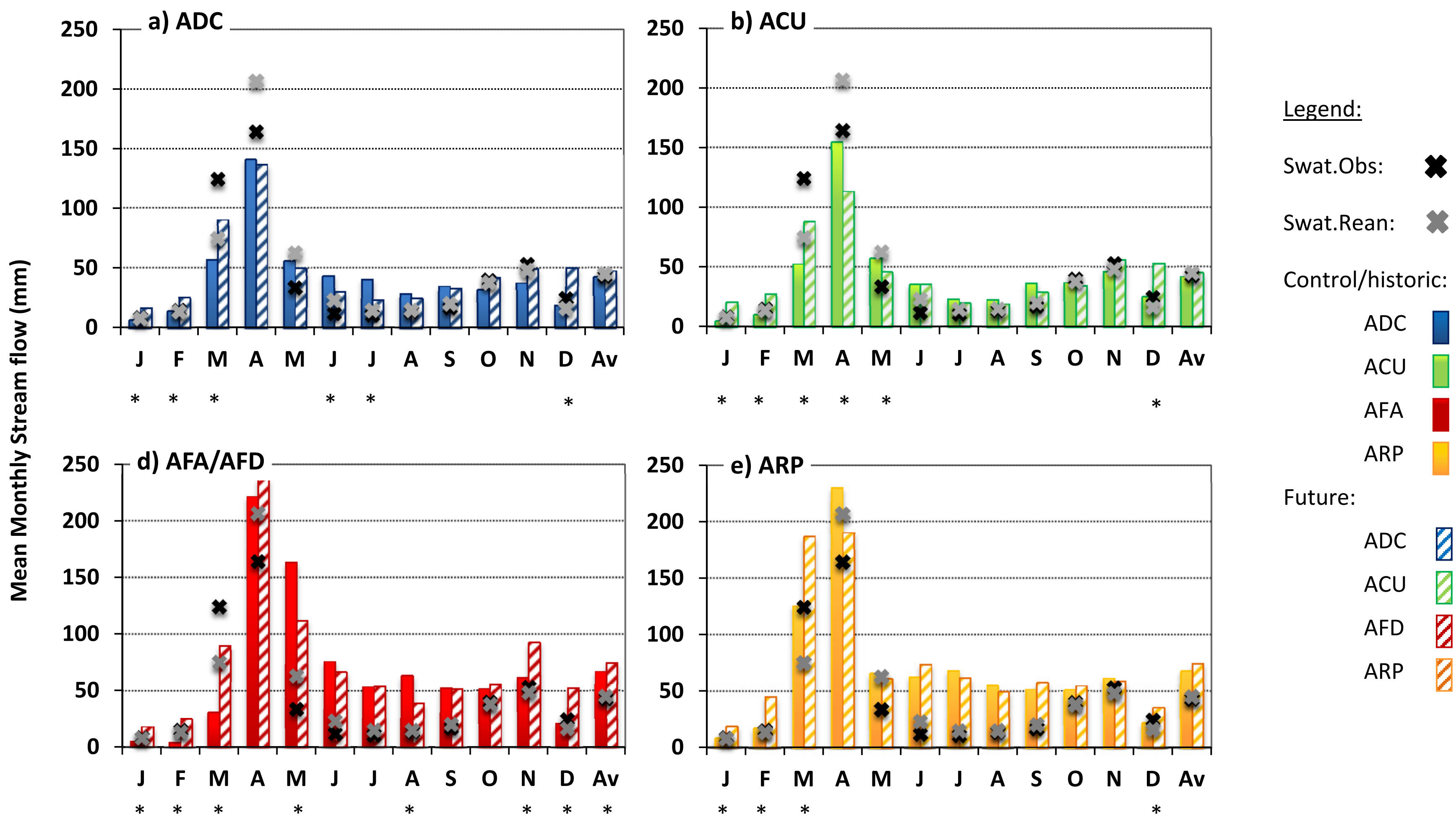

Figure 4.11: Mean annual stream flow simulated with observed climate and the nine datasets produced by the CRCM and VRGCM Arpège, for the current (historical) (1971-2000) and future climates (2041-2070). * indicate significant changes (Paired *t*-test, $P \leq 0.05$).

Despite discrepancies between the simulations, a common pattern can be observed with similar studies performed in other Québec watersheds (Minville et al., 2008; Boyer et al., 2010). For example, Minville et al. (2008) summarized these trends as an increase in winter flow, an earlier spring flood, and a decrease in summer-fall flow.

These changes are mostly attributable to higher precipitation but also to higher temperatures in winter which increase liquid precipitation and snowmelt episodes and reduce the storage of water in the snowpack. Similarly, the early onset of spring flooding is a result of an increase in the daily mean temperatures of the month of March. The temperatures often exceed the snowfall/melt temperature, and trigger earlier snowmelt runoff. The decrease of spring peak flow is a direct result of winter changes which shift spring snowmelt runoff from April to the earlier winter months. Decreases in summer stream flows are generally explained by the higher evapotranspiration which results from an increase in temperature and a decrease in rainfall.

This also most likely explains simulated changes for stream flow in the Pike River watershed. The influence of the four projected climates on the watershed's hydrological processes occurred through changes to the main components of the water cycle (Figure 4.12).

4.3.3 Seasonal changes within the hydrologic cycle

Differences between the historical and future period for 30-year mean precipitation (PCP), evapotranspiration (AET), water yield or total runoff (WYLD), surface runoff (RnQ), subsurface flow (SubSQ), and temperatures (Temp in °C) are presented in figure 4.12. Paired *t*-tests were also performed on the water yield.

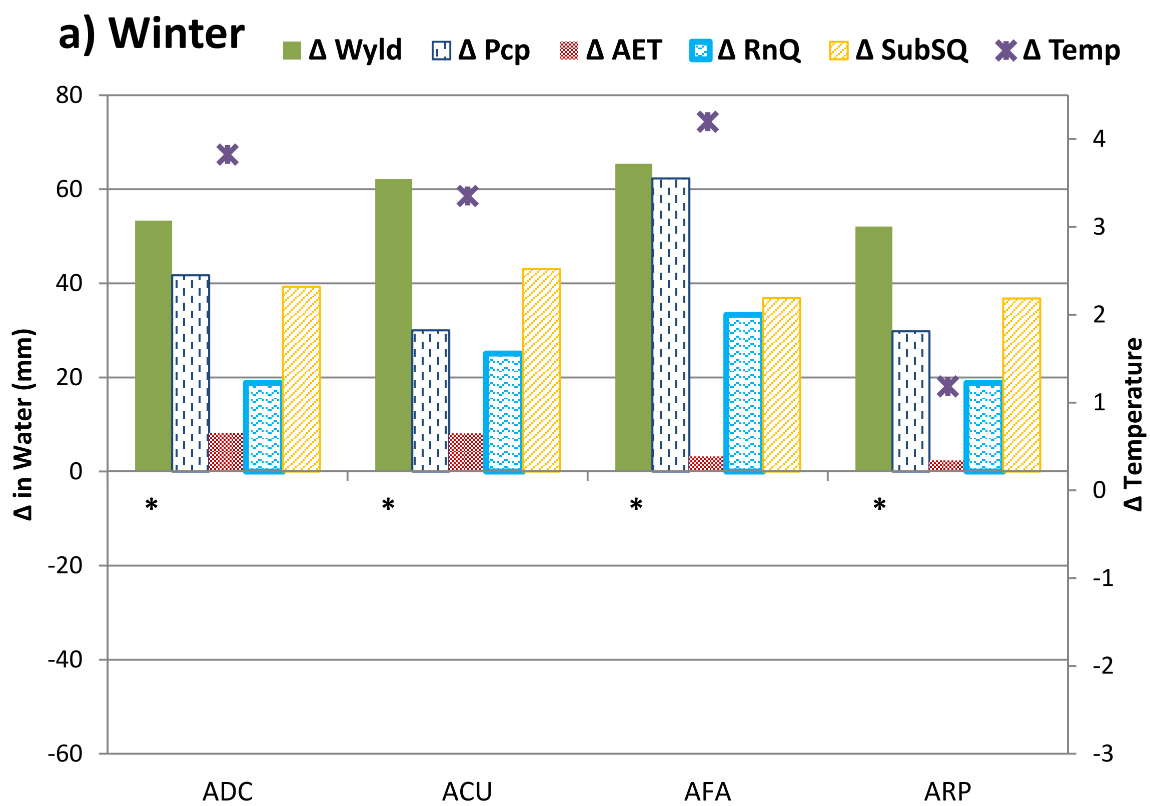

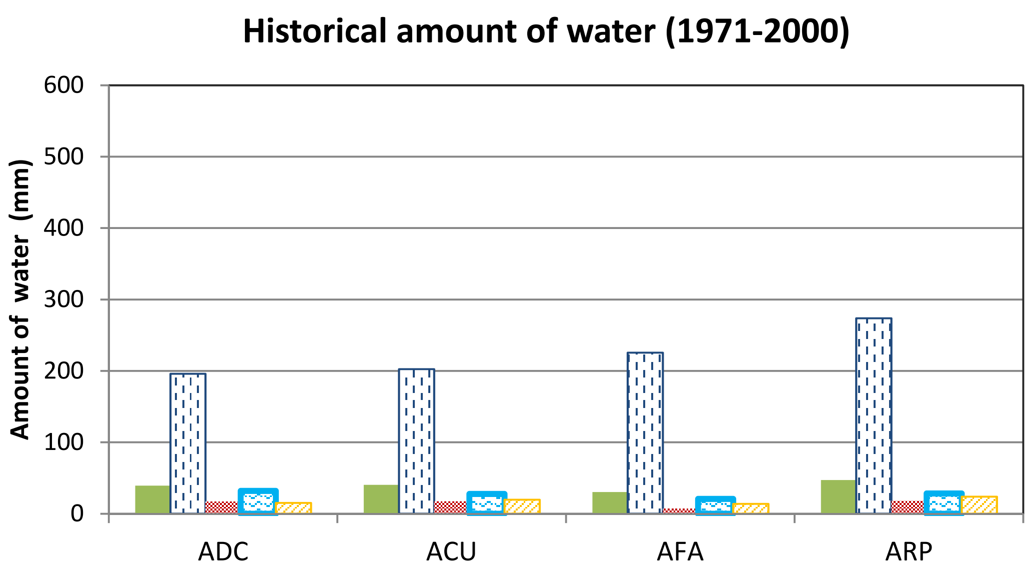

Figure 4.12 a): 30-year mean absolute changes in the components of the hydrological cycle on a seasonal basis: winter (December, January and February).

PCP: precipitation, ET: evapotranspiration, WTLD: Wateryield (Q_{sur}+SubSurQ), Q_{surf}: Surface Runoff, SubSurQ: subsurface flow (mm), and T: change in monthly averaged temperatures in °C for the season for each climate projection.

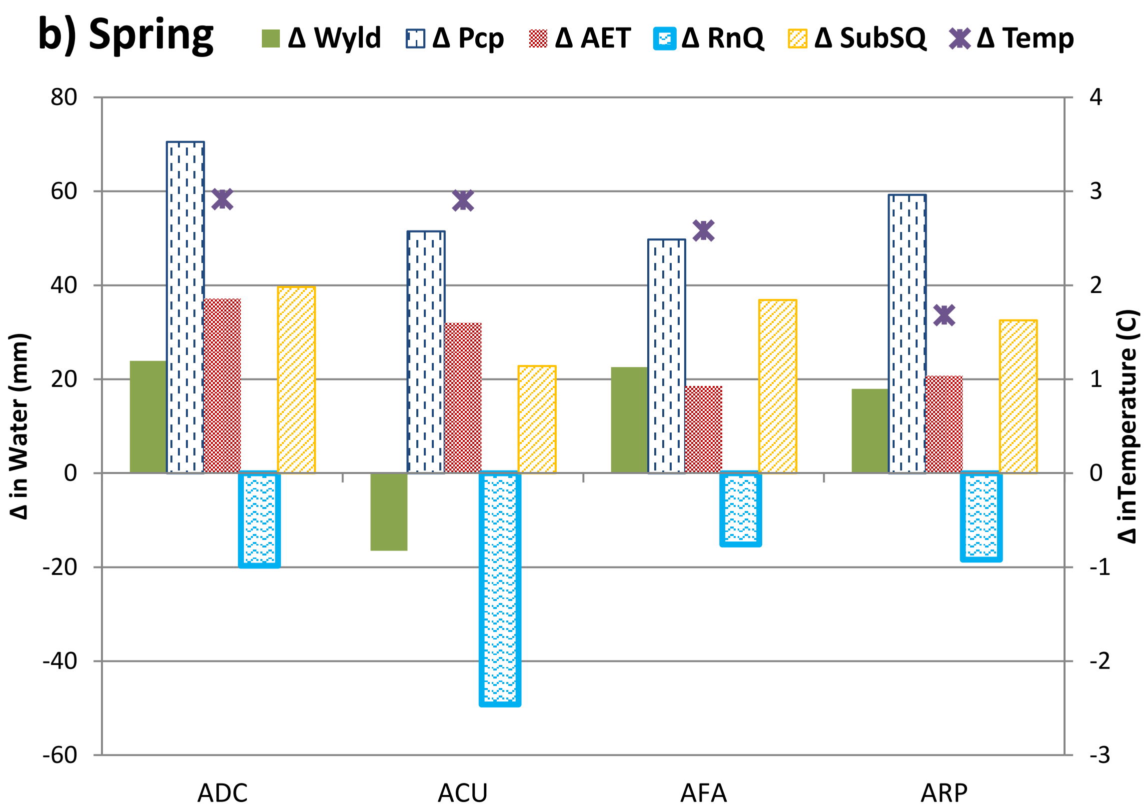

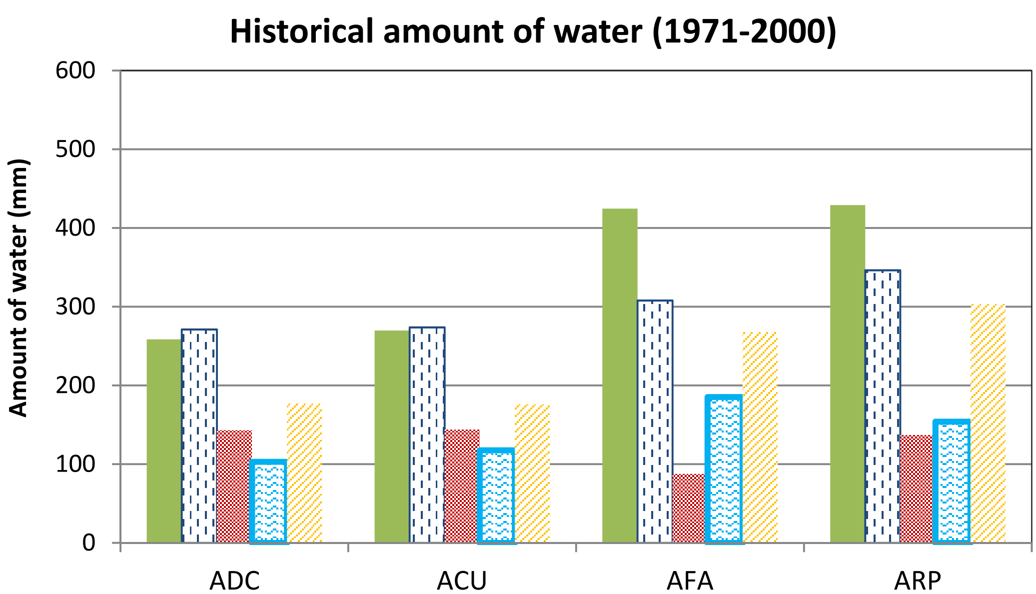

Figure 4.12 b): 30-year mean absolute changes in the components of the hydrological cycle on a seasonal basis: spring (March, April and May).

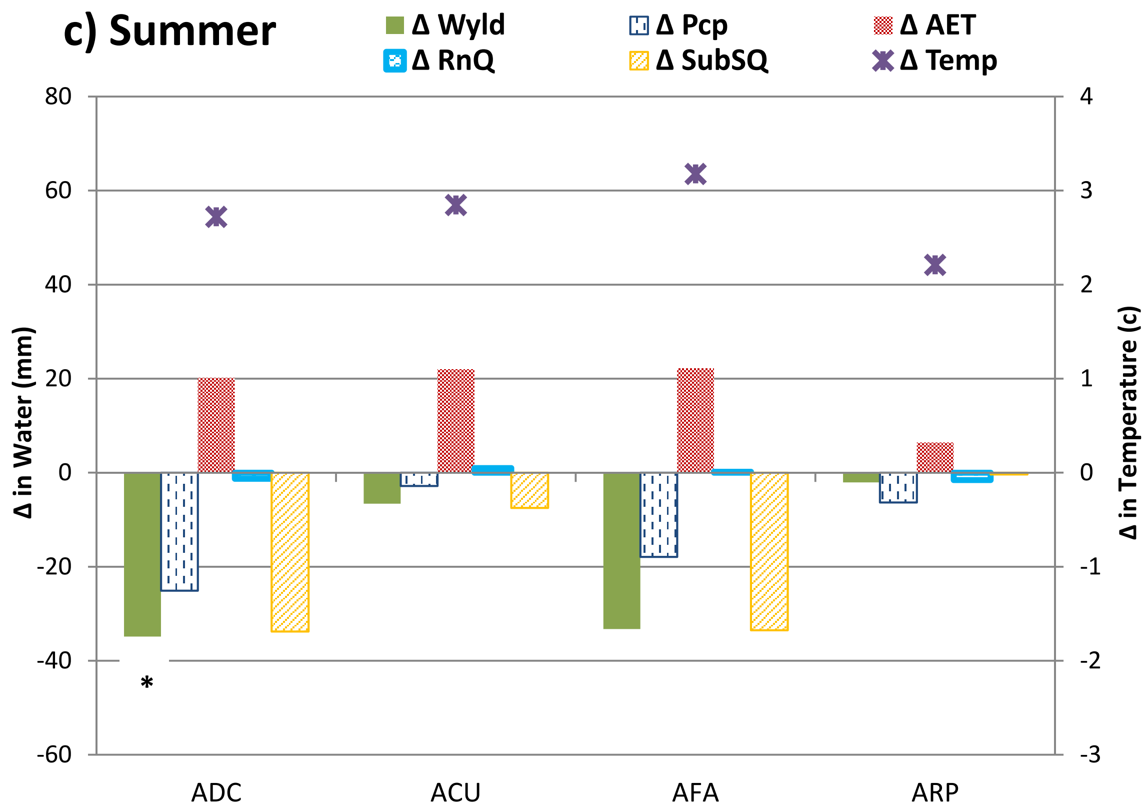

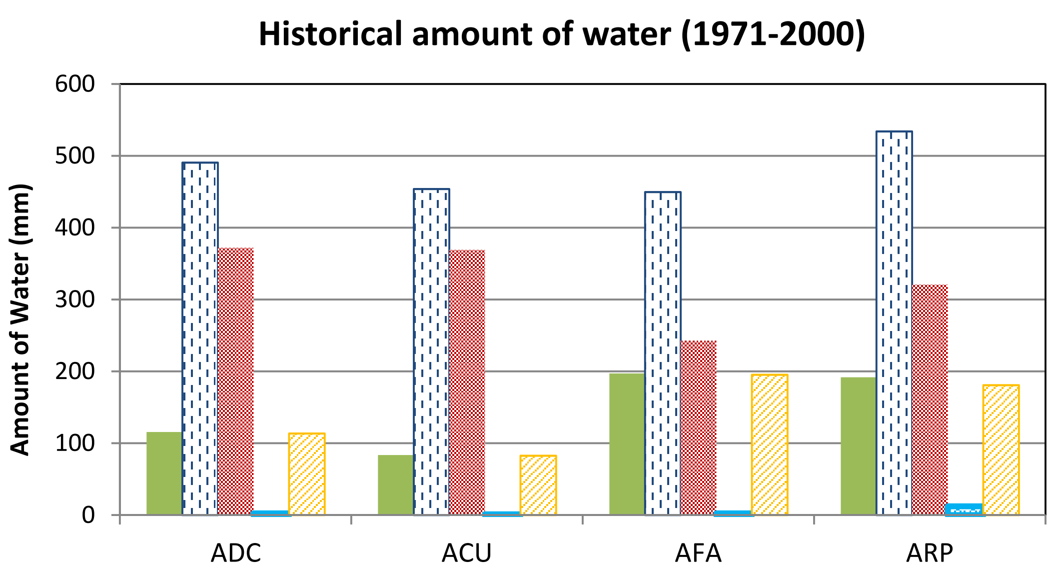

Figure 4.12 c): 30-year mean absolute changes in the components of the hydrological cycle on a seasonal basis: summer (June, July and August).

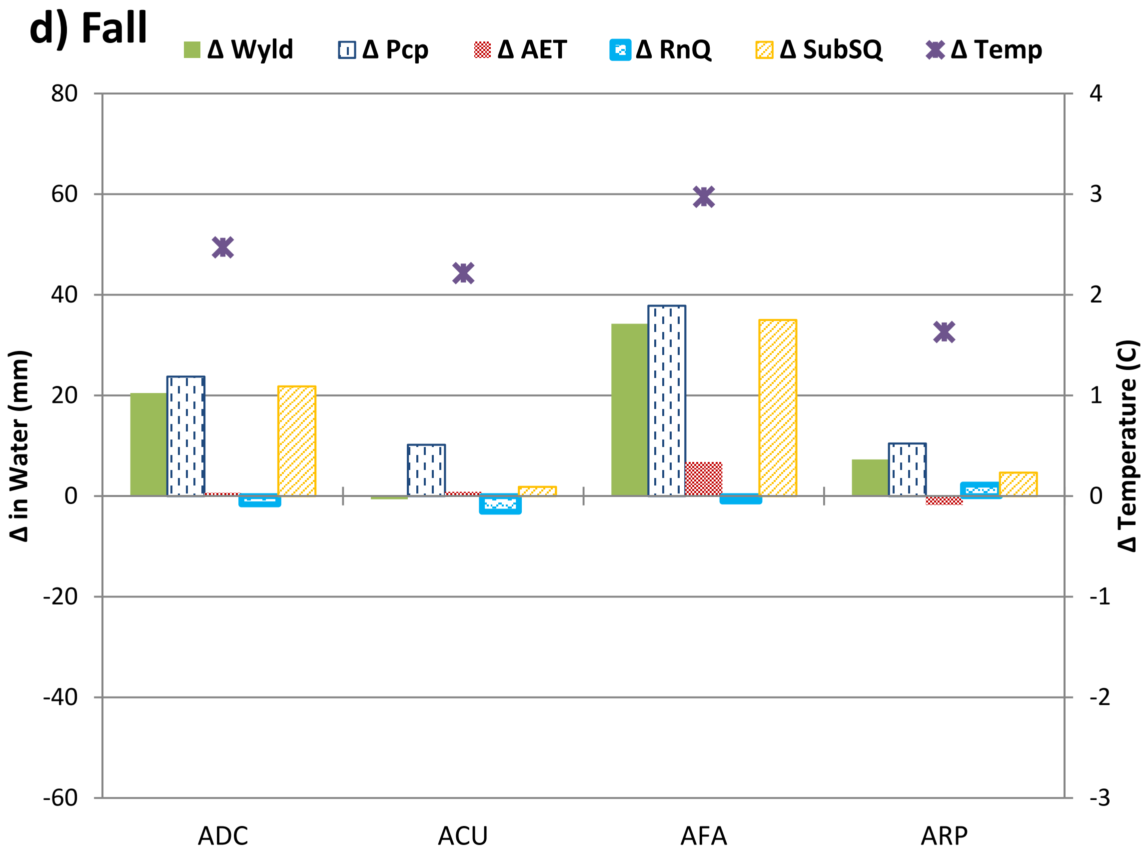

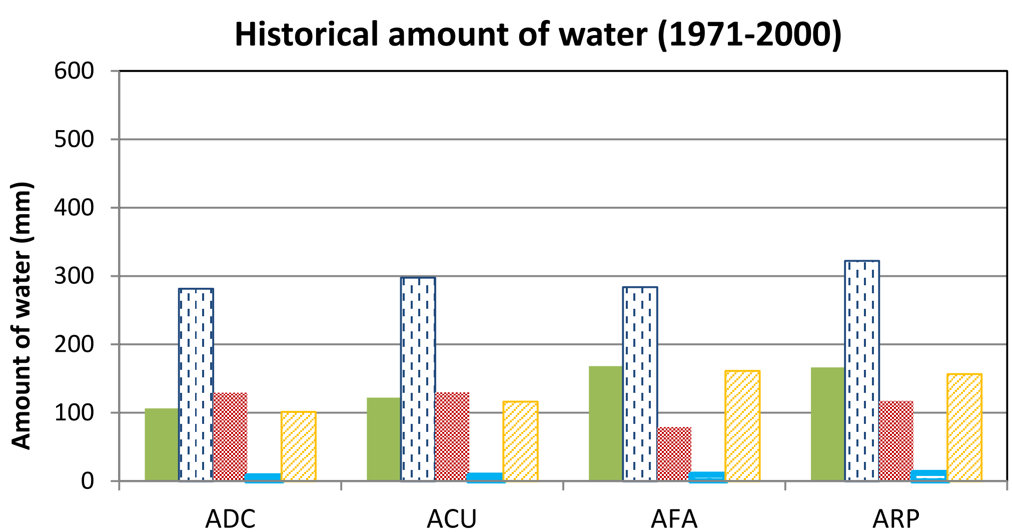

Figure 4.12 d): 30-year mean absolute changes in the components of the hydrological cycle on a seasonal basis: summer (September, October and November).

Winter

Winter is the only season for which all simulations predict significant increases in stream flow for every month. Predictions suggest an increase in precipitation of between 30 mm and 60 mm within the watershed. It is the second biggest seasonal increase in precipitation after spring. Similarly, the increases in temperature are among the largest during the year, with the three projections of the Canadian model predicting a 3.35°C to 4.20°C rise compared to the historical period of 1971-2000. These combined changes had the effect of increasing water yield by 53 to 65 mm, resulting in total runoff 2- to 3-fold greater than historical levels of the current period, thus contributing to a significant increase in stream flow.

Despite higher evapotranspiration rates, increases in water yield and stream flow are always much higher than those of precipitation. The increase in snowmelt episodes and rainfall, provoked by mild spells in the winter, might explain this observation. The resulting surplus in winter runoff, historically stored in the snowpack, adds to the increase in precipitation and contributes for a major part to the increase in water yield.

The only exception occurred in the case of the AFA simulation which predicts an increase in water yield that closely matches the increase in precipitation. This may be explained by a bias present within AFA temperatures.

This bias was noted when comparison of observed and simulated temperatures revealed that the AFA simulation significantly underpredicted temperatures in January and February (-15°C;-14°C *vs.* the observed -10°C;-8°C) (Figure C2). Because of this bias, the 4°C increase in temperatures which-as explained above- should have triggered more runoff events, might not have been sufficient to trigger enough increase in rainfall (instead of snowfall) and snowmelt events to produce notable differences between the precipitation and water yield increase.

In fact, if one adds 4°C to the historical simulation AFA, the future projection of AFA matches observed temperatures (-15°C+4°C=-11°C; -14°C+4°C=-10°C). If temperatures were not biased, one can suppose that the increase of AFA water yield might be greater than for other simulations. On this last note, it may be important to mention that as AFA presents the highest increase in stream flow, the upper bound of climate change effects in the winter might be underpredicted.

Evapotranspiration was affected in the same way, since despite the 4°C increase, evapotranspiration remained as low as evapotranspiration of the ARP simulation, which only projected a small increase in temperature.

Finally, while both surface and subsurface flow increase, the latter does so to a greater extent than the former. This might be due to fewer days with frozen soil fostering water infiltration during winter mild spells (Jyrkama and Sykes, 2007). Subsurface flow was simulated to be 37 mm to 43 mm (or 2.5- to 3.7-fold) greater in the future horizon than for the historical horizon. As a result, subsurface flow contribution to water yield became equal or superior to contributions of surface flow. In the case of AFA simulation, increases in surface and subsurface flow were similar, again likely due to the negative bias of the temperature keeping soils frozen as in current conditions.

<u>Spring</u>

Spring temperatures were 1.68°C to 2.92°C higher and precipitation 50 mm to 71 mm (16% to 21%) greater, in the future (*vs.* historical) horizon. Despite the fact that on a monthly basis, changes in stream flow and water yield were significant for the four projections; no significant changes could be detected for the season because the monthly results aggregated on a seasonal basis balanced out each other.

Moreover, higher temperatures increased evapotranspiration by 19 to 37 mm (15% to 26%) partially offsetting the increase in precipitation, and limiting the increase in water yield to a volume ranging from 18 mm to 24 mm (4% to 9%). Added to this, a decrease in snowmelt due to the reduction of water storage during the winter explains also the moderate increase in spring water yield. ACU simulation even showed that water yield could decrease if the reduction in snowmelt and increase in evapotranspiration were important. For example ACU water yield decreased by 17 mm (6%) as a result of evaporation increase of 30 mm and reduction in runoff of 50 mm. This likely explains the decrease in spring peak flow in figure 4.11.

Only one simulation (AFA/AFD) showed a slight increase in peak flow. Minville et al. (2008) noted that the simulations predicting the greatest increase in winter/spring temperatures were also the ones which predicted the greatest decrease in spring peak flow. However, when future temperatures were not high enough, the increase in precipitation would thicken the snowpack resulting in higher peak flow in spring. Although this simulation projects the greatest increase in temperature, the negative winter bias (see preceding section on winter) keeps the future temperature sufficiently low for snow to accumulate in the snowpack, despite more rain and snowmelt episodes (Minville et al., 2008).

Spring surface runoff decreased by 15 to 50 mm (8 to 42%) most likely because of a decrease in snowmelt, and also due to better infiltration of water through the soil profile due to earlier and more frequent freeze/thaw periods as previously discussed in winter (Jyrkama and Sykes, 2007). As a result subsurface flow increases by 23 and 40 mm (11% to 22%).

Summer:

While most projections showed no significant change in summer water yields, one simulation (ADC) showed a significant decrease in water yield, while another (AFA) showed a clear downward trend attributable to a significant decrease in water yield for a single month. The 2 to 35 mm (1% to 30%) decrease in water yield can be explained by a decrease in precipitation (6 mm to 20 mm, or 1% to 5%) and an increase in evapotranspiration (6 mm to 22 mm, or 2% to 9%). Water yields, however, do not decrease as much as the combined amounts of precipitation decrease and evapotranspiration increase. In fact, the increase in subsurface flow during spring and winter indicates that aquifers benefit from an increased recharge (Table E1). Thus, as explained in Sulis et al. (2011) the recharge feeds summer base flow, which mitigates the effect of temperature increases and precipitation decreases during this season.

In summer, the four climate projections overestimated precipitation and slightly underestimated temperatures. However, contrary to the biases in winter and spring, daily thresholds governing evapotranspiration during the summer and fall, like snowmelt/snowfall temperatures governing moisture storage and runoff in winter and spring, did not appear to exist or to be significant. Therefore, these biases may not have an important effect on the results given that the resulting hydrological bias will be eliminated through comparing the historical and future simulations.

The physiological effects of increasing CO_2 concentration ($[CO_2]$) on vegetation were not taken into account in this study. One effect involves the reduction of stomatal aperture of plant which reduces the evapotranspiration of the vegetation. A second effect involves an increase in leaf area index (LAI) leading to greater moisture interception by the plants leaves and greater transpiration (Betts et al., 1997). The net effect of these two mechanisms could either be slightly positive, significantly negative or null according to the region and vegetation types (Kergoat et al., 2002; Leipprand and Gerten, 2006). For a better estimation of future evapotranspiration, information on stomatal and leaf area response to $[CO_2]$ for each type of vegetation growing in the watershed should have been integrated into the modified version of SWAT used in this study, as did Eckhardt and Ulbrich (2003). However, these specific responses are still poorly understood (Andrews et al., 2011) and therefore difficult to integrate. Eckhardt and Ulbrich (2003), studying a German snowmelt watershed, found that a doubling of $[CO_2]$ in the 2070-2099 horizon, would lead to respective decreases of 3% and 4%, in mean annual groundwater recharge and stream flow. This would be due to the counteracting effect of temperature rise, stomatal conductance reduction and an increase in LAI. The same counterbalancing effect might be present in the Pike River watershed, suggesting therefore that only a small under- or overestimation of evapotranspiration occurs, along with its consequences on runoff.

Fall:

In the fall, changes in stream flow were not significant even if three simulations predicted an upward trend in response to the increase in precipitation. Typically, for an increase in precipitation of 10 mm to 38 mm, water yield would increase between 0 mm and 34 mm, with base flow increasing and runoff remaining as low as under current conditions. However, evapotranspiration remains rather constant. Therefore, when an increase in precipitation does not correspond to an increase in water yield, the surplus of water would likely be allocated to soil or aquifer recharge, as was found by Sulis et al. (2011) for the des Anglais watershed in Southern Québec. A quick increase in end-of-month soil moisture can be observed between September and October (Figure 4.13). As a worst case scenario, ACU presents the greatest decrease in soil moisture during the preceding seasons and the lowest moisture content. As a result, the total amount of precipitation serves to replenish soil and aquifer recharge.

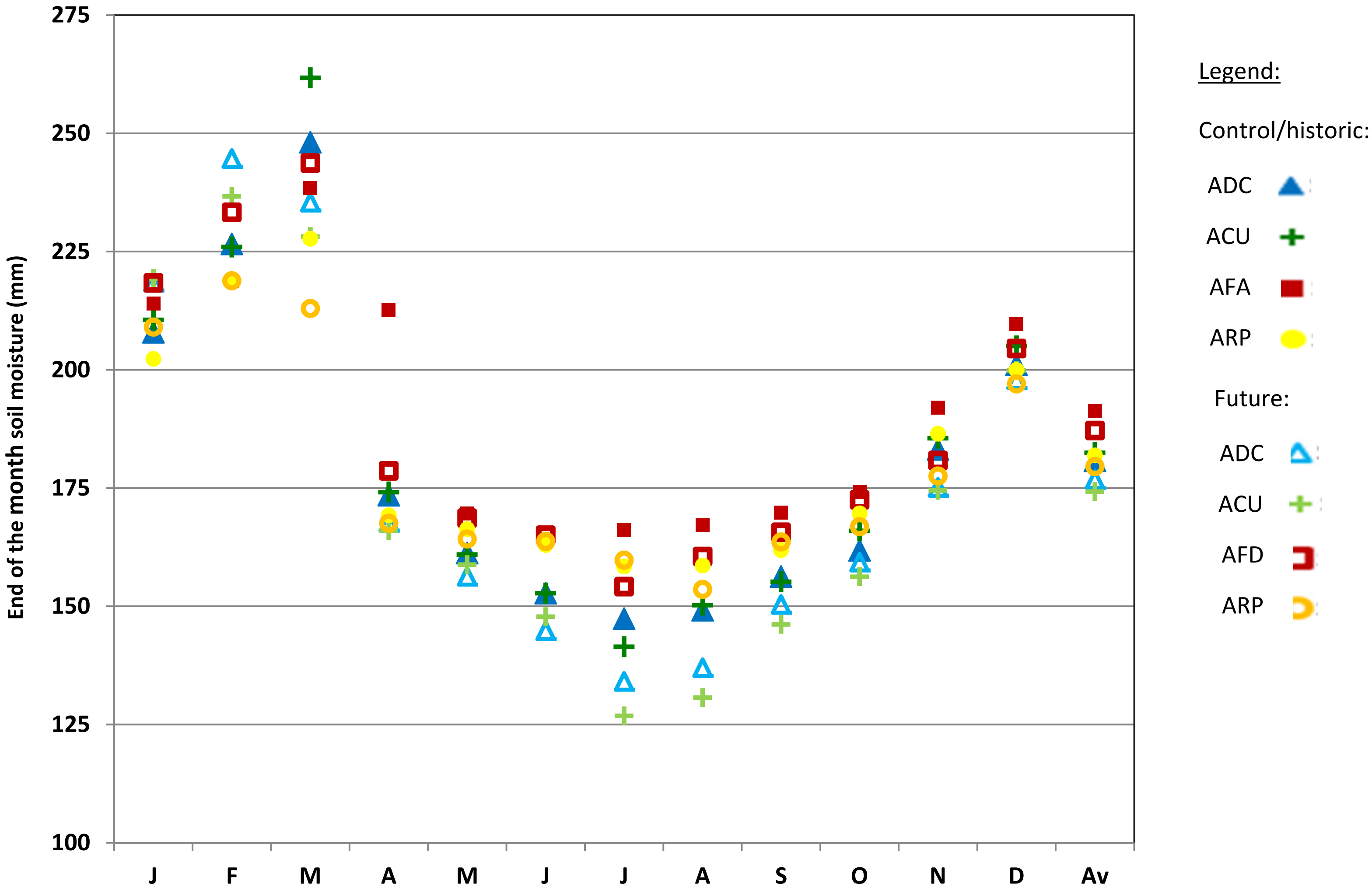

Figure 4.13: Thirty-year mean values for end-of-the-month soil moisture for the historical and the future period.

4.4 Potential changes in water quality

Average changes in sediment, total P and N loading simulated for the periods between 1971-2000 and 2041-2070 are displayed in table 4.12 for annual results, and tables 4.13 a,b,c,d, for the winter, spring, summer and fall seasons, respectively. Similarly to hydrological changes, the four simulations predicted results of equal probability despite their different accuracy in reproducing historical loadings. Finally, the average of several climate simulations likely provides more robust estimates than a single prediction (Gleckler et al., 2008). Assuming this would also be the case for water quality variables, the average of the four simulations is also given here as a point of reference. Changes in stream flow and surface runoff (RnQ) are also presented in this section for discussion purposes.

On a yearly basis, changes in mean annual loadings range from -16 kg ha^{-1} to 46 kg ha^{-1}(-11% to 15%) for sediments, from 0.04 kg ha^{-1} to 0.17 kg ha^{-1} (6% to 14%) for TP and from -1.1 kg ha^{-1} to 4.1 kg ha^{-1} (-3% to 17%) for TN. Future sediment, TP and TN loads tended to increase. However, in one simulation (ACU) a decrease in surface runoff was predicted, though not for P and N. Only climate projection AFD, with the greatest increase in temperature and precipitation in winter (>30% for precipitation and 4°C for temperature) triggered a significant increase in sediments and TP, as it did for stream flow. As for projection ADC, with the greatest increase in spring temperature and precipitation, it triggered a significant annual change in total N loading. In other words, only these simulations stand out from natural variability.

While changes in concentration were not analysed *per se,* the comparison between percentage changes in stream flow and loadings may provide a good insight. TP and TN may be either diluted or concentrated depending on whether changes in stream flow are substantially different from changes in TP and TN. Sometimes change in stream flow and nutrient loads differ by as much as 100% (ADC for TP) or are opposite (AFD for TN). Overall, no clear trend was detected as the different projections are at odds. Their average indicates that concentrations in total P and N tend to remain constant because the percentage increases of stream flow and of the loadings are similar. In contrast turbidity may slightly decrease. All simulations, but one, also indicate the N:P ratio could change. In contrast, the scenario average indicates overall changes in P and N to be similar. Although P and N concentrations and ratios fluctuate during the year due to biological and chemical processes, these results indicate climate change may harden the achievement of the water quality standards of 0,03 mg P L^{-1} to avoid eutrophication. In fact, even if changes are insignificant or rather small, changes are far from the required reduction of 40 Mg of P an^{-1} planned within the Québec-Vermont agreement (Missisquoi Bay Phosphorus reduction Task Force, 2005).

Table 4.12: Mean annual changes in sediments (Sed), total phosphorus (TP) and nitrogen (TN) loadings between 1971-2000 and 2041-2070

Annual	Stream flow		RnQ		Sed			TP			TN		
	mm	%	mm	%	kg ha^{-1}	Mg	%	kg ha^{-1}	Mg	%	kg ha^{-1}	Mg	%
ADC	61	12%	-4	<u>-3%</u>	7.50	475.4	<u>5%</u>	0.040	2.55	6%	**4.1**	260.02	**17%**
ACU	37	7%	-26	-17%	-16.09	-1 019.6	<u>-11%</u>	0.040	2.52	<u>5%</u>	3.0	188.20	12%
AFD	**89**	**<u>11%</u>**	17	8%	**45.96**	**2 912.2**	**15%**	**0.171**	10.83	**14%**	-1.1	-71.01	<u>-3%</u>
ARP	75	9%	1	1%	18.75	1 187.7	6%	0.101	6.42	8%	3.7	236.24	10%
Average	65	10%	-3	-2%	14.03	888.9	6%	0.088	5.58	9%	2.4	153.36	8%

<u>Explanation of abbreviations:</u> RnQ : Surface Runoff

As expected from the hydrological results, the effects of climate change appear stronger when analysed on a seasonal and monthly basis. In fact, stream flow, as well as sediment, P and N loadings increase significantly in winter (DJF) under the four scenarios. The increase in sediment loadings ranges from 24 to 45 kg $ha^{-1}winter^{-1}$, that for TP loadings from 0.127 to 0.195 kg $ha^{-1}winter^{-1}$ and the one for TN loading from 2.9 to 3.5 kg $ha^{-1}winter^{-1}$. Significant changes appeared also for the other seasons but to a lesser extent and with a maximum of only two significant simulations for each season.

After the increase in winter, spring loadings (MAM) tended to decrease. Indeed, the four simulations predicted from 1.23 to 43.88 kg $ha^{-1}spring^{-1}$(-1% to -38%) less sediments and from 18 to 80 g $ha^{-1}spring^{-1}$ (-2% to -17%) less TP for the period

2041-2070. Changes in TN are unclear; two simulations predicted a 12% decrease, corresponding to -1.5 kg ha^{-1} and -2.8 kg ha^{-1}. The two others predicted a very weak increase (<6%), while the average of the four predictions resulted in a 0.8 kg $ha^{-1}spring^{-1}$ (5%) decrease. Only the 38% decrease in sediments triggered by simulation ACU is significant. Surprisingly, ACU's TP also decreased, but to a smaller degree (17%) and the decrease was not significant. This is what partly explains why mean annual sediment loading decreased whereas mean annual P loading increased for this simulation. Indeed, spring sediment decreased enough to counterbalance the winter increase. In spring TP decreases were not as high to produce the same effect on annual TP loadings. This will be further discussed in the next section.

Thus, as for the water yield, significant changes invisible on an annual or seasonal scale are observed on a monthly scale, especially during spring and summer (Appendix E). In fact, two simulations predicted a significant increase in March sediment and P loadings as a result of the earlier onset of the spring flood. On the other hand, April and May loadings tended to decrease significantly for half of the simulations.

For summer and fall results, it is important to note that some results displayed a high percent change which corresponded to rather small actual changes. This is a result of the fact that loadings are generally much smaller during these seasons. Value of percentage loadings during these seasons are therefore easily affected by small increase or decrease.

Summer sediments, TP and TN loadings decreased by 0.74 to 1.77 kg ha^{-1} (10% to 64%), 0.011 to 0.029 kg ha^{-1} (6% to 35%) and 0.5 to 2.8 kg ha^{-1} (10% to 46%), respectively, with an exception of simulation ACU for sediment and TP loadings which increased by 1.53 kg ha^{-1} (81%) and 1 g ha^{-1}(2%). Significance is null for sediment, but positive for simulation ADC for both TP and TN as well as for simulation AFD for TN only. Again, some simulations show significant changes on a monthly basis which did not appear on a seasonal basis.

Finally, fall sediments and TP loadings (SON) tended to increase according to the scenario average, but simulations ADC and ACU predicted a decrease in sediment loads, which resulted in a decrease in P loads for ACU but not for ADC. None of the predictions stood out from natural variability. In contrast, loadings in TN increased much more and were significant for at least two simulations.

Table 4.13: Mean seasonal changes in sediments (Sed), total phosphorus (TP) and nitrogen (TN) loadings between 1971-2000 and 2041-2070, for (a) winter, (b) spring, (c) summer, (d) fall

a) Winter	Stream flow		RnQ		Sed		TP		TN	
	mm	%	mm	%	kg ha^{-1}	%	kg ha^{-1}	%	kg ha^{-1}	%
ADC	**53**	**139%**	19	59%	**23.83**	**88%**	**0.127**	**99%**	**3.5**	**225%**
ACU	**62**	**156%**	25	91%	**28.94**	**119%**	**0.129**	**110%**	**3.5**	**191%**
AFD	**65**	**214%**	33	161%	**45.40**	**219%**	**0.195**	**178%**	**2.9**	**227%**
ARP	**52**	**110%**	19	66%	**31.57**	**101%**	**0.133**	**88%**	**3.0**	**138%**
Average	**58**	**148%**	24	88%	**32.44**	**125%**	**0.146**	**116%**	**3.2**	**188%**

b) Spring	Stream flow		RnQ		Sed		Total P		Total N	
	mm	%	mm	%	kg ha^{-1}	%	kg ha^{-1}	%	kg ha^{-1}	%
ADC	23	9%	-20	-19%	-12.48	-12%	-0.063	-14%	0.7	6%
ACU	-18	-7%	-49	-42%	**-43.88**	**-38%**	-0.08	-17%	-1.5	-12%
AFD	23	5%	15	-8%	-1.23	-1%	-0.018	-2%	-2.8	-12%
ARP	17	4%	-18	-12%	-14.84	-6%	-0.031	-4%	0.5	3%
Average	11	3%	-26	-18%	-18.11	-10%	-0.048	-8%	-0.8	-5%

c) Summer	Stream flow		RnQ		Sed		Total P		Total N	
	mm	%	mm	%	kg ha^{-1}	%	kg ha^{-1}	%	kg ha^{-1}	%
ADC	**-34**	**-31%**	-2	-49%	-2.77	-64%	**-0.029**	**-35%**	**-2.6**	**-46%**
ACU	-6	-8%	1	85%	1.53	81%	0.001	2%	-0.5	-14%
AFD	-33	-17%	0.2	9%	-0.74	-10%	-0.018	-15%	**-2.8**	**-14%**
ARP	-0.9	0.5%	-2	-13%	-3.50	-14%	-0.011	-6%	-0.9	-10%
Average	-19	-13%	-0.4	29%	-1.37	-14%	-0.014	-5%	-1.7	-24%

d) Fall	Stream flow		RnQ		Sed		Total P		Total N	
	mm	%	mm	%	kg ha^{-1}	%	kg ha^{-1}	%	kg ha^{-1}	%
ADC	19	19%	-2	-33%	-1.08	-14%	0.005	6%	**2.6**	**55%**
ACU	-0.7	-1%	-3	-38%	-2.69	-30%	-0.011	-12%	1.5	27%
AFD	34	20%	-1	-11%	2.53	21%	0.013	10%	**1.6**	**25%**
ARP	7	4%	2	20%	5.52	31%	0.010	7%	1.2	17%
Average	15	11%	-0.9	-9%	1.07	9%	0.004	4%	1.7	29%

Explanations of abbreviations: RnQ : Surface Runoff

In this section are presented the magnitude and variability of the effect of climate change on water quality of the Pike river watershed. Similar to other studies performed in wet or snowmelt basins from Finland and Sweden (Pierson et al., 2010), Denmark (Jeppesen et al., 2009), Ireland (Jennings et al., 2009), and England (Bouraoui et al., 2002), future N and P loadings increased in winter and early spring. The early onset of the spring flood shifted nutrient loadings towards the beginning of the year, while from April to the end of the summer, loadings decreased (Appendix E). The few cases showing an increase in sediment and nutrient loadings between the period from May to July and the fall period may be related to greater rainfall depths and intensities on bare soil. This can be explained by the fact that plants may not cover and protect the soil enough due to their early growth stage in spring or their harvest in fall (for precise dates of planting and harvesting see Appendix A1 on field management). The cases showing a decrease in sediment and nutrient loadings correspond generally to a decrease in stream flow and runoff. However, for most of these cases, changes were not significant and may thus only represent natural variability in the climate.

Also, in most of the studies mentioned above, spring peak loads decreased as a result of the drop in spring peak flood. In this watershed, such decrease appear less evident for TP, indeed two simulations show a peak increase. As noted on the monthly graphs, the effect of the climate models' bias on the predicted hydrology (Section 4.2.5) especially on the timing and magnitude of spring flood peaks also affected nutrient loading in the same manner. Great uncertainty is therefore related to the prediction of this peak. However, because it is always simulated late for all historical simulations, it is likely that its shift toward winter months may be greater than predicted. Overall changes in TN seemed more important than changes in TP.

Not surprisingly in most cases and for each time step, changes in TP mirrored changes in sediment which mirrored changes in surface runoff and changes in TN mirrored changes in stream flow (corresponding to total runoff or water yield). However underlined values in the tables 4.12 and 4.13 a,b,c and d show a few interesting exceptions, briefly explained in the next section.

4.4.1 A change in nutrient losses pathway and forms

Changes in TP or TN were not always consistent with changes in sediment or stream flow and changes in sediments were not always consistent with changes in surface runoff. Though changes are not statistically significant, some of them may provide important information about future effects of climate change. In tables 4.12 and 4.13 are underlined instances of inversely related or disproportionate changes, such as a decrease of 3% in runoff accompanied by an increase of 5% in sediment loading (Table 4.12, simulation ADC).

Four patterns were found in these "inconsistencies":i) a decrease in surface runoff with an increase in sediment and P losses (ADC annual, AFD Fall), ii) an increase in surface runoff with a decrease in sediment and P (AFD summer), iii) a decrease in sediment with an increase or much smaller decrease in P (ACU Annual; ACU, spring, AFD, Fall) and iv) an increase in stream flow with a decrease in N (AFD Annual, AFD, spring) or vice versa (ACU fall).

Marshall and Randhir (2008) found the same pattern i) between June and October for a large watershed, near our region of study (New-England close to the US-Canada border) using SWAT and climate change projections. This could be related to a greater occurrence of heavy rainfall events with greater erosive power but which do not necessarily result in a greater quantity of water within the season (Pruski and Nearing, 2002a). However, SWAT had difficulty in reproducing high and extreme events within the Pike river watershed, which limits the strength of this argument. On this note, it is important to highlight that results obtained within the Pike River watershed during the growing season (April to November) are therefore very conservative and that this region could display, in the future, erosion rates and nutrient losses greater than predicted. Another explanation of contrasted results between surface runoff and sediment losses is the increased vulnerability of soil to rainfall when vegetation cover and soil protection decrease due to water stress (Pruski and Nearing ,2002a).

In contrast, the second pattern may be due to greater soil protection by vegetation boosted by higher temperatures as observed for certain types of Mediterranean vegetation in Nunes et al. (2008). In Southern Québec, the crops most likely benefitting from an increase in temperature would be corn and sorghum while soybean and cereals would experience water stress (Brassard and Singh, 2008; Almaraz et al., 2009). The third pattern, in turn, may indicate a change in the relative proportion of soluble vs. particulate P exported, as well as a change in the pathway through which they are exported. Indeed, the increase in TP along with a decrease in sediments is likely explained by an increase in soluble P counterbalancing the decrease in particulate P which would be associated to any sediment decrease.

Bouraoui et al. (2002) used SWAT to assess the impact of climate change on nutrients loads within an Irish catchment and noted that for scenarios with higher temperatures, crop nutrient uptake was higher. They attributed this phenomenon to a higher rate of P mineralisation, and subsequently increased available P to be taken up. SWAT allows mineralisation to occur when the temperature of the soil layer is above 0°C and increases the rate of mineralisation with increased temperature. In our case, higher temperatures in winter, spring and fall may increase mineralization releasing available P when plants are not present for its consumption. This may result therefore in possible higher loss in soluble P, especially if soil P concentration is already high.

Likewise, changes within the relative contribution of surface and subsurface flow to stream flow found in section 4.3.3 could be responsible for higher export in soluble P. Although SWAT does not simulate P processes below the first 10 mm of the soil, it allows modellers to enter a concentration of soluble P to account for groundwater contribution in P to the reach. In this study concentrations were fixed at 0.07 mg P L^{-1} and 0.08 mg P L^{-1} for upstream and downstream sections of the watershed respectively. These concentrations were based on field measurements and calibration results. Soluble P export through subsurface flow might therefore have increased under the future climate projections as a result of the predicted increases in subsurface runoff.

Finally, the fourth pattern showing an increase in stream flow and a decrease in N (Table 4.13b, AFD) may be explained by the substantial decrease in N and TN caused by the decrease in surface runoff. In this case, the increase in stream flow is explained by an increase in base flow. It is, however, surprising that base flow has not been found to result in greater nitrate losses. Inversely, a decrease in stream flow accompanied by an increase in N loadings

(Table 4.13d, ACU) may be explained by an increase in the rate of N mineralisation and residue decomposition in autumn as a result of higher temperatures (Jennings et al., 2009). Therefore, although, runoff and stream flow decreased, the amount of N in total runoff has increased compared to the period of reference.

CHAPTER 5: SUMMARY AND CONCLUSIONS

Summary

In order to assess future risks related to eutrophication and blue-green algae contamination of Missisquoi Bay, future exports in sediments and nutrients entering the Bay were simulated. A version of the SWAT2005 model, adapted for Québec agroclimatic conditions (Michaud *et al.*, 2008) was applied to the Pike River watershed using four climate projections provided by the Ouranos Consortium. Potential changes in the Pike river watershed hydrology and N and P loads were assessed for the 2041-2070 horizon based on the 1971-2000 reference period.

Three climate projections originated from the Canadian Regional Climate Model (CRCM4) driven by its homologue global model CGCM3, and a fourth one from the French Global Climate Model Arpège with variable resolution. The four simulations assumed an increase in GHG following the IPCC SRES scenario A2. These simulations were chosen to encompass a wide range of possible changes especially in winter and spring temperatures and precipitation, because these seasons presented greater uncertainties and because of the high sensitivity of temperature snowmelt. Simulations also differed as to the domain they covered, the version of the model, and the initial conditions or the model used.

As the four climate projections bracketed a large range of possible temperature and precipitation changes, it is assumed that the simulations also bracketed a wide range of the possible watershed responses and potential changes in water quality. Having these high, medium and low responses provides an estimate of the magnitude of the uncertainty related to the predictions.

SWAT was first calibrated and validated for the watershed hydrology, sediment and nutrient exports between the years 2001 and 2006 with observed climate data, and was revalidated for a longer period of 20 years (1980-2000) to test its ability under varied climate conditions. SWAT performance driven by outputs of regional climate models data was also assessed over the historical period in order to better understand sources of bias in the simulations.

The following conclusions were drawn from this study:

SWAT performance in simulating hydrology and water quality

i. After calibration, the customized version of SWAT satisfactorily reproduced components of the annual water cycle as well as daily, monthly and annual stream flow. For the calibrated period of November 2001 to May 2003, coefficients of performance computed on a daily, monthly and annual scale were all above the criteria of acceptability. On a monthly and yearly basis, R^2 values exceeded 0.7; NSE values exceeded 0.5, and the absolute % deviation remained below 25%.

ii. The short validation performance for the period extending from November 2004 to May 2006 did not meet acceptability criteria likely due to heavy rainfalls that SWAT could not capture. The coefficients of performance were however close to the threshold for the two Wallbridge subwatersheds supporting the calibration of water quality. Nonetheless, performance in the long term validation was rated as very good, with R^2, NS and % deviation of 0.6, 0.55 and -14% on monthly basis.

iii. Similar to hydrology, SWAT performed rather well in simulating sediment, total P and N loadings of the Pike River over the calibration period and rather satisfactorily during the long term validation of 20 years. R^2, NS and % deviations, computed for sediments and TP over the long term validation were 0.44,-2.8 and 55% for sediment and 0.52, -0.67 and 42% for TP. The low NSE values are likely due to the use of constant land-use and management practices for the model parameterization which reflected overly intensive agriculture for the beginning of the simulation, provoking a strong overestimation of predictions.

Validation periods did not show improvements in model predictions that were as marked as for the calibration period. This situation is not uncommon because models are often optimized for conditions prevailing during the calibration period, which may differ significantly from the validation period. In this study wetter conditions and more intense hydrologic events prevailed during the validation (vs. calibration) period, which explains why acceptability thresholds could not be met during the second evaluation period (Engel et al., 2007). However, this does not mean the model is unsuitable. The same authors point out that acceptability criteria vary according to the project objective. When absolute and accurate predictions need to be made to enable decision-making regarding the security and efficiency of an applied solution or financial investments, it is understood that acceptability criteria need to remain high in all conditions. For example, projects which assess urban drainage needs or flood probability near potential development need much higher coefficients of performance.

For climate change assessments, we assume that the ability of SWAT to reproduce the principal processes in regional erosion and nutrient losses with appropriate seasonal and inter-annual variability would be good because: i) coefficients of performance indicate that predictions significantly improved compared to uncalibrated predictions and ii) because most of the assessment is based on a relative comparison rather than providing absolute values.

<u>Integrating regional climate data into SWAT</u>

The historical historical simulations reproduced current hydrological conditions rather well, but gave a mixed performance.

iv. Besides higher mean annual precipitation, the proportions of water allocated to the main components of the water cycle were generally respected, except for simulations AFA and ARP which allocated too much water to total runoff (60% instead of 40%) and not enough for evapotranspiration (30%, to low of 10%). Otherwise, the relative partition between and subsurface flow corresponded to observed annual conditions for all simulations.

v. Annual and monthly stream flow matched the validated stream flow of the reference simulation (SWAT.OBS). Positively biased precipitation combined with the slightly negatively biased temperatures of the GCM simulations led to an overestimation of summer flow ranging between 40 to 73 mm (156%-360%), while negatively biased temperature in March, brought about by the CRCM, created a delay in the onset of the spring flood.

vi. Similar to stream flow, biases resulting from both the CRCM and GCM projections significantly influenced sediments, P and N loading predictions in a number of ways (decrease or increase depending on the projections) especially during the spring season.

The March peak load was simulated with fifteen days to one month delay for sediment and TP. Large absolute uncertainties were therefore present and only a relative assessment comparing the historical and future period was therefore valid.

Potential changes in the Pike river watershed hydrology and nutrient loadings

vii. Similar to other snowmelt basins for this time horizon (2041-2070), climate change projections specifically affected the timing of spring floods along with those of sediment and nutrient delivery.

viii. On a yearly basis, monthly or seasonal changes tend to balance each other out, hiding the effect of climate change. Mean annual stream flow increased by 7% to 12% and changes in mean annual loadings ranged from -11% to +15% for sediments, 6% to 14% for TP and from 3% to 17% for TN. Generally speaking, sediment, TP and TN loads tend to increase, but are not significantly distinct from natural variability, except for simulation AFA/AFD which projected the highest precipitation and temperature changes in winter, summer and fall. On the other hand, ADC triggered the only significant annual change in TN loading.

ix. The higher temperatures, rainfall, snowmelt and more numerous freeze-thaw events in winter, significantly increased (2- to 3-fold) winter stream flow and loadings from their current levels, and shifted the peak discharge from April to March. In winter, the Pike River would deliver from 24 to 45 kg ha^{-1} additional sediment loadings, from 0.13 to 0.19 kg ha^{-1} additional TP loadings and from 2.9 to 3.5 kg ha^{-1} additional nitrogen loadings.

x. However, spring stream flow increased much less than for winters, although spring discharge remains the highest peak of the year. **An important point to remember about these two seasons is the change in surface and subsurface flow linked to fewer days with frozen soil in winter. In winter subsurface flow increased between 2.5 to 3.7 times while surface runoff decreased by 20% to 42%, in spring.** On the other hand, spring and summer stream flows tended to decrease, increasing risks of water stress but decreasing risks of nutrient losses for the season. Finally, fall stream flow increased but not significantly.

xi. Changes in surface and subsurface flow due to the increase in temperature may impact P pathways. Temperature increase may also affect P mineralization by increasing its release in soil during fall, winter and spring when plants may not be there to consume the nutrients, thereby resulting in higher risks of soluble P losses.

Final Remarks

xii. Despite the use of unbiased synthetic data as direct inputs to SWAT, general results are similar to other studies conducted in Québec. However, it seems negative bias in temperature prediction led to snowmelt, runoff and stream flow underestimation in winter and spring. Despite using a time slice approach to cancel the effect of climatic biases on the response of the watershed, these biases may lead to significant errors. This is particularly due to the high sensitivity of snowfall and snowmelt events to temperature thresholds. And it may partly explain the uncertain direction of change seen in spring peak flow results, when all other studies for southern Québec watersheds show significant decreases in spring peak flow for most of their climate projections (Minville et al., 2008; Boyer et al., 2010; Sulis et al., 2011).

xiii. There is no certainty that the calibration parameters developed for the present climate remain appropriate for a changing climate, since important processes like runoff and erosion processes are still mainly based on an empirical relationship (Fowler et al., 2007).

xiv. The use of a small number of climate and water quality models does not provide a full assessment of uncertainties and the climatic impacts may extend beyond the range of the results summarized above (Coulibaly and Dibike, 2004; Minville et al., 2008).

xv. Increases in GHGE predicted in scenario A2 have been considered until recently as one of the highest increases predicted. Nonetheless, concentrations in GHG recorded between 2000 and 2005 already exceed concentrations predicted by scenario A2 for this period (Raupach et al., 2007). Results of this impact assessment can therefore be considered conservative.

xvi. Similarly, intense precipitation events are expected to increase in the future but SWAT's difficulty at reproducing intense events might also have led to underestimation of possible increases in sediment and nutrients loadings to Missisquoi Bay.

xvii. Finally, the annual and seasonal scales may not be precise enough to detect the detailed effect of climate change. Indeed, aggregating the data on a seasonal scale made some significant monthly changes disappear. Consequently, over the entire spring (March-April-May) no significant changes were detected, though in terms of absolute values, March experienced the greatest increase in water yield (scenario average: 47 mm) in the year. Similarly, during the summer (June, July, August) stream flow did not appear to decrease significantly though ADC and AFA projections showed some months may still experience water stress due to substantial decrease in soil moisture and water yield. Likewise, results on the annual scale did not show an important increase in winter runoff. New measures of erosion mitigation would be necessary if winter runoff were to increase to limit further loss of nutrients. Similarly, increase in summer water stress may also require measures of adaptation which may not be judged necessary when results are examined at the seasonal or annual scale.

CHAPTER 6: FUTURE RESEARCH

Assessment Improvement

i. SWAT was not designed to simulate intense rainfall events, but because intense rainfall events are among the key factors generating erosion and because these events are expected to increase, it would be interesting to include or develop another water quality model capable of simulating storm erosion processes in a future study.

ii. It would always be important to continue the monitoring of stream flow and water quality on tributaries as well as on the main section of the river, especially for the agricultural downstream section. This would allow the improvement of the calibration and validation of water quality models in the context of a changing climate.

iii. Improving subsurface P modelling in SWAT would help understanding more precisely the impact of climate change on future pathways and forms of exported P.

iv. Including heightened CO_2concentration effects on plant growth and evapotranspiration in future simulations could improve accuracy of the predictions.

Further Assessments Opportunities

v. Assessing the spatial impact of climate change by examining runoff and nutrient loss for each crop type could help identifying future critical areas (HRU) and target better solutions to limit TP export.

vi. Simulating BMPs under climate change scenarios would help determine the best strategies to meet the P concentration standard of 0.025 mg P L^{-1}, to prevent eutrophication and blue-green algae outbreaks.

REFERENCES

Abbaspour, K.C., M. Faramarzi, S.S. Ghasemi, and H. Yang. 2009. Assessing the impact of climate change on water resources in Iran. *Water Resources Research* 45.W10434.

Adhikari, B.K., C.A. Madramootoo, and A. Sarangi. 2010. Temporal variability of phosphorus flux from pike river watershed to the Missisquoi Bay of Quebec. *Current Science* 98: 58-64.

Akhtar, M., N. Ahmad, and M.J. Booij. 2008. The impact of climate change on the water resources of Hindukush–Karakorum–Himalaya region under different glacier coverage scenarios. *Journal of Hydrology* 355 (1-4): 148-163.

Aladin, N., D.R. Barker, B. Gordana, J. Brouwer, N. Davidson, L. Duker, W. Junk, H. Kaplowitz, M.D. Ketelaars, E. Kreuzberg-Mukhina, G. de la Lanza Espino, C. Lévêque, A. Lopez, R.G. Milton, P. Mirabzadeh, D. Pritchard, C. Revenga, M. Rivera, A.S. Hussainy, M. Silvius, and M. Steinkamp. 2005. Inland Water System. In: Hassan, R., R. Sholes, and N. Ash, (Eds.), *Ecosystems and Human Well-Being:Current State and Trends*. Millennium Ecosystem Assessment. Island Press, Washinghton, D.C.

Almaraz, J.J., F. Mabood, X. Zhou, I. Strachan, B. Ma, D.L. Smith. 2009. Performance of Agricultural Systems under Contrasting Growing Season Conditions in South-western Quebec. *Journal of Agronomy and Crop Science* 195 (5): 319-327.

Andersen, H.E., B. Kronvang, S.E. Larsen, C.C. Hoffmann, T.S. Jensen, and E.K. Rasmussen .2006. Climate-change impacts on hydrology and nutrients in a Danish lowland river basin. *Science of the Total Environment* 365(1-3): 223-237.

Andrews, T., M. Doutriaux-Boucher, O. Boucher, and P.M. Forster. 2011. A regional and global analysis of carbon dioxide physiological forcing and its impact on climate. *Climate Dynamics* 36 (3-4):783-792.

Aqua Terra Consultants, 2010. Watershed Modelling to Evaluate Potential Impacts of Climate and Land-use Change on the Hydrology and Water Quality of Major U.S. Drainage Basins. Aqua-Terra Consultant. Available at : http://www.aquaterra.com/projects/descriptions/gcrp.php. Accessed August 2011.

Arheimer, B., J. Andreasson, S. Fogelberg, H. Johnsson, C.B Pers, and K. Persson. 2005. Climate Change Impact on Water Quality: Model Results from Southern Sweden. *Ambio* 34(7):559-566.

Arnold, J.G., R. Srinivasan, R.S. Muttiah, and J.R. Williams. 1998. Large area hydrologic modelling and assessment part I: Model development. *Journal of the American Water Resources Association* 34(1): 73-89.

Assemblée Nationale. 2009. Loi affirmant le caractère collectif des ressources en eau et visant à renforcer leur protection. Projet de loi no 27 (2009, chapitre 21). Éditeur Officiel du Québec, Québec.

Atmospheric Environment Service. 1975.Canadian Hydrologic Atlas: Plate 25:Water Balance – Derived precipitation and evapotranspiration.

Auger, P., and J. Baudrand. 2004. Gestion Intégrée de l'eau par bassin versant au Québec: Cadre de référence pour les organismes de bassins versants prioritaires. In: Direction des politiques de l'eau (Ed.). Ministère de l'Environnement, Québec. Available at :Envirodoq ENV/2004/0009. Accessed April 2011

Bates, B.C., Z.W. Kundzewicz, S. Wu, and J.P. Palutikof. 2008. Climate Change and Water. Technical Paper of the Intergovernmetal Panel on Climate Change, IPCC Secretariat, Geneva, p. 210.

Beasley, D.B., L.F. Huggins, and E.J, Monke. 1980. Answers - a Model for Watershed Planning. *Transactions of the ASAE* 23 (4) : 938-944.

Beaudin, I., J. Deslandes, A. Michaud, and F. Bonn. 2006. Variabilité spatio-temporelle des exportations des sédiments et de phosphore dans le bassin versant de la Rivière aux Brochets au sud-ouest du Québec. *Agrosolutions* 17(1) : 1-17.

Beck, E., E. van Bochove, E. Smeltzer, and D. Leblanc. 2012. Missiquoi Bay Critical Source Area Study, Final report to the International Joint Comission. International Missisquoi Bay Study Board.

Bedient, P.B., W.C. Huber, and B.E. Vieux. 2008. *Hydrology and Floodplain Analysis.*4th ed. Prentice Hall. Upper Saddle River, NJ.

Benaman, J., and C.A. Shoemaker. 2005. An analysis of high-flow sediment event data for evaluating model performance. *Hydrological Processes* 19(3): 605-620.

Benaman, J., C.A. Shoemaker, and D.A. Haith. 2005. Calibration and validation of soil and water assessment tool on an agricultural watershed in upstate New York. *Journal of Hydrologic Engineering* 10 (5) :363-374.

Bernard, C. 1996. Estimation de l'érodabilité des principales séries de sol du Québec, à l'aide du nomographe de Wischmeier. [Estimation of different Quebec soil types' erodibility, by way of Wishmeier's nomograph]. *Agrosol* 9: 6-12.

Betts, R.A., P.M. Cox, S.E. Lee, and F.I. Woodward. 1997. Contrasting physiological and structural vegetation feedbacks in climate change simulations. *Nature.* 387 : 796-799.

Blais, S. 2002. La problématique des cyanobactéties (algues bleu-vert) à la baie Mississquoi en 2001. *Agrosolutions* 13(2) :103 :110.

Boe, J., L. Terray, E. Martin, and F. Habets. 2009. Projected changes in components of the hydrological cycle in French river basins during the 21st century. *Water Resources Research* 45 W08426.

Booty, W., D. Lam, G. Bowen, O. Resler, and L. Leon. 2005. Modelling Changes in Stream Water Quality Due to Climate Change in a Southern Ontario Watershed. *Canadian Water Resources Journal* 30(3):211-226.

Booty, W., and G. Benoy. 2009. Multicriteria review of nonpoint source water quality models for nutrients, sediments, and pathogens. *Water Quality Research Journal of Canada* 44(4): 365-377.

Borah, D.K., R. Xia, and M. Bera. 2002. DWSM - A dynamic watershed simulation model. In: Singh, V.P., Frevert, D.K. (Eds.), Mathematical Models of Small Watershed Hydrology and Applications*. Water Resources Publications*, Highlands Ranch, Colo.

Borah, D.K., and M. Bera. 2003. Watershed-scale hydrologic and nonpoint-source pollution models: Review of mathematical bases. *Transactions of the American Society of Agricultural Engineers* 46 (6):1553-1566.

Borah, D.K., and M. Bera. 2004. Watershed-scale hydrologic and nonpoint-source pollution models: Review of applications. *Transactions of the American Society of Agricultural Engineers* 47(3): 789-803.

Bos, R., C. Caudill, J. Chilton, E.M Douglas, M. Meybeck, and D. Prager. 2005. Freshwater Resources. In: Hassan, R., Sholes, R., Ash, N. (Eds.), *Ecosystems and Human Well-being: Current State and Trends. Millennium Ecosystem Assessment.* Island Press, Washinghton, D.C.

Bouraoui, F., L. Galbiati, and G. Bidoglio. 2002. Climate Change Impacts on Nutrient Loads in the Yorkshire Ouse Catchment (UK). *Hydrology and Earth System Sciences* 6(2):.197-209.

Bourque, A., and G. Simonet. 2008. "Québec" in *Vivre avec les changements climatiques au Canada: édition 2007,*. In: Lemmen, D.S., Warren, J., Lacroix, J., Bush, E. (Eds.). Gouvernement du Canada, Ottawa (Ontario), pp. 171-226.

Boutin, D. 2006. The Challenge of Reconciling Water and Agricultural Policies – The Role of Public Hearings In *Water and Agriculture: Sustainability, Markets and Policies,* 453-468. OECD Publishing, Paris, France.

Boyer, C., D. Chaumont, I. Chartier, and A.G. Roy. 2010. Impact of climate change on the hydrology of St. Lawrence tributaries. *Journal of Hydrology* 384(1-2): 65-83.

Brassard, J.-P., and B. Singh. 2008. Impacts of climate change and CO2 increase on agricultural production and adaptation options for Southern Québec, Canada. *Mitigation and Adaptation Strategies for Global Change* 13(3): 241-265.

Bunce, J.A. 2004. Carbon dioxide effects on stomatal responses to the environment and water use by crops under field conditions. *Oecologia* 140(1): 1-10.

Burakowski, E.A., C.P. Wake, B. Braswell, and D.P. Brown. 2008. Trends in wintertime climate in the northeastern United States: 1965-2005. *Journal of Geophysical Research - Atmospheres* 13-D20114

Campbell, J.L., S.V. Ollinger, G.N. Flerchinger, H. Wicklein, K. Hayhoe, and A.S Bailey. 2010. Past and projected future changes in snowpack and soil frost at the Hubbard Brook Experimental Forest, New Hampshire, USA. *Hydrological Processes* 24: 2465-2480.

Campbell, J.L., C.T. Driscoll, A. Pourmokhtarian, and K. Hayhoe. 2011. Stream flow responses to past and projected future changes in climate at the Hubbard Brook Experimental Forest, New Hampshire, United States. *Water Resources Research* 47-W02514.

Cann, D.B., P.Lajoie, and P.C. Stobbe. 1948. Soil Survey of Shefford, Brome and Missisquoi Counties in the Province of Québec. 3M-10358-12-47. Experimental Farms Services, Dominion Department of Agriculture in Co-operation with the Québec Departement of Agriculture and Macdonald College, McGill University. 94 p.

Carpenter, S.R., N.F. Caraco, D.L. Correll, R.W. Howarth, A.N. Sharpley, V.H. Smith. 1998. Nonpoint pollution of surface waters with phosphorus and nitrogen. *Ecological Applications* 8(3): 559-568.

Cattaï, J. 2004. Contour Detection in a Stratified field-scale approach to the Classification of an Agricultural Landscape from LANDSAT TM data, Case Study of the Pike River Watershed, Southern Québec. Msc. Thesis. Département de Géographie et Télédétection, Faculté des Lettres et Sciences Humaines. Université de Sherbrooke, Sherbrooke, Qc. 120p.

Chapin, F.S., P.A. Matson, and H.A. Mooney. 2002. *Principle of terrestrial ecosystem ecology*. New-York, NY. Springer-Verlag.

Cohen, S.J., and M.W. Waddell. 2009. *Climate change in the 21st century*. Montréal. McGill-Queen's University Press.

Corporation Bassin Versant Baie Missisquoi, 2003. Développement de l'agriculture durable dans le bassin versant de la baie Missisquoi. Mémoire du Comité de Bassin Versant de la Baie Missisquoi (CBVBM) pour la consultation publique sur le développement durable de la production porcine au Québec. Corporation de Bassin Versant de la Baie Missisquoi, Saint-Jean-sur-Richelieu,Québec,Canada, p. 45.

Coulibaly, P., and B.Y. Dibike. 2004. Downscaling and Climate Change Impact Study in Saguenay River System. Projet n° S02-15-01. McMaster University, Department of Civil Engineering/School of Geography and Geology, Hamilton Ontario, p. 85.

CRAAQ. 2010. *Guide de référence en fertilisation, 2d édition.*Eds : Parent., L.E. and G.Gagné. Québec. CRAAQ. 470p.

Dayyani, S., S.O. Prasher, A. Madani and C.A.Madramootoo. 2012. Impact of climate change on the hydrology and nitrogen pollution in a tile drained agricultural watershed in eastern Canada. Transactions of the ASABE. 55(2): 389-401

de Elia, R. and H. Cote. 2009. Climate and climate change sensitivity to model configuration in the Canadian RCM over North America. Meteorologische Zeitschrift 19(4): 325-339.

De Jong, R., B. Qian, and J.Y. Yang. 2008. Modelling nitrogen leaching in Prince Edward Island under climate change scenarios. *Canadian Journal of Soil Science* 88(1): 61-78.

Déqué, M. and J.P. Piedelievre. 1995. High resolution climate simulation over Europe. *Climate Dynamics* 11(6): 321-339.

Deslandes, J., A. Michaud, A.,and F. Bonn. 2002. Développement et validation des indicateurs agroenvironnementaux associés aux pertes diffuses de phosphore dans le bassin-versant de la rivière aux Brochets. *Agrosol*, 13(2):111-123.

Deslandes, J., I. Beaudin, A. Michaud, F. Bonn, and C.A. Madramootoo. 2007. Influence of landscape and cropping system on phosphorus mobility within the pike river watershed of Southwestern Quebec: Model parameterization and validation. *Canadian Water Resources Journal* 32(1) : 21-42.

Di Luzio, M., R. Srinivasan, J.G., Arnold, and S.L. Neitsch. 2002. ArcView interface For SWAT2000 User's Guide. Blackland Research & Extension Center - Texas Agricultutal Experiment Station / Grassland, Soil and Water Research Laboratory - USDA Agricultural Research Service, Temple, Texas p. 351.

Donigian, A.S.J., B.R. Bicknell, and J.C. Imhoff. 1995. Hydrological simulation program - Fortran. In: Singh, V.P. (Ed.), Computer Models of Watershed Hydrology. *Water Resource Publications*, Highlands Ranch, Colo. pp395-442.

Douglas-Mankin, K.R., R. Srinivasan, and J.G. Arnold. 2010. Soil and Water Assessment Tool (Swat) Model: Current Developments and Applications. *Transactions of the ASABE* 53(5): 1423-1431.

Eastman, M., 2007. Filed-Scale Nutrient Transport Monitoring and Modelling of Subsurface and Naturally Drained Agricultural Lands. Msc. Thesis. Bioresource Engineering Dept. McGill University, Montréal.109p.

Eckhardt, K., and U. Ulbrich. 2003. Potential impacts of climate change on groundwater recharge and stream flow in a central European low mountain range. *Journal of Hydrology* 284(1-4): 244-252.

Engel, B., D. Storm, M. White, J. Arnold, and M. Arabi. 2007. A hydrologic/water quality model application protocol. *Journal of the American Water Resources Association* 43(5): 1223-1236.

Enright, P., and C.A. Madramootoo. 2004. Phosphorus losses in surface runoff and subsurface drainage waters on two agricultural fields in Quebec. In *Proceedings of the 8th International Drainage Symposium - Drainage VIII*, pp. 160-170. Sacremento, California.

Environment Canada, 2007. Canadian Climate Data On-Line Customized Search - Canada's National Climate Archive. National Climate Data and Information Archive. Environment Canada. Available at: http://www.climate.weatheroffice.gc.ca/climateData/canada_e.html. Accessed July 2008.

Environment Canada, 2008. Canadian Climate Normals or Averages 1971-2000. National Climate Data and Information Archive. Environment Canada. Available at: http://www.climate.weatheroffice.gc.ca/climate_normals/index_e.html . Accessed October 2009.

Environment Canada, 2011. Canadian Climate Normals or Averages 1971-2000. National Climate Data and Information Archive. Environment Canada. Available at: http://www.climate.weatheroffice.gc.ca/climate_normals/index_e.html . Accessed January 2012.

EPA, 2009. National Water Quality Inventory report to Congress - 2004 Reporting Cycle. United States Environmental Protection Agency Office of Water, EPA 841-R-08-001, Washington, DC 20460.

ESCER, 2009. Réseau canadien en modélisation et diagnostics du climat régional (MDCR) - Projets de recherche (2006-2010). Centre pour l'étude et la simulation du climat a l'échelle régionale (ESCER), Faculté des sciences de l'UQAM. Available at : http://www.mrcc.uqam.ca/ Accessed February 2009.

Ewen, J., G. Parkin, and P.E. O'Connell. 2000. SHETRAN:Distributed River Basin Flow and Transport Modelling System. *ASCE J Hydrologic Eng*. 5(3): 250-258.

Ficklin, D.L., Y. Luo, E. Luedeling, S.E. Gatzke, and M. Zhang. 2010. Sensitivity of agricultural runoff loads to rising levels of CO2 and climate change in the San Joaquin Valley watershed of California. *Environmental Pollution* 158 (1):223-234.

Flato, G.M., and G.J. Boer. 2001. Warming asymmetry in climate change simulations. *Geophysical Research Letters* 28(1): 195-198.

Follett, F.R. 1995. Fate and Transport of Nutrients: Nitrogen, Working Paper No 7. In: Agricultural Research Service: Soil-Plant-Nutrient Research Unit (Ed.). USDA, NRCS, Fort Collins, Colorado.

Fowler, H.J., S. Blenkinsop, and C. Tebaldi. 2007. Linking climate change modelling to impacts studies: Recent advances in downscaling techniques for hydrological modelling. *International Journal of Climatology* 27(12):1547-1578.

Gagnon, P., B. Konan, A.N Rousseau, and M. Slivitzky. 2009. Hydrometeorological Validation of a Canadian Regional Climate Model Simulation within the Chaudière and Châteauguay Watersheds (Québec, Canada). *Canadian Journal Civil Engineering* 36(2) : 253-266.

Gangbazo, G., J. Roy, and A. Le Page. 2005. Capacité de support des activitées agricoles par les rivières: le cas du phosphore total. In: *Direction* du suivi de l'état de l'environnment, M. (Ed.), Québec, p. 36.

Gleckler, P.J., K.E. Taylor, and C. Doutriaux. 2008. Performance metrics for climate models. *Journal of Geophysical Research- Atmospheres* 113-D06104.

Global Environment Facility. 2010. Strenghtening Cooperation in the Danube River Basin. Available at: http://www.thegef.org/gef/node/2183. Accessed November 2011

Gollamudi, A. 2006. Hydrological and Water Quality Modelling of Agricultural Fields in Québec. Msc Thesis. Department of Bioresource Engineering. McGill University, Montréal, 117p.

Gollamudi, A., C.A. Madramootoo, P. Enright. 2007. Water quality modelling of two agricultural fields in southern Quebec using SWAT. *Transactions of the ASABE* 50 (6): 1973-1980.

Graham, L.P., L. Andréasson, B. Carlsson. 2007. Assessing climate change impacts on hydrology from an ensemble of regional climate models, model scales and linking methods - A case study on the Lule River basin. *Climatic Change* 81(Supplement):293-307.

Green, W.H. and G.A. Ampt. 1911. Studies on soil physics,1. The flow of air and water through soils. *Journal of Agricultural Sciences* 4: 11-24.

Groupe de travail Québec-Vermont. 2000. Partage des responsabilités entre le Québec et le Vermont pour la réduction des charges de phosphore dans la baie Missisquoi. In: Gruessner, B., P. Benedict, R. Hopkins, R. Lauzier, M. Mimeault, M. Simoneau, E. Smeltzer (Eds.). Groupe de travail Vermont-Québec sur la réduction du phosphore au Comité directeur du lac Champlain. 29p.

Hades,A. 2003. Nos Lacs. *Les connaître pour mieux les protéger*. Nouv. Ed. Québec,Québec. Fides.

Hargreaves, G.L., G.H. Hargreaves, and J.P. Riley. 1985. Agricultural Benefits for Senegal River Basin. *Journal of Irrigation and Drainage Engineering* 11(2): 113-124.

Hesse, C., V. Krysanova, J. Pazolt, F. Hattermann. 2008. Eco-Hydrological modelling in a highly regulated lowland catchment to find measures for improving water quality. *Ecological Model* 218(1-2):135-148.

Hodgkins, G.A., R.W.Dudley, and T.G. Huntington. 2003. Changes in the timing of high river flows in New England over the 20th Century. *Journal of Hydrology* 278 (1): 244-252.

Hodgkins, G.A., and R.W. Dudley. 2006. Changes in the timing of winter-spring stream flows in eastern North America, 1913-2002. *Geophysical* Research Letters 33-L06402

Horan, R.D., and M.O. Ribaudo. 1999. Policy Objectives and Economic Incentives for Controlling Agricultural Sources of NonPoint Pollution. *Journal of the American Water Resources Association* 35.(5):1023-1035.

Huntington, T.G., G.A. Hodgkins, B.D. Keim, R.W. Dudley. 2004. Changes in the proportion of precipitation occurring as snow in New England (1949-2000). *Journal of Climate* 17(13):2626-2636.

Huntington, T.G. 2006. Evidence for intensification of the global water cycle: Review and synthesis. *Journal of Hydrology* 319(1-4): 83-95.

IPCC, 2007. *Climate Change 2007: The Physical Science Basis.* . In: Solomon, S., Qin, D., Manning, Z., Chen, Z., Marquis, M., Averyt, K.B., Tignor, M., Miller, H.L. (Eds.), Contribution of Working Group I to the Fourth Assessment Report of the Intergovernmental Panel on Climate Change,. Cambridge University Press, Cambridge, UK and New York,NY,USA. 996p.

Jamieson, A., C.A. Madramootoo, and P. Enright. 2003. Phosphorus losses in surface and subsurface runoff from a snowmelt event on an agricultural field in Quebec. *Canadian Biosystems Engineering / Le Genie des biosystems au Canada* 45:1.1-1.7

Jennings, E., N. Allott, D.C. Pierson, E.M. Schneiderman, D. Lenihan, P. Samuelsson, and D. Taylor. 2009. Impacts of climate change on phosphorus loading from a grassland catchment: Implications for future management. *Water Research* 43(17):4316-4326.

Jeppesen, E., B. Kronvang, M. Meerhoff, M. Søndergaard, K.M. Hansen, H.E. Andersen, T.L. Lauridsen, L. Liboriussen, M. Beklioglu, A. Ozen, and J.E. Olesen. 2009. Climate change effects on runoff, catchment phosphorus loading and lake ecological state, and potential adaptations. *Journal of Environmental Quality* 38(5): 1930-1941.

Jha, M., Z. Pan, E.S. Tackle, and R. Gu. 2004. Impacts of climate change on stream flow in the Upper Mississippi River Basin: A regional climate model perspective. *Journal of Geophysical Research-Atmospheres* 109-D09105

Jones, C.A., C.V. Cole, A.N. Sharpley, and J.R. Williams. 1984. A simplified soil and plant phosphorus model: I. Documentation. *Soil Science Society of America Journal* 48 (4): 800-805.

Jyrkama, M.I. and J.F. Sykes. 2007. The impact of climate change on spatially varying groundwater recharge in the grand river watershed (Ontario). *Journal of Hydrology* 338(3-4) 237-250.

Kergoat, L., S. Lafont, H. Douville, B. Berthelot, G. Dedieu, S. Planton, and J.F. Royer2002. Impact of doubled CO_2 on global-scale leaf area index and evapotranspiration: Conflicting stomatal conductance and LAI responses. *Journal of Geophysical Research-Atmospheres* 107-4808

La Financière agricole. 2008. Événements - État des cultures. Gouvernement du Québec. Available at: http://www.fadq.qc.ca/acces_medias/evenements/etats_des_cultures/etat_des_cultures_2012.html. Accessed September 2008 and July 2011.

La Financière agricole. 2009. Programme d'assurance stabilisation des revenues agricoles. Mesures D'écoconditionalité.

Lake Champlain Basin Program. 2008. State of of the lake and ecosystem indicators report - 2008. Available at http://www.lcbp.org/PDFs/SOL2008-web.pdf Accessed May 2009.

Laprise, R. 2008. Regional climate modelling. *Journal of Computational Physics* 227(2008) : 3641-3666.

Lavoie, I., I. Laurion, A. Warren, and W. Vincent. 2007. Les fleurs d'eau de cyanobactéries, revue de littérature. INRS. Rapport n°916. 124p.

Leavesley, G.H., R.W. Lichty, B.M. Troutman, and L.G. Saindon. 1983. Precipitation-Runoff Modelling System - User's Manual. In: 83-4238, U.W.R.I.r.N. (Ed.). U.S. Geologial Survey, Washinghton, D.C.

Leipprand, A., and D. Gerten. 2006. Global effects of doubled atmospheric CO_2 content on evapotranspiration, soil moisture and runoff under potential natural vegetation. *Hydrological Sciences Journal-Journal Des Sciences Hydrologiques* 51(1):171-185.

Levesques, G. (2003).Mise en oeuvre du modèle SWAT sur le bassin de la rivière Aux Brochets. Mémoire de DESS. Institut de Recherche et Développement en Agroenvironnement, Québec. Université Monnet de Saint-Étienne, France and École nationale d'ingénieurs de Saint-Étienne, France.

Lettenmaier, D., D. Major, L. Poff, and S. Running. 2008. Water Resources. The effects of climate change on agriculture, land resources, water resources, and biodiversity in the United States. A report by the U.S. Climate Change Science Program and the Subcommittee on Global Change Research, Washington, DC., USA. 362p.

Leung, L.R., Y. Qian, and X. Bian. 2003. Hydroclimate of the western United States based on observations and regional climate simulation of 1981-2000. Part I: Seasonal statistics. *Journal of Climate* 16(12): 1892-1911.

Madramootoo, C.A., P. Enright, C. Laflamme, G. Simard, H. Fyles. 2004. Towards a Better Understanding of Phosphorus Dynamics in Baie Missisquoi. Restoring the Health of the Lake Champlain Basin. Brace Center for Water Resources Management, McGill University, Montréal,Canada. 40p.

Mailhot, A., S. Duchesne, D. Caya, and G. Talbot. 2007. Assessment of future change in intensity-duration-frequency (IDF) curves for Southern Quebec using the Canadian Regional Climate Model (CRCM). *Journal of Hydrology* 347(1-2) :197-210.

MAPAQ, 2009a. Prime-Vert.Publication 09-0013. Québec.Gouvernement du Québec.

MAPAQ, 2009b. Rapport Annuel de Gestion 2008-2009. Québec. Gouvernement du Québec.

Marshall, E., and T. Randhir. 2008. Effect of climate change on watershed system: A regional analysis. *Climatic Change* 89 (3-4):263-280.

McElroy, A.D., S.Y. Chiu, J.W. Nebgen, A. Aleti, and F.W. Bennett. 1976. Loading functions for assessment of water pollution from nonpoint sources. EPA document EPA 600/2-76-151, USEPA, Athens,GA.

McFarlane, N.A., J.F. Scinocca, M. Lazare, R. Harvey, D. Verseghy, and J. Li. 2005. The CCCma third generation atmospheric general circulation model. Rapport interne du Centre Canadien de la Modélisation et de l'Analyse Climatique, 25p. Available at http://www.cccma.ec.gc.ca/papers/jscinocca/AGCM3_report.pdf.

MDDEP, 2002. Politique Nationale de l'Eau. L'eau. La vie. L'avenir. Gouvernement du Québec, Québec. Available at http://www.mddep.gouv.qc.ca/eau/politique/ Accessed July 2010.

MDDEP. 2008. Bilan des lacs et cours d'eau touchés par une fleur d'eau d'algues bleu-vert au Québec de 2004-2010. Québec.Gouvernement du Québec. Available at : http://www.mddep.gouv.qc.ca/eau/algues-bv/bilan/liste_comparative.asp. Accessed June 2009.

MDDEP. 2009. Les fleurs d'eau d'algues bleu-vert en 2009, une responsabilité collective. Bilan final des plans d'eau touchés par une fleur d'eau d'algues bleu-vert en 2009. Gouvernement du Québec.

MDDEP. 2011. Les plans d'eau touchés par une fleur d'eau d'algues bleu-vert. Bilan final de la gestion des épisodes en 2011. Québec. Gouvernement du Québec.

MENV, 2003. Synthèse des informations environnementales disponibles en matière agricole au Québec. Direction des politiques du secteur agricole, Ministère de l'Environnement. Envirodoq ENV/ 2003/0025. 143p.

Michaud, A., J. Deslandes, and J. Desjardin. 2004. Réseau d'actions concertées en bassins versants agricoles., [Network of holistic undertakings on agricultural watersheds] Rapport Final Projet 212, to the Fonds d'action québécois pour le développement durable. Québec City, Qc. Institut de Recherche et Developpment Durable en Agroenvironnement. 23p.

Michaud, A., J. Deslandes, and I. Beaudin. 2006. Modélisation de l'hydrologie et des dynamiques de pollution diffuse dans le bassin-versant de la Rivière Aux Brochets à l'aide du modèle SWAT.Rapport Final. Sainte-Foy. Institut de Recherche et Développement en Agroenvironnement. 117p

Michaud, A.R., I. Beaudin, J. Deslandes, F. Bonn, and C.A. Madramootoo. 2007. SWAT-predicted influence of different landscape and cropping system alterations on phosphorus mobility within the Pike River watershed of south-western Québec. *Canadian Journal of Soil Science* 87(3):329-344.

Michaud, A., S. Seydoux, I. Beaudin, and C. Gombault. 2008. Beneficial Management Practices and Water Quality:Hydrological Modelling of Two Basins in the Montérégie Region (Québec). National Agri-Environmental Standards Initiative Technical Series Report No. 4-65. Québec. Institut de Recherche et Développement en Agroenvironnemnt. 129p.

Michaud, A., S.-C. Poirier, J. Desjardins, M. Grenier, and I. Saint-Laurent. 2009a. Évaluation des exportation de surface et souterraines de phosphore en sol drainé. Raport Final de projet. Québec. Institut de Recherche et Développement en Agroenvironment (IRDA) et MAPAQ. 39p.

Michaud, A.R., F. Ruyet, and I. Beaudin. 2009b. Évaluation des outils de gestion agroenvironnementale à l'échelle du bassin versant dans un cadre opérationnel de service-conseil à la ferme. Dans le cadre du projet Lisière verte. Institut de recherche et de développement en agroenvironnement (IRDA), Coopérative de solidarité du bassin versant de la rivière au Brochet, Dura-Club, AAC (PASCAA) et MAPAQ, Québec. p63.

Michaud, A. 2010. Personal communication.July 2010. At Institut de Recherche et Developement en Agroenvironmment.

Mimeault, M. 2004. Missisquoi Bay and Lake Champlain Management. In: Brace Centre for Watershed Resources Management (Ed.), Restoring the Health of the Lake Champlain Basin. Brace Centre for Watershed Resources Management, McGill University Montréal, Canada. 40p.

Minville, M., F. Brissette, and R. Leconte. 2008. Uncertainty of the impact of climate change on the hydrology of a nordic watershed. *Journal of Hydrology* 358(1-2): 70-83.

Minville, M., F. Brissette, S. Krau, and R. Leconte. 2009. Adaptation to Climate Change in the Management of a Canadian Water-Resources System Exploited for Hydropower. *Water Resources Management* 23 (14):2965-2986.

Missisquoi Bay Phosphorus reduction Task Force. 2005. Workplan of the Missisquoi Bay Watershed Phophorus Load Monitoring Program. Vermont Agency of Natural Resource, Ministère du Développment Durable, de l'environnement et des Parcs du Québec. 14p.

Monteith, J.L. 1965. Evaporation and the environment. In *The state and movement of water in the living organism, XIXth symposium Society for Experimental Biology*, Swansea, Cambridge University Press.

Moriasi, D.N., J.G. Arnold, M.W. Van Liew, R.L. Bingner, R.D. Harmel, and T.L. Veith. 2007. Model evaluation guidelines for systematic quantification of accuracy in watershed simulations. *Transactions of the ASABE* 50(3): 885-900.

Nakicenovic, N., J. Alcamo, G. Davis, B. de Vries, J. Fenhann, S. Gaffin, K. Gregory, A. Grübler, T.Y. Jung, T. Kram, E.L.L. Rovere, L. Michaelis, S. Mori, T. Morita, W. Pepper, H. Pitcher, L. Price, K. Riahi, A. Roehrl, H.H. Rogner, A. Sankovski, M. Schlesinger, P. Shukla, S. Smith, R. Swart, H. van Rooijen, and N. Victor, a.Z.D. 2000. *IPCC Special Report on Emissions Scenarios*. Cambridge, U.K.: Cambridge University Press.

Nearing., M.A., L. Darrell Norton, and X. Zhang. 2001. Chapter2: Soil erosion and sedimentation. In *Agricultural NonPoint Source Pollution : watershed management and hydrology.*29-58. Ritter, W.F., and A. Shirmohammadi. Boca raton, Fla. Lewis Publishers.

Nearing, M.A., F.F. Pruski, and M.R. O'Neal. 2004. Expected climate change impacts on soil erosion rates: A review. *Journal of Soil and Water Conservation* 59(1): 43-50.

Nearing, M.A., V. Jetten, C. Baffaut, O. Cerdan, A. Couturier, M. Hernandez, Y. Le Bissonnais, M.H. Nichols, J.P. Nunes, C.S. Renschler, V. Souchère, and K. van Oost. 2005. Modelling response of soil erosion and runoff to changes in precipitation and cover. *CATENA* 61(2-3), 131-154.

Neitsch, S.L., J.G. Arnold, J.R. Kiniry, R. Srinivasan, and J.R Williams. 2004. Input/Output File Documentation. Version 2005. Grassland, Soil and Water Research Laboratory - Agricultural Research Service ; Blackland Research Center - Texas Agricultural Experiment Station Temple,Texas. 541p.

Neitsch, S.L. 2005. Differences between SWAT2000 and SWAT2005. Grassland, Soil and Water Research Laboratory - Agricultural Research Service ; Blackland Research Center - Texas Agricultural Experiment Station, Texas. 7p.

Neitsch, S.L., J.G. Arnold, J.R. Kiniry, and J.R. Williams. 2005. Soil and Water Assessment Tool, Theoretical Documentation. Grassland, Soil and Water Research Laboratory - Agricultural Research Service ; Blackland Research Center - Texas Agricultural Experiment Station, Texas.494p.

Nunes, J.P., J. Seixas, and N.R. Pacheco. 2008. Vulnerability of water resources, vegetation productivity and soil erosion to climate change in Mediterranean watersheds. *Hydrological Processes* 22 (16): 3115-3134.

Orr, P., J. Colvin, and D. King. 2007. Involving stakeholders in integrated river basin planning in England and Wales. *Water Resources Management* 21(1): 331-349.

Ouranos. 2010a. Climate Sciences, Climate Simulations. Montréal. Consortium Ouranos. Available at http://www.ouranos.ca/en/scientific-program/climate-sciences/climate-simulations/ Accessed: January 2010.

Ouranos, 2010b. Consortium On Regional Climatology and Adaptation to Climate Change. Montréal, Qc, Canada. Available at:http://www.ouranos.ca/en/default.php

Overton, D.E. 1966. Muskingum Flood Routing of Upland Stream flow. *Journal of Hydrology* 4(1966): 185-2000.

Pan, Z., J.H. Christensen, R.W. Arritt, W.J. Gutowski Jr, E.S. Takle, and F. Otieno. 2001. Evaluation of uncertainties in regional climate change simulations. *Journal of Geophysical Research -Atmospheres* 106 (D16): 17735-17751.

Parker, G.T., R.L Droste, and K.J. Kennedy. 2008. Modelling the effect of agricultural best management practices on water quality under various climatic scenarios. *Journal of Environmental Engineering and Science* 7(1):9-19.

Perrone, J., and C.A. Madramootoo. 1998. Improved curve number selection for runoff prediction. *Canadian Journal of Civil Engineering* 25(4):728-734.

Pierson, D., L. Arvola, N. Allott, M. Järvinen, E. Jennings, L. May, K. Moore, and E. Schneiderman. 2010. Chapter 9. Modelling the effects of climate change on the supply of phosphate-phosphorus. In *The impact of climate change on european lakes. Aquatic Ecologic Series* 2010. Vol4. G.Georges. @Us Government 2010. Springer.

Plummer, D.A., D.Caya, A. Frigon, H.Côté, M. Giguère,D. Paquin, S. Biner, R. Harvey, and R. De Elia. 2006. Climate and climate change over North America as simulated by the Canadian RCM. *Journal of Climate* 19(13): 3112-3132.

Priestley,C.H.B, and R.J. Taylor. 1972. On the Assessment of Surface Heat Flux and Evaporation Using Large-Scale Parameters. *Monthly Weather Review* 100(2):81-92.

Prudhomme, C., and H. Davies. 2009. Assessing uncertainties in climate change impact analyses on the river flow regimes in the UK. Part 2: Future climate. *Climatic Change* 93(1-2): 197-222.

Pruski, F.F., and M.A. Nearing. 2002a. Climate-induced changes in erosion during the 21st century for eight US locations. *Water Resources Research* 38(12):1298-1109

Pruski, F.F.and M.A. Nearing. 2002b. Runoff and soil-loss responses to changes in precipitation: A computer simulation study. *Journal of Soil and Water Conservation* 57(1):7-16.

Québec. 2012. Politique de protection des rives, du littoral et des plaines inondables. Loi sur la qualité de l'environnement (L.R.Q. ,c.Q-2,a.2.1). Gouvernement du Québec.

Quilbé, R., A.N. Rousseau, J.S. Moquet, N.B. Trinh, Y. Dibike, P. Gachon, and D. Chaumont. 2008. Assessing the effect of climate change on river flow using general circulation models and hydrological Modelling - Application to the chaudière River, Québec, Canada. *Canadian Water Resources Journal* 33(1):73-94.

Rahman, M., T. Bolisetti, and R. Balachandar. 2010. Effect of climate change on low-flow conditions in the Ruscom river watershed, Ontario. *Transactions of the ASABE* 53(3): 1521-1532.

Raupach, M.R., G. Marland, P. Ciais, C. Le Quéré, J.G. Canadell, G. Klepper, and C.B. Field.2007. Global and regional drivers of accelerating CO_2 emissions. *Proceedings of the National Academy of Sciences of the United States of America* 104(24): 10288-10293.

Refsgaard, J.C., B. Storm, and A. Refsgaard. 1995. Recent developments of the Systeme Hydrologique Europeen (SHE) towards the MIKE SHE. In *Modelling and Management of Sustainable Basin-Scale Water Resource Systems.Proc. Boulder Symp., July 1995.*Ed:Simonovic. S.P.,Z. Kundzcwicz, D.Rosberg., and K Takeuchi.IAHS Publ n° 231:427-434.

Ribaudo, M.O., R.D. Horan, and M.E. Smith. 1999. Economics of Water Quality Protection From Nonpoint Sources:Theory and Practice. Resource Economics Division, Economic Research Service, U.S Department of Agriculture. Agricultural Economic Report No. 782.

Ritter, W.F., and A. Shirmohammadi. 2001. Agricultural nonpoint source pollution: watershed management and hydrology. Boca Raton, Fla. Lewis Publishers.

Scinocca, J.F., and N.A. McFarlane. 2004. The variability of modeled tropical precipitation. *Journal of the Atmospheric Sciences* 61(16): 1993-2015.

Sharpley, A.N., S.C. Chapra, R. Wedepohl, J.T. Sims, T.C. Daniel, and K.R. Reddy. 1994. Managing agricultural phosphorus for protection of surface waters - Issues and options. *Journal of Environmental Quality* 23(3): 437-451.

Sharpley, A.N. 1995. Soil phosphorus dynamics: agronomic and environmental impacts. *Ecological Engineering* 5(2-3): 261-279.

Sharpley, A.N., T. Daniel, T. Sims, J. Lemuyon, R. Stevens, and R. Parry. 2003. Agricultural phosphorus and eutrophication, Second Edition. U.S. Department of Agriculture - Agricultural Research Service. ARS-149 (Ed.) 44p.

Simoneau, M. 2007. État de l'écosystème aquatique du bassin versant de la baie Missisquoi:faits saillants 2001-2004. In: Direction du suivi de l'état de l'environnment (Ed.). Ministère du Développement Durable, de l'environement et des Parcs, Québec.18p.

Singh, J., H.V. Knapp, J.G. Arnold, and M. Demissie. 2005. Hydrological modelling of the iroquois river watershed using HSPF and SWAT. *Journal of the American Water Resources Association* 41(2): 343-360.

Smeltzer, E., F.Dunlap, and M. Simoneau. 2009. Lake Champlain phosphorus concentrations and loading rates, 1990-2008. Fall 2009.Technichal report No.57. LCBP. Grand Isle, VT.

Stager, C.T. and M. Thill. 2010. Climate Change in the Champlain Basin, What natural resource managers can expect and do. The Nature Conservancy. 44p.

Statistiques Canada. 2008. Recencement de l'agriculture 2006; Tableaux de données sur les exploitations et les exploitants agricoles : Bétail, volail et abeille. Available at : http://www.statcan.gc.ca/pub/95-629-x/2007000/4123855-fra.htm. Accessed September 2011.

Sulis, M., C. Paniconi, C. Rivard, R. Harvey, and D. Chaumont. 2011. Assessment of climate change impacts at the catchment scale with a detailed hydrological model of surface-subsurface interactions and comparison with a land surface model. *Water Resources Research* 47-W01513

SWCS. 2003. Conservation Implications of Climate Change:Soil Erosion and Runoff From Cropland. Soil and Water Conservation Society. Iowa. Report No 68-4A75-2-98.25p.

Tabi, M., L. Tardif, D. Carrier, G. Laflamme, and M. Rompré. 1990. Inventaire des problèmes de dégradation des sols agricoles du Québec -Région agricole 6, Richelieu, Saint-Hyacinthe [Quebec Inventory of Agricultural Soil Degradation Problems - Agricultural Region 6, Richelieu, Saint-Hyacynthe]. Governemnet of Quebec Publication 91-0025.Quebec City, QC.

Thériault, J.E., L. Choinière, E. Pageau, and H. Talbot. 1943. Carte des sols du comté d'Iberville. Service de la grande culture du Ministère de l'agriculture du Ministère de l'agriculture et Service de la cartographie économique du Ministère de l'industrie et du commerce, Québec, QC, Canada.

Tian, Y., Z. Huang, and W. Xiao. 2010. Reductions in non-point source pollution through different management practices for an agricultural watershed in the Three Gorges Reservoir Area. *Journal of Environmental Sciences* 22(6): 184-191.

Tolson, B.A., and C.A. Shoemaker. 2004. Watershed modelling of the cannonsville basins using SWAT2000:Model development, calibration and validation for the prediction of flow, sediment, and phosphorus transport to the cannonsville reservoir. Version 1.0., Technical Report. School of Civil and Environmental Engineering,Cornell University, Ithaca, NY.

Troy, A., W. Wang, and D. Capen. 2007. Updating the Lake Champlain Basin Land-use Data to Improve Prediction of Phosphorus Loading. Grande-Isle, VT.121p.

UCAR. 2007. North American Regional Climate Change Assessment Program NARCCAP. In: Research, U.C.f.A. (Ed.). University Corporation for Atmospheric Research. Available at http://www.narccap.ucar.edu/. Accessed August 2011

Uppala, S. M., P. W. KÅllberg, A. J. Simmons, U. Andrae, V. Da Costa Bechtold, M. Fiorino, J. K. Gibson, J. Haseler, A. Hernandez, G. A. Kelly, X. Li, K. Onogi, S. Saarinen, N. Sokka, R. P. Allan, E. Andersson, K. Arpe, M. A. Balmaseda, A. C. M. Beljaars, L. Van De Berg, J. Bidlot, N. Bormann, S. Caires, F. Chevallier, A. Dethof, M. Dragosavac, M. Fisher, M. Fuentes, S. Hagemann, E. Hólm, B. J. Hoskins, L. Isaksen, P. A. E. M. Janssen, R. Jenne, A. P. Mcnally, J.-F. Mahfouf, J.-J. Morcrette, N. A. Rayner, R. W. Saunders, P. Simon, A. Sterl, K. E. Trenberth, A. Untch, D. Vasiljevic1, P. Viterbo, J. Woollen. 2005. -The ERA-40 re-analysis. *Quarterly Journal of the Royal Meteorological Society* 131 (612):2961-3012

USDA-NRCS. 1999. Soil Survey Geographic (SSURGO) Database for Franklin County VT011. . U.S Departement of Agriculture, Natural Resources Conservation Service.

USDA-SCS, 1972. Section 4 Hydrology. In *National Engineering Handbook*, US Departement of Agriculture-Soil Conservation Service:Washinghton DC.

USDA-SCS, 2006. Section 4-10.Hydrology. In *National Engineering Handbook*, Part 630. US Departement of Agriculture-Soil Conservation Service:Washinghton DC.

Vadas, P.A., and M.J White. 2010. Validating soil phosphorus routines in the SWAT model. *Transactions of the ASABE* 53(5): 1469-1476.

Van Liew, M.W., J.G. Arnold, and J.D. Garbrecht. 2003. Hydrologic simulation on agricultural watersheds: Choosing between two models. *Transactions of the ASAE* 46(6): 1539-1551.

Verseghy, D.L. 1991. CLASS - a Canadian land surface scheme for GCMs. I. Soil model. *International Journal of Climatology* 11: 111-133.

Verseghy, D.L., N.A. McFarlane, and M. Lazare. 1993. CLASS - a Canadian land surface scheme for GCMs, II. Vegetation model and coupled runs. *International Journal of Climatology* 13: 347-370.

Walker, W. 1998. Flux, Stream loads computations, version 5.0. Environmental laboratory USAE Waterways Experiment Station. Vischsburg, Misissipi, USA.

Wang, Q.G., G. Gu, and Y. Higano. 2006a. Toward integrated environmental management for challenges in water environmental protection of lake Taihu basin in China. *Environmental Management* 37(5): 579-588.

Wang, S., R. McGrath, T. Semmler, C. Sweeney, and P.Nolan. 2006b. The impact of the climate change on discharge of Suir River Catchment (Ireland) under different climate scenarios. *Natural Hazards and Earth System Science* 6(3): 387-395.

Webster, A.J., P.J. Thorburn, P.C. Roebeling, H.L. Horan, and J.S. Biggs. 2009. The expected impact of climate change on nitrogen losses from wet tropical sugarcane production in the Great Barrier Reef region. *Marine and Freshwater Research* 60(11):1159-1164.

Whitfield, P.H. and A.J. Cannon. 2000. Recent variations in climate and hydrology in Canada. *Canadian Water Resources Journal* 25(1): 19-65.

Williams, J.R. 1975. Sediment routing for agricultural watersheds. *JAWRA Journal of the American Water Resources Association* 11(5): 965-974.

Williams, J.R. and R.W. Hann. 1978. Optimal operation of large agricultural watersheds with water quality constraints., Technical Report No.96. Texas Water Resources Institute, Texas A&M University.

Wischmeier, W.H., C.B. Jonhson, and B.V. Cross. 1971. A Soil Erodibility nomograph for farmland and construction sites. *Journal of Soil and Water Conservation* 26(5): 189-192.

Wischmeier, W.H. and D.D Smith. 1978. Predicting rainfall erosion losses. A guide to conservation planning. U.S. Department of Agriculture, Agricultural Handbook n° 537 In *Conservation Implications of Climate Change:Soil Erosion and Runoff From Cropland.* Soil and Water Conservation Society. 2003. Iowa. Report No 68-4A75-2-98.25p.

Yagouti, A., G. Boulet, L. Vincent, L. Vescovi, and E. Mekis. 2008. Observed changes in daily temperature and precipitation indices for southern Québec, 1960-2005. *Atmosphere - Ocean* 46(2):243-256.

Yang, J., P.Reichert, K.C. Abbaspour, J. Xia, and H. Yang. 2008. Comparing uncertainty analysis techniques for a SWAT application to the Chaohe Basin in China. *Journal of Hydrology* 358(1-2):1-23.

Yang, Y., and L. Wang. 2010. A Review of Modelling Tools for Implementation of the EU Water Framework Directive in Handling Diffuse Water Pollution. *Water Resources Management* 24(9):1819-1843.

Young, R.A., C.A. Onstad, D.D Bosch, and W.P Anderson. 1989. Agnps - a Nonpoint-Source Pollution Model for Evaluating Agricultural Watersheds. *Journal of Soil and Water Conservation* 44(2):168-173.

Zhang, X., L.A. Vincent, W.D. Hogg.and A. Niitsoo. 2000. Temperature and precipitation trends in Canada during the 20th century. *Atmosphere - Ocean* 38(3):395-429

APPENDIX A : Inputs for SWAT calibration and parameterization

Table A1: Tables displaying schedules of simulated field operation management per crops

Crop	Year	Pre-plant manure spreading (N and P) (45% of annual inputs for crops)	N mineral fertilization (1/2 of total input)	Spring field work (Harrowing)	Seedling and P minral fertilization	First hay harvest	Manure spreading after first hay harvest (1/2 annual input)	Post-emergence manure spreading (36% of annual inputs for crop)	N mineral fertilization (1/2 total input)	Second hay harvest	Manure spreading after second hay harvest (Mineral N and P)	Third hay harvest	Manure spreading after third hay harvest (1/2 of annual input)	Crop harvest	Fall manure spreading (19% of annual inputs for crops)	Fall field work (ploughing tilling)
Pasture	1998	Apr 23,				Jun 9,	Jun 10,			Aug 5,	Aug 6,	Sep 18,	Sep 24,			
	1999	Apr 29,				Jun 12,	Jun 13,			Aug 10,	Aug 11,	Sep 3,	Sep 4,			
	2000	Apr 30,				Jun 13,	Jun 14,			Jul 6,	Jul 7,	Sep 18,	Sep 19,			
	2001	Apr 27,				Jun 6,	Jun 7,			Jul 19,	Jul 20,	Sep 15,	Sep 16,			
	2002	Apr 24,				Jun 30,	Jul 1,			Aug 5,	Aug 10,	Sep 18,	Sep 19,			
	2003	Apr 29,				Jun 21,	Jun 22,			Aug 15,	Aug 16,	Sep 18,	Sep 20,			
	2004	Apr 29,				Jun 27,	Jun 28,			Aug 15,	Aug 16,	Sep 28,	Sep 29,			
	2005	May 5,				Jun 26,	Jun 27,			Aug 18,	Aug 19,	Sep 23,	Sep 24,			
	2006	Apr 28,				Jul 7,	Jul 8,			Aug 16,	Aug 17,	Oct 8,	Oct 9,			

*No fertilizer application on Soya

Rules to set the dates and practices

Earlier manure spreading :	Last week of April		
Tillage and spreading :	48 hours after and before rainfall		
Field work practice :	Single soil tillage	Spring Harrowing	Fall ploughing
Fertilizer distribution in time :	45 % before sowing	36 % growing season	19% after harvest

Sources: Deslandes et al. (2007); Michaud et al. (2008)

Crop	Year	Pre-plant manure spreading (N and P) (45% of annual inputs for crops)	N mineral fertilization (1/2 of total input)	Spring field work (Harrowing)	Seedling and P minral fertilization	First hay harvest	Manure spreading after first hay harvest (1/2 annual input)	Post-emergence manure spreading (36% of annual inputs for crop)	N mineral fertilization (1/2 total input)	Second hay harvest	Manure spreading after second hay harvest (Mineral N and P)	Third hay harvest	Manure spreading after third hay harvest (1/2 of annual input)	Crop harvest	Fall manure spreading (19% of annual inputs for crops)	Fall field work (ploughing tilling)
Soybean	1998			Apr 30,	May 12,									Sep 25,		Oct 6,
	1999			May 2,	May 14,									Sep 26,		Sep 28,
	2000			May 16,	May 21,									Sep 18,		Sep 30,
	2001			May 3,	May 5,									Sep 18,		Oct 1,
	2002			May 6,	May 19,									Sep 18,		Sep 26,
	2003			May 4,	May 5,									Sep 18,		Oct 7,
	2004			May 9,	May 13,									Sep 27,		Oct 8,
	2005			May 6,	May 19,									Oct 2,		Oct 5,
	2006			Apr 29,	Jun 14,									Nov 3,		Nov 6,

Crop	Year	Pre-plant manure spreading (N and P) (45% of annual inputs for crops)	N mineral fertilization (1/2 of total input)	Spring field work (Harrowing)	Seedling and P minral fertilization	First hay harvest	Manure spreading after first hay harvest (1/2 annual input)	Post-emergence manure spreading (36% of annual inputs for crop)	N mineral fertilization (1/2 total input)	Second hay harvest	Manure spreading after second hay harvest (Mineral N and P)	Third hay harvest	Manure spreading after third hay harvest (1/2 of annual input)	Crop harvest	Fall manure spreading (19% of annual inputs for crops)	Fall field work (ploughing tilling)
Oats	1998	Apr 23,	Apr 23,	Apr 30,	May 12,				Jul 6,					Aug 31,	Sep 17,	Sep 25,
	1999	Apr 29,	Apr 29,	May 2,	May 14,				Jun 22,					Aug 25,	Sep 1,	Sep 12,
	2000	Apr 30,	Apr 30,	May 16,	May 21,				Jun 14,					Aug 22,	Sep 7,	Sep 10,
	2001	Apr 27,	Apr 27,	May 3,	May 5,				Jun 14,					Aug 22,	Sep 7,	Sep 15,
	2002	Apr 24,	Apr 24,	May 6,	May 19,				Jun 30,					Aug 21,	Sep 7,	Sep 18,
	2003	Apr 29,	Apr 29,	May 4,	May 5,				Jun 17,					Aug 21,	Sep 7,	Sep 10,
	2004	Apr 29,	Apr 29,	May 9,	May 13,				Jun 28,					Sep 4,	Sep 13,	Sep 14,
	2005	May 5,	May 5,	May 6,	May 19,				Jun 30,					Aug 26,	Sep 5,	Sep 6,
	2006	Apr 28,	Apr 28,	Apr 29,	May 28,				Jul 9,					Aug 29,	Sep 7,	Sep 11,

Crop	Year	Pre-plant manure spreading (N and P) (45% of annual inputs for crops)	N mineral fertilization (1/2 of total input)	Spring field work (Harrowing)	Seedling and P minral fertilization	First hay harvest	Manure spreading after first hay harvest (1/2 annual input)	Post-emergence manure spreading (36% of annual inputs for crop)	N mineral fertilization (1/2 total input)	Second hay harvest	Manure spreading after second hay harvest (Mineral N and P)	Third hay harvest	Manure spreading after third hay harvest (1/2 of annual input)	Crop harvest	Fall manure spreading (19% of annual inputs for crops)	Fall field work (ploughing tilling)
Corn	1998	Apr 23,	Apr 23,	Apr 30,	May 12,			Jun 10,	Jun 10,					Oct 22,	Oct 22,	Oct 25,
	1999	Apr 29,	Apr 29,	May 2,	May 14,			Jun 22,	Jun 22,					Oct 28,	Oct 28,	Oct 29,
	2000	Apr 30,	Apr 30,	May 16,	May 21,			Jun 14,	Jun 14,					Oct 13,	Oct 13,	Oct 21,
	2001	Apr 27,	Apr 27,	May 3,	May 5,			Jun 14,	Jun 14,					Oct 20,	Oct 20,	Oct 30,
	2002	Apr 24,	Apr 24,	May 6,	May 19,			Jun 30,	Jun 30,					Oct 12,	Oct 12,	Oct 23,
	2003	Apr 29,	Apr 29,	May 4,	May 5,			Jun 17,	Jun 17,					Oct 12,	Oct 12,	Oct 24,
	2004	Apr 29,	Apr 29,	May 9,	May 13,			Jun 28,	Jun 28,					Oct 26,	Oct 26,	Oct 27,
	2005	May 5,	May 5,	May 6,	May 19,			Jun 30,	Jun 30,					Oct 30,	Oct 30,	Nov 3,
	2006	Apr 28,	Apr 28,	Apr 29,	May 28,			Jul 9,	Jul 9,					Nov 3,	Nov 3,	Nov 4,

Table A2: Values of calibration parameters for the experimental Wallbridge watersheds and the upstream and downstream sections of the entire watershed

Parameter files	Calibration parameters	Set up 1		Setup 2		Parameter ranges	Parameter definitions
		PR up	PR dw	Wal up	Waldw		
SUB.dbf	SFTMP	0.5		-1.5		-5 ; 5	Snowfall temperature
	SMTMP	-1		-1.5		-5 ; 5	Snow melt base temperature
	SMFMX	5		4		0-10	Maximum melt rate for snow during year (occurs on summer solstice)
	SMFMN	0.5		1		0-10	Minimum melt rate for snow during the year (occurs on winter solstice)
	TIMP	0,25		0.87		0-1	Snow pack temperature lag factor.
	SNOCOVMX	50		100		0-500	Minimum snow water content that corresponds to 100% snow cover.
	SNOCOV50	1		1		0-1	Snow water equivalent that corresponds to 50% snow cover.
	SURLAG	25		0.5		1-24	Surface runoff lag time (days)
	ADJ_PKR	0.5		0.5		0.5-2	Peak rate adjustment factor for sediment routing in the subbasin (tributary channels).
	PRF	0.5		0.5		0-2	Peak rate adjustment factor for sediment routing in the main channel.
	SPCON	0.0005		0.0005		0.0001-0.01	Linear parameter for calculating the maximum amount of sediment that can be re-entrained during channel sediment routing.
	SPEXP	1		1		1-1.5	Exponent parameter for calculating sediment reentrained in channel sediment routing.
	Crakflow	on		on			Allow crack flow to occur
	MSK_CO1	3		8		0-10	Calibration coefficient used to control impact of the storage time constant for normal flow.
	MSK_CO2	0		3		0-10	Calibration coefficient used to control impact of the storage time constant for low flow
	MSK_X	0.2		0.2		0-0.3	Weighting factor controlling relative importance of inflow rate and outflow rate in determining water storage in reach segment.

Parameter file	Calibration parameters	Set up 1		Setup 2		Parameter ranges	Parameter definitions
		PR up	PR dw	Wal up	Waldw		
GW.dbf	SHALLST	500	500	500	500	0-1000	Initial depth of water in the shallow aquifer.
	DEEPST	50	50	50	50	0-3000	Initial depth of water in the deep aquifer
	GW DELAY	10	20	**10:**Forest, Apple **2:**Others	**10:**Forest, Apple **2:**Others	0-500	Groundwater delay
	ALPHA_BF	1	1	1	1	0-1	Baseflow alpha factor
	GWQMN	100	150	100	100	0-5000	Threshold depth of water in the shallow aquifer required for return flow to occur
	GW_REVAP	**0.2:**Urban areas **0.1:**Pasture, Rangebrush, soybean **0.15:**Corn Oats **0.2:**Forest, Apple		0,2	0,2	0.02-0.2	Groundwater "revap" coefficient.
	REVAPMN	175	175	125	125	0-500	Threshold depth of water in the shallow aquifer for "revap" to occur
	RECHRG_DP	0,2	0,25	0,15	0,15	0-1	Deep aquifer percolation fraction.
	GWSOLP	0,7	0,8	0,7	0,8	0-1000	Concentration of soluble phosphorus in groundwater contribution to stream flow from subbasin.
HRU.dbf	SLSUBBSN[1]	**50**:Soybean, Corn, Pasture **40**:Others	**55:** Soybean, Corn, Pasture, Vegetables **45:**Oats, rangebrush, forest, apple	**75:** crops and pasture **65:**others	**80:** crops and pasture **70:**others	10-150	Average slope length.

[1]Cultivated field were allocated with longer slope length. These length are likely too short and should be increased to improve this calibration in subsequent studies. For this study these values were chosen as a solution to excessive erosion but it is acknowledged further efforts should be put into calibration to set this parameter closer to field values (around ≥80 m).

Parameter file	Calibration parameter	Set up 1		Setup 2		Parameter ranges	Parameter definitions
		PR up	PR dw	Wal up	Waldw		
HRU.dbf	SLOPE	Lidar values for each HRU as in previous set-up		Lidar values for each HRU as in previous set-up		0-0.6	Average slope steepness.
	OV_N	**0.1:**Urban area:0.1 **0.12:**Crops: 0.12 **0.35:**Pasture, rangebrush: 0.35 **0.5:**Wetland: 0.5 **0.7:** Forest and apple **0.35:** Corn on Milton (no till)		**0.1:**Urban area:0.1 **0.12:**Crops: 0.12 **0.35:**Pasture, rangebrush: 0.35 **0.5:**Wetland: 0.5 **0.7:** Forest and apple **0.35:** Corn on Milton (no till)		0.01-30	Manning's "n" value for overland flow.
	ESCO	**0.5**: Soybean, Corn, Oats (crops) **1:** Others		1	1	0-1	Soil evaporation compensation factor
	EPCO	**0:** Urban areas **0.4:** Pasture, rangebrush **0.6:** Soybean, Oats **0.7:** Corn **1:**Apple,forest		**0:** Urban areas **0.4:** Pasture, rangebrush **0.6:** Soybean, Oats **0.7:** Corn **1:**Apple,forest		0-1	Plant uptake compensation factor.
	ERORG_P	**0.7:** crops **1:** others		**0.7:** crops **1:** others		0-5	Organic P enrichment ratio.
SOL.dbf	SOL_BD	Untouched because physical parameters measured on field without uncertainty bounds		Untouched because physical parameters measured on field without uncertainty bounds			Soil Bulk Density
	SOL_K						Soil saturated hydraulic conductivity
	SOL_AWC						Soil available water capacity
	USLE_K						USLE soil erodibility factor

Parameter files	Calibration parameters	Set-up 1		Set-up 2		Parameter ranges	Parameter definitions
		PR up	PR dw				
RTE.dbf (main channel)	CH_K2	1		6		-0.001; 150	Effective hydraulic conductivity in main channel alluvium.
	CH_D2	**3:** Pike river channel **1.5:** tributaries		1.5		1-30	Average depth of main channel.
	CH_S2	Untouched		0.004		-0.01; 10	Average depth of main channel
	CH_N2	0.01	0.06	0.07	0.02	-0.01; 0.03	Manning's "n" value for the main channel.
	CH_EROD	0.01				-0.05;0.6	Channel erodibility factor.
	CH_COV	0.05				-0.001;1	Channel cover factor.
SUB.dbf (tributaries)	SNO_SUB	16				0-150	Initial snow water conte
	CH_S1	Untouched		0.002	0.001	0.0001-10	Average slope of tributary channels.
	CH_K1	10	12	8	4	0-150	Effective hydraulic conductivity in tributary channel alluvium.
	CH_N1	0.1	0.55	0.06	0.06	0.01-30	Manning's "n" value for the tributary channels.
	CN	-80%	-90%	-80%	-90%	35 -98	SCS runoff curve number for moisture condition II.
MGT.dbf	FILTERW	1 for crop	1 for crop	1	1	0-100	Witdth of edge of field filter strip
	DDRAIN	900		900		0-2000	Depth to subsurface drain
	TDRAIN	18		23		0-72	Time to drain soil to field capacity
	GDRAIN	12		12		0-100	Drain tile lag time
	K_P	0.7 for crop only		0.7 for crop only		0.1-1	USLE equation support practice (P) factor.
BSN.dbf for Water Quality	CMN	0.0003		0.0003		0.0001-0.0003	Rate factor for humus mineralization of active organic nitrogen.
	N_UPDIS	1		1		0-100	Nitrogen uptake distribution parameter.
	P_UPDIS	100		100		0-100	Phosphorus uptake distribution parameter.
	NPERCO	0.2		0.2		0-1	Nitrogen percolation coefficient.

Parameter files	Calibration Parameters	Set-up 1		Set-up 2		Parameter ranges	Parameter definitions
		PRup	PRdw	Prup	PRdw		
BSN.dbf	PPERCO	10		10		10-17.5	Phosphorus percolation coefficient.
	PHOSKD	200		200		100-200	Phosphorus soil partitioning coefficient.
	PSP	0.7		0.7		0.01-0.7	Phosphorus sorption coefficient.

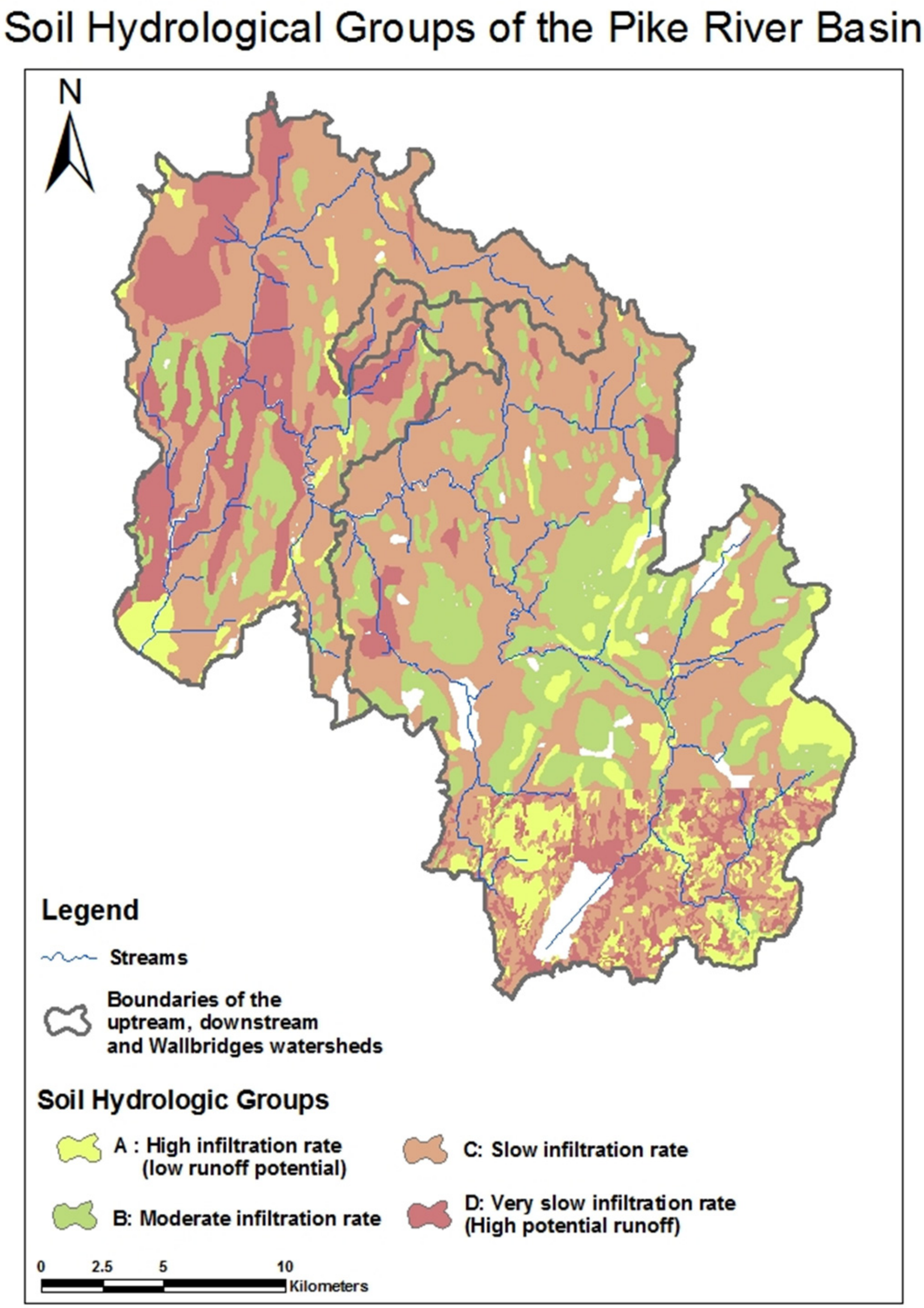

Figure A3: Maps of hydrological soil groups

APPENDIX B: Extra results for SWAT calibration and validation

Table B1: Average annual values of the water budget components within the Pike(PRup and PRdw) and Wallbridges (WCup and WCdw) watersheds.

* Ground water (GW) comprises base flow, lateral flow and tile flow. Tile flow was estimated at about 60% (between 300-400 mm) of the water yield when crop are drained. The Wallbridges present smaller numbers as about 40% of the water yield is evacuated on crop field. The setup was built with **60** % of drained land within the entire Watershed.

Unit : mm H_2O	**Period**	**Precipitation**	**Evapotranspiration**	**Deep Aquifer Recharge**	**Wateryield (Total Runoff)**	**In mm or % of water yield**	
						Surface Runoff	**GW*** (Ground-water)
Uncalibrated Watershed	Calibration and Validation	1 106	462 (42%)	17 (2%)	613 (55%)	279 (45%)	339 (55%)
Uncalibrated WC Up&Dw	Calibration and Validation	1 105	449 (40%)	16 (2%)	626 (57%)	331 (53%)	294 (47%)
WCup	Calibration	1 073	525 (49%)	47 (4%)	509 (47%)	141 (28%)	368 (72%)
	Validation	1 137	524 (46%)	62 (5%)	617 (54%)	177 (29%)	440 (71%)
WCdw	Calibration	1 073	545 (51%)	41 (4%)	474 (44%)	195 (41%)	279 (59%)
	Validation	1 137	546 (48%)	54 (5%)	583 (51%)	230 (39%)	353 (61%)
PRup	Calibration	1 160	612 (53%)	75 (6%)	468 (40%)	114 (24%)	354 (76%)
	Validation	1 034	585 (53%)	81 (7%)	495 (43%)	121 (25%)	374 (76%)
PUdw	Calibration	1 087	584 (54%)	63 (6%)	529 (49%)	138 (26%)	390 (74%)
	Validation	1 034	562 (54%)	64 (6%)	552 (53%)	162 (29%)	390 (74%)
Calibrated Watershed	Calibration	1 159	590 (51%)	72 (6%)	501 (45%)	128 (26%)	373 (74%)
Validated Watershed	Validation 20 years	1 147	597 (52%)	68 (6%)	522 (45%)	167 (32%)	355(68%)

Figure B2: Daily hydrograph of the calibration period for the upstream (PR_{up}), downstream (PR_{dw}) and Wallbridges (WC_{up} and WC_{dw}) watersheds

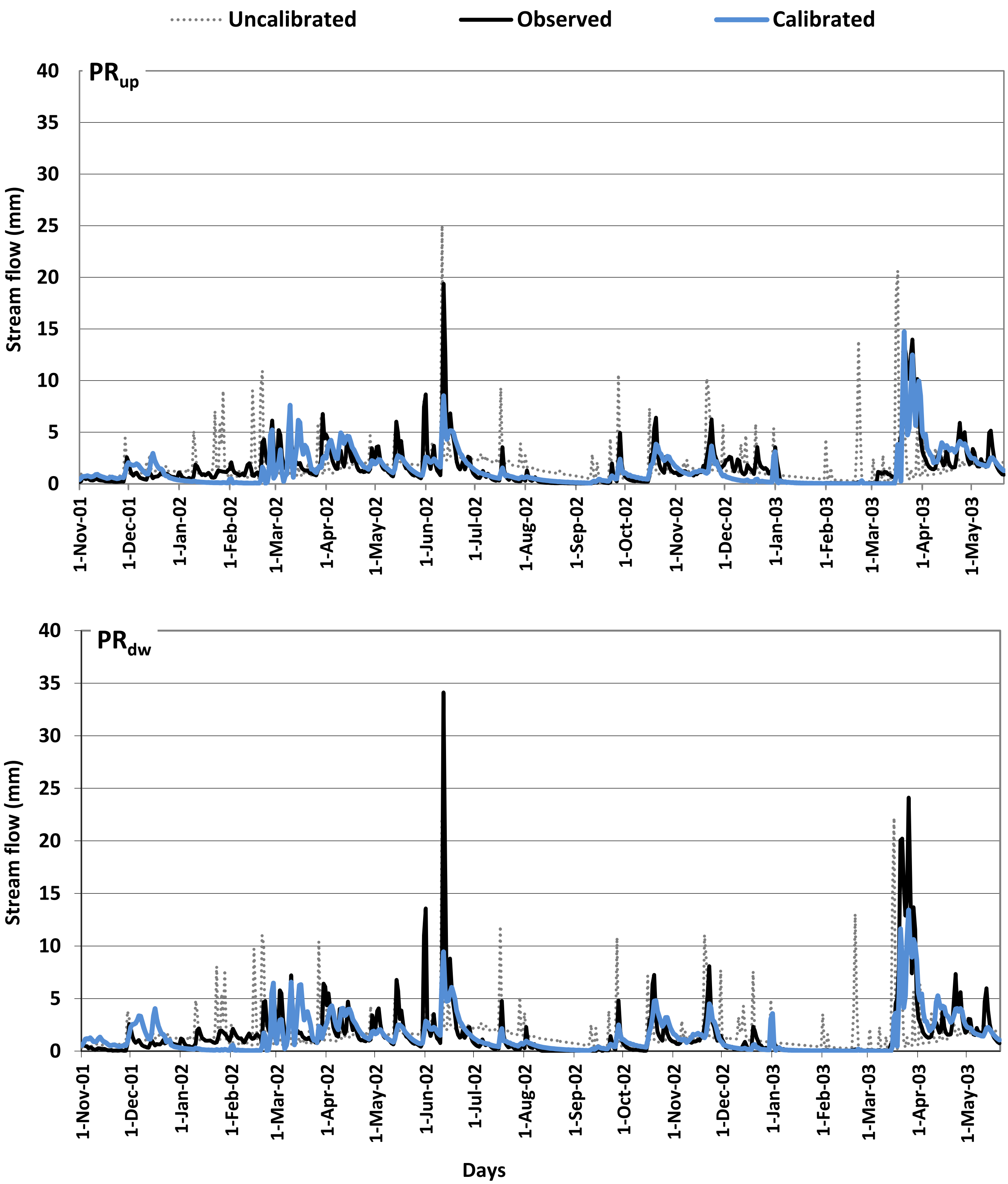

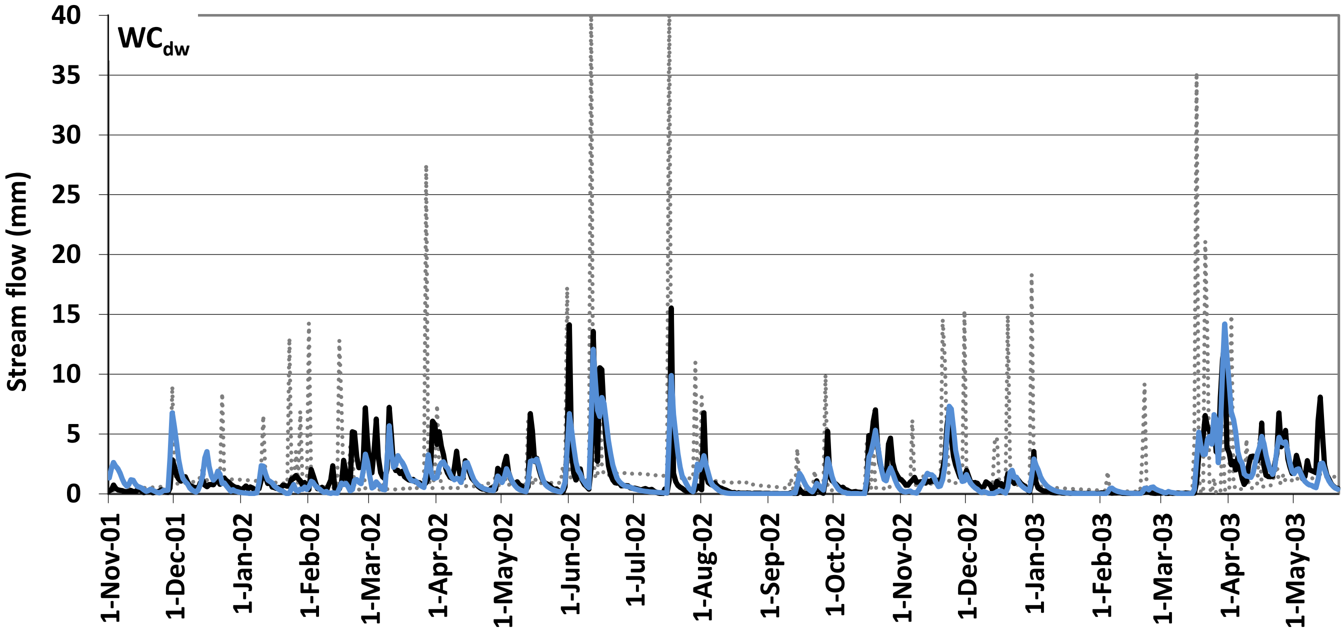
WC$_{dw}$
Stream flow (mm)
0
5
10
15
20
25
30
35
40
1-Nov-01
1-Dec-01
1-Jan-02
1-Feb-02
1-Mar-02
1-Apr-02
1-May-02
1-Jun-02
1-Jul-02
1-Aug-02
1-Sep-02
1-Oct-02
1-Nov-02
1-Dec-02
1-Jan-03
1-Feb-03
1-Mar-03
1-Apr-03
1-May-03

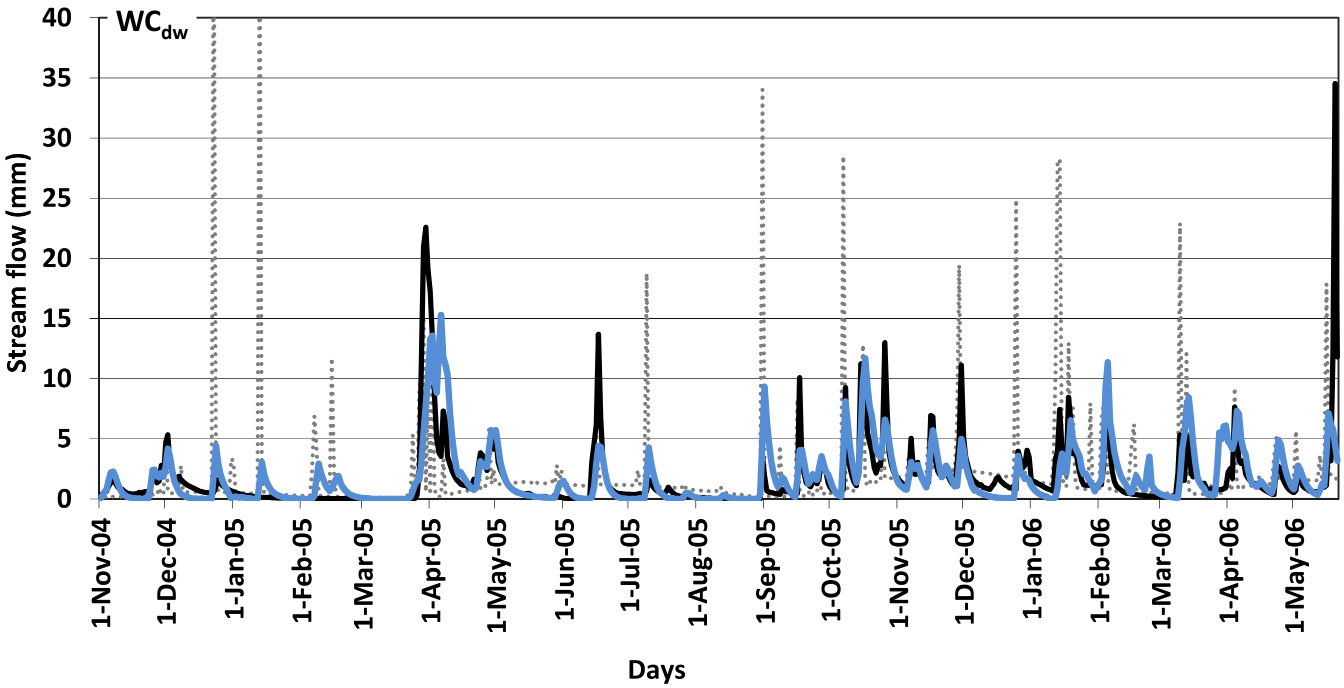
WC$_{dw}$
Stream flow (mm)
0
5
10
15
20
25
30
35
40
1-Nov-04
1-Dec-04
1-Jan-05
1-Feb-05
1-Mar-05
1-Apr-05
1-May-05
1-Jun-05
1-Jul-05
1-Aug-05
1-Sep-05
1-Oct-05
1-Nov-05
1-Dec-05
1-Jan-06
1-Feb-06
1-Mar-06
1-Apr-06
1-May-06
Days

Table B3: SWAT performance statistics for stream flow

SWAT performance statistics for stream flow prediction during calibration (November 2001-May 2003)

Station	R^2		NSE		PBIAS (%)	Diff (mm)
	Daily	Monthly	Daily	Monthly	Computed on cumulative stream flow for the period	
PR_{up}	0.61	0.75	0.59	0.70	-13	-118
PR_{dw}	0.56	0.71	0.53	0.67	-14	-132
WB_{up}	0.52	0.87	0.45	0.85	-2	-22
WB_{dw}	0.60	0.75	0.58	0.71	-3	-23

SWAT performance statistics for stream flow prediction during validation (November 2004-May 2006). Values in brackets were calculated omitting spring 2006

Station	R^2		NSE		PBIAS (%)	Diff (mm)
	Daily	Monthly	Daily	Monthly	Computed on cumulative stream flow for the period	
PR_{up}	0.38	0.34	0.33	0.12	-23	-220
PR_{dw}	0.05	0.25	-0.05	0.06	-14	-131
WB_{up}	0.36	0.5 (0.6)	0.24	0.28 (0.43)	-6	-55
WB_{dw}	0.41	0.6 (0.7)	0.39	0.47 (0.58)	4	40

Figure B4: Water quality results for sediments

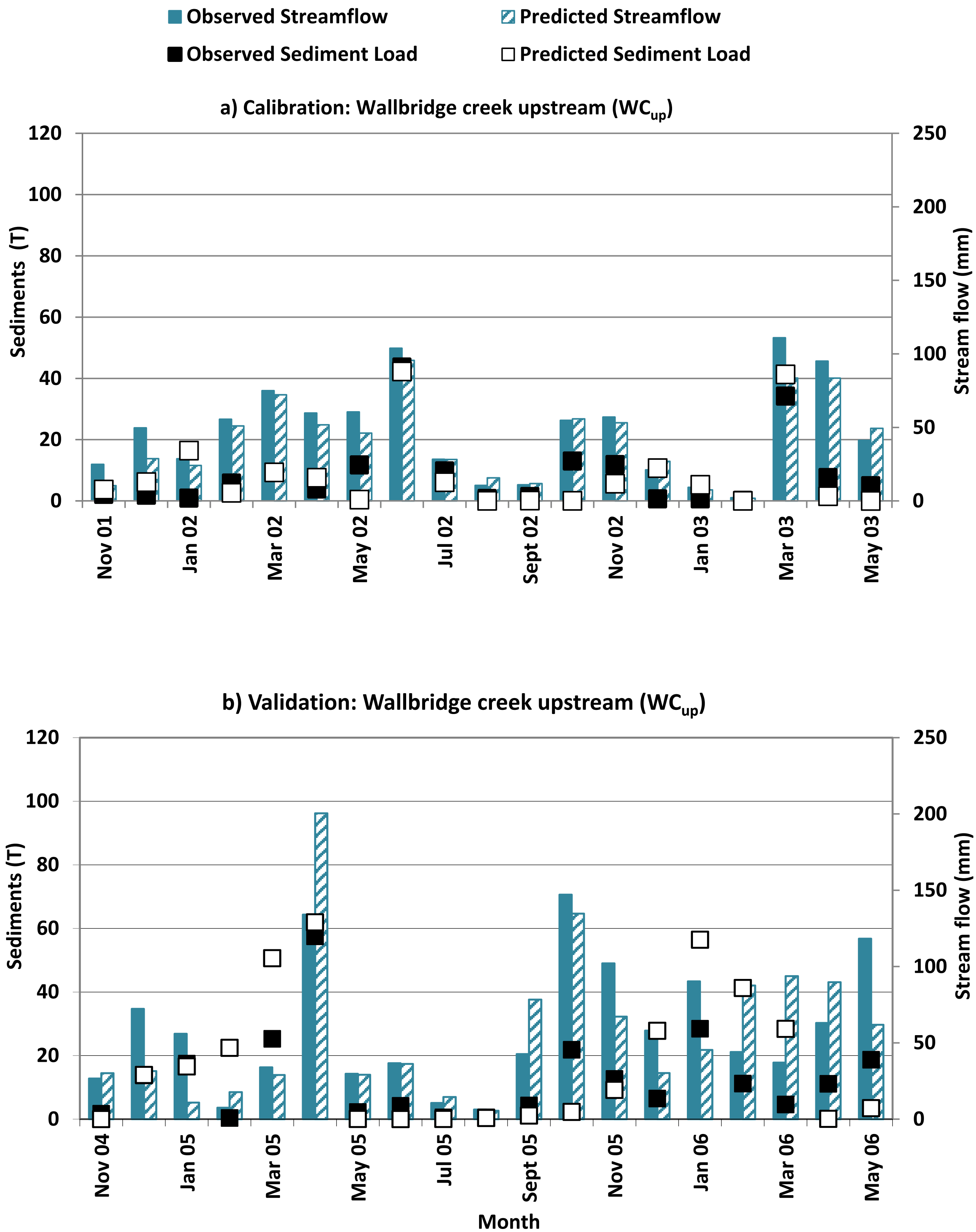

Figure B5: Water quality results for total phosphorus

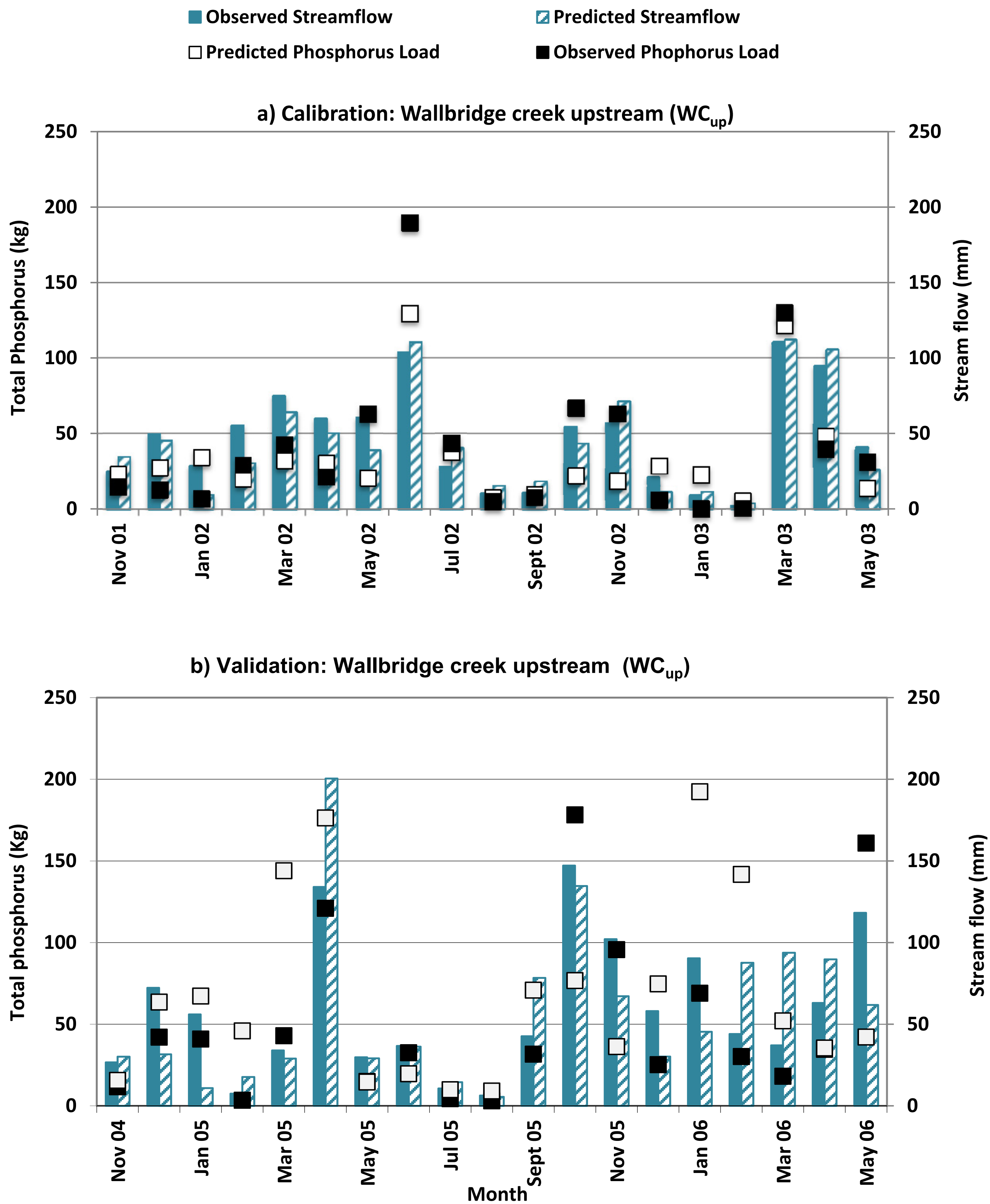

Figure B6: Water quality results for total nitrogen

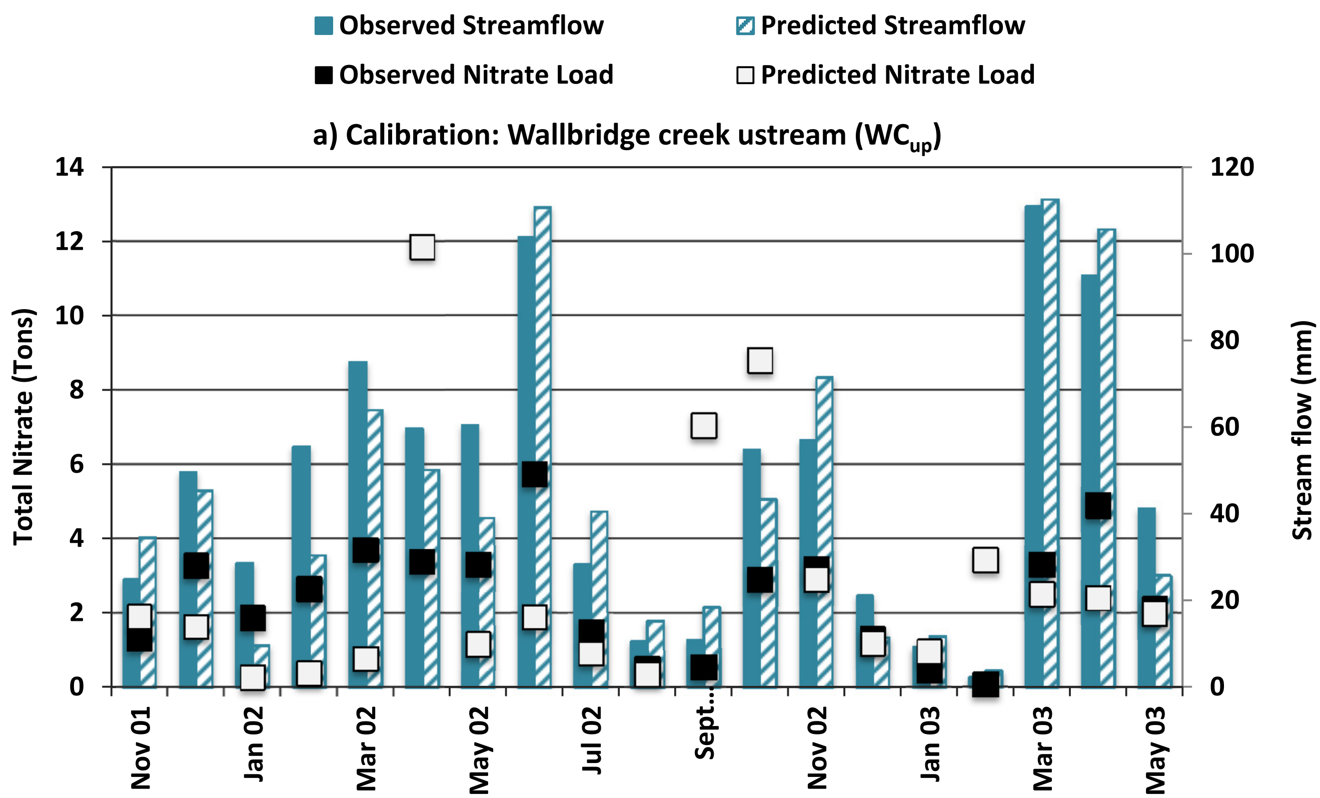

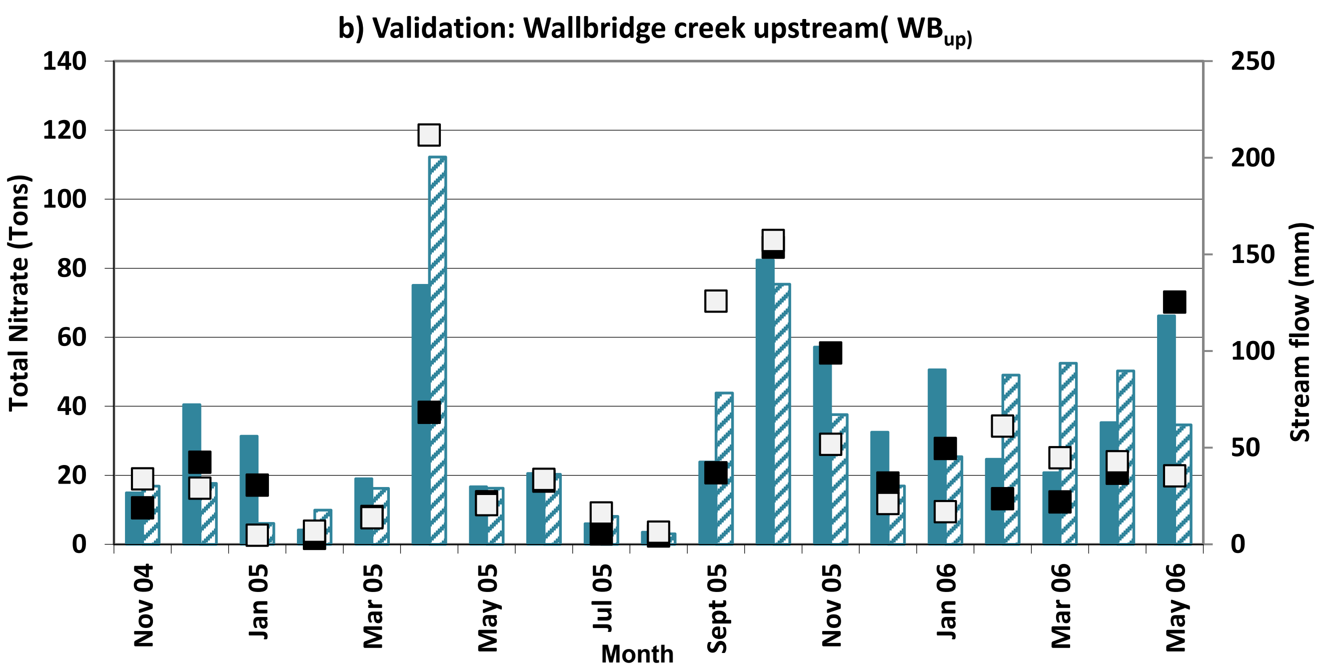

APPENDIX C: Comparison of predicted precipitation and temperatures to observed values

Figure C1

Comparison of predicted and recorded mean monthly precipitation over the historical period (1971-2000). The three weather stations are averaged on a weighted area basis.

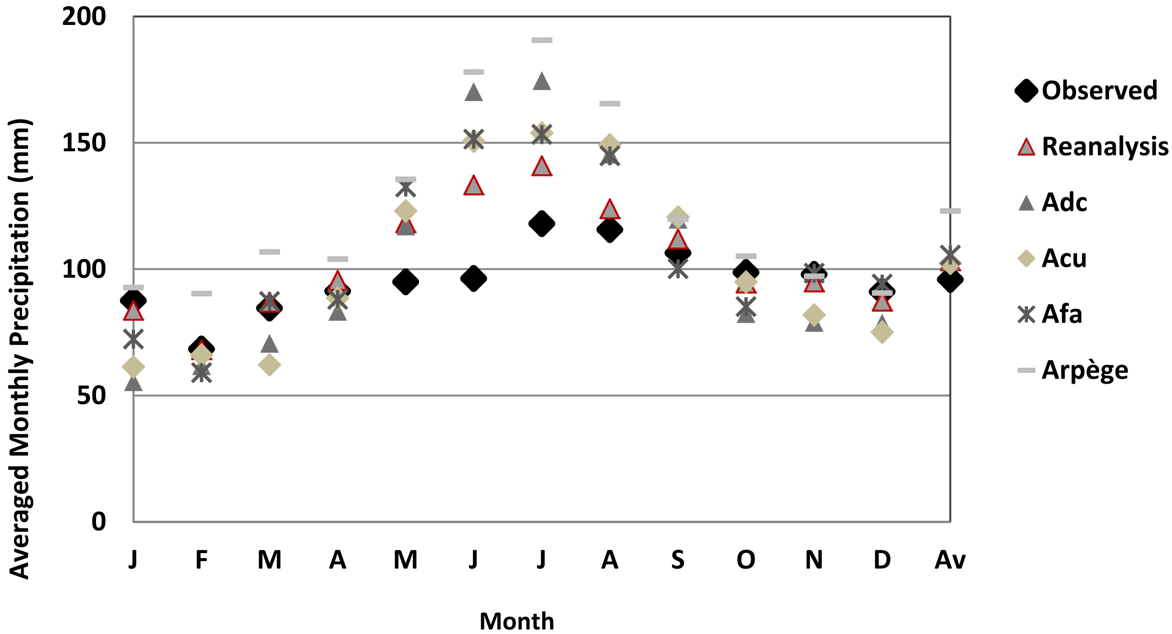

Comparison of predicted and recorded monthly average of daily mean temperature over the historical period (1971-2000). The stations are weighted averaged.

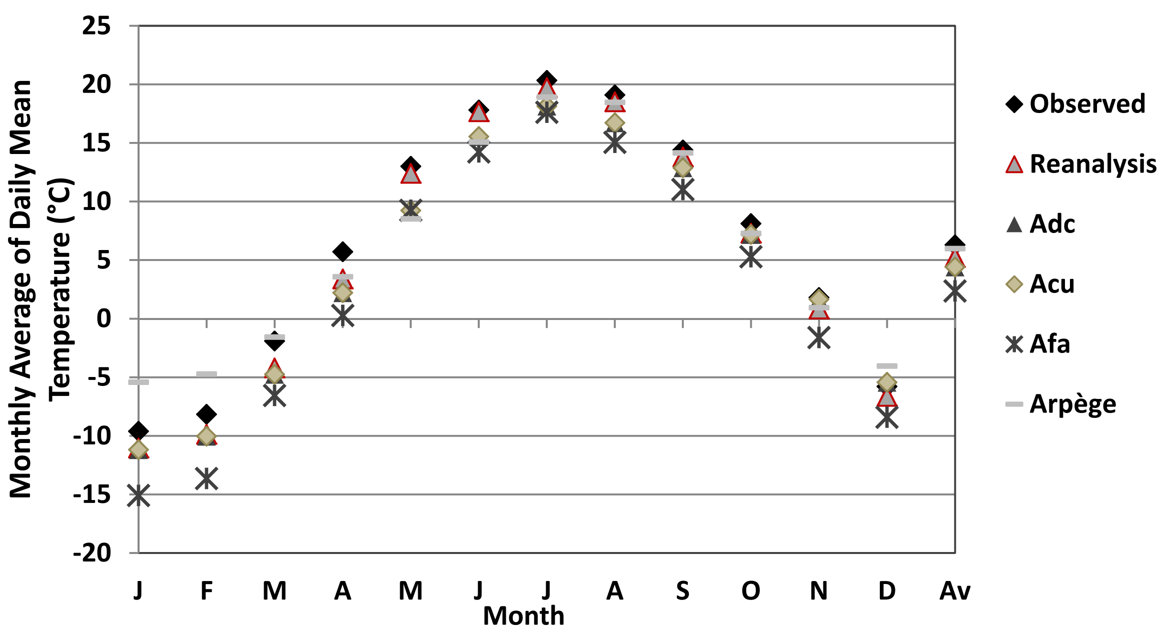

Figure C2: Daily mean temperature, averaged over the period of reference 1971-2000.

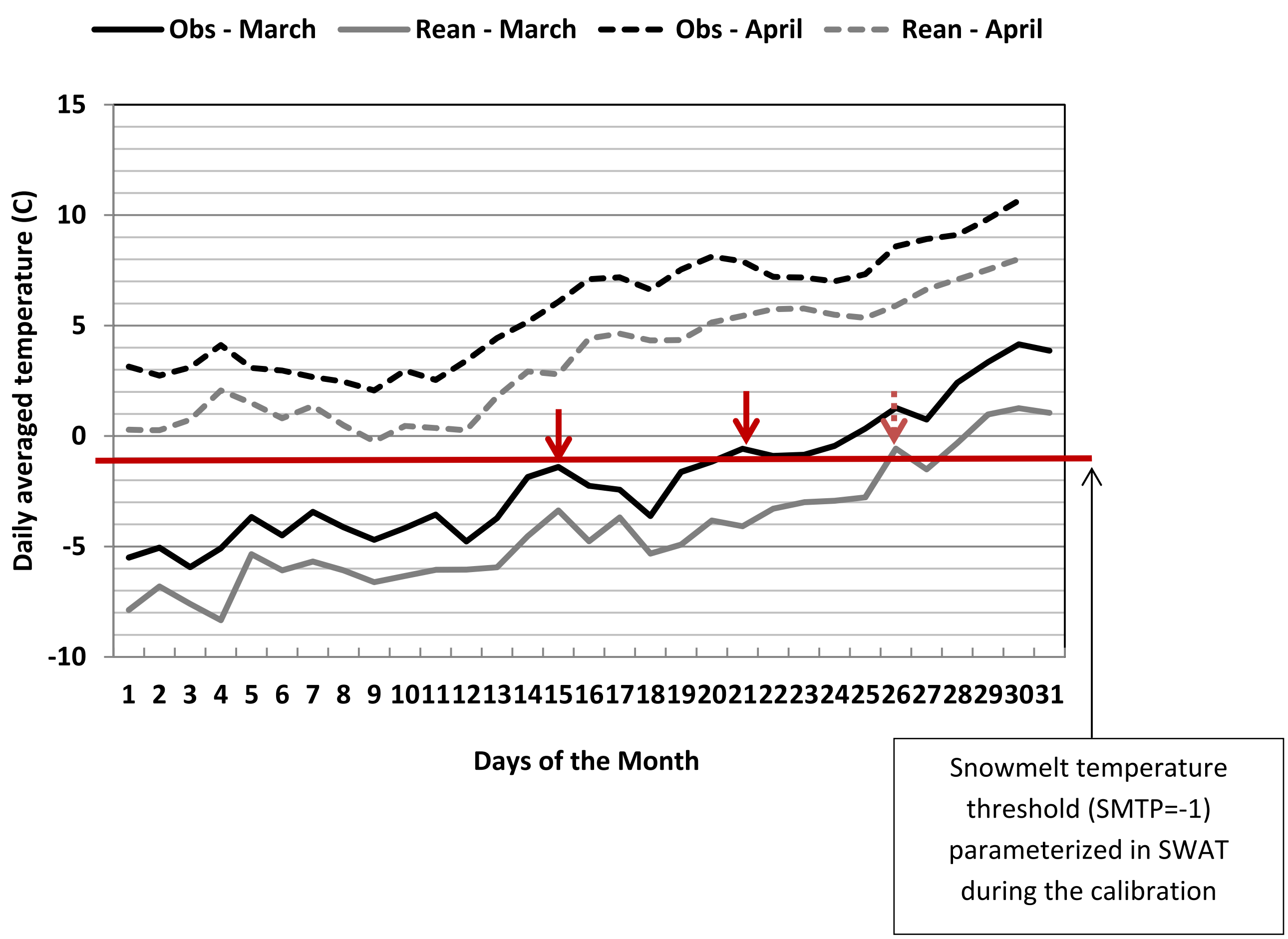

APPENDIX D : Return period calculation

Qp : Calculated Flow for the Return Period
Qp = a+bu, determined graphically in this study
Reduced Variable of Gumbel: u =LN (-LN (Non-Exceedence Probability)
Non-Exceedence Probability = 1-(1/T)
T= Return Period (years)

Annual results

Figure D1: Gumbel diagram for annual flow to determine Qp (y) for a given return period

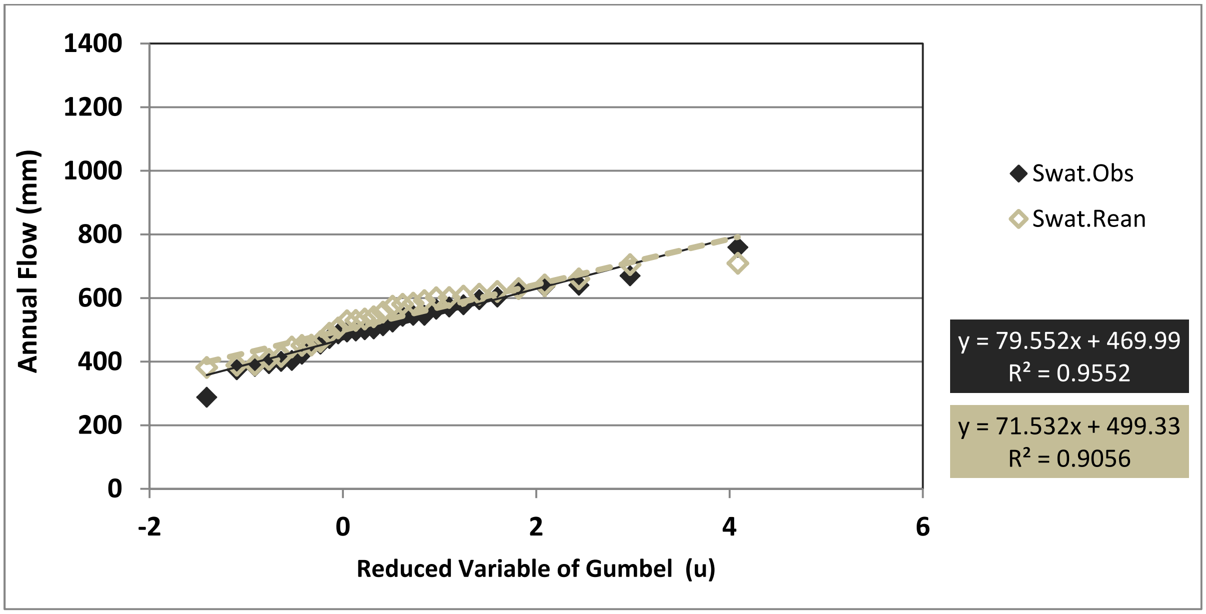

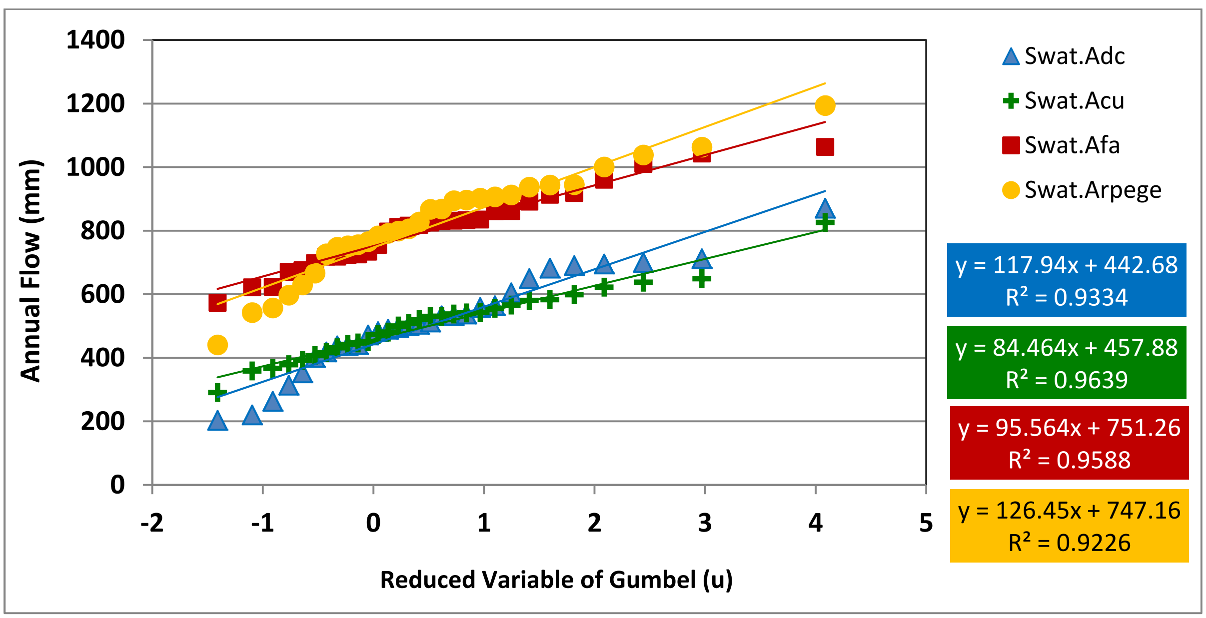

Table D2: Annual stream flow values for different return periods with their probability of exceedence or non-exceedence for each simulation over the historical period (1961-2000)

Return Period T		100	75	50	20	10	5	2.33	2	1.5	1.1	[years]
Non-Exceedence Probability		99%	99%	98%	95%	90%	80%	57%	50%	33%	9%	%
Probability of Exceedence		1%	1.3%	2%	5%	10%	20%	43%	50%	67%	91%	%
Reduced Variable of Gumbel		4.6	4.3	3.9	3.0	2.3	1.5	0.6	0.4	-0.1	-0.9	
SWAT.OBS	Qp for the Return Period T	**835.9**	**812.9**	**780.4**	**706.3**	**649.0**	**589.3**	**516.0**	**499.1**	**462.5**	**400.4**	mm
SWAT.ACZ	Qp for the Return Period T	**828.4**	**807.7**	**778.4**	**711.8**	**660.3**	**606.6**	**540.7**	**525.6**	**492.6**	**436.8**	mm
	% Difference of Qp with SWAT.OBS	-1%	-1%	0%	1%	2%	3%	5%	5%	7%	9%	%
SWAT.ADC	Qp for the Return Period T	**985.2**	**951.1**	**902.9**	**793.0**	**708.1**	**619.6**	**510.9**	**485.9**	**431.6**	**339.5**	mm
	% Difference of Qp with SWAT.OBS	18%	17%	16%	12%	9%	5%	-1%	-3%	-7%	-15%	%
SWAT.ACU	Qp for the Return Period T	**846.4**	**822.0**	**787.4**	**708.7**	**648.0**	**584.6**	**506.7**	**488.8**	**449.9**	**384.0**	mm
	% Difference of Qp with SWAT.OBS	1%	1%	1%	0%	0%	-1%	-2%	-2%	-3%	-4%	%
SWAT.AFA	Qp for the Return Period T	**1190.9**	**1163.2**	**1124.1**	**1035.1**	**966.3**	**894.6**	**806.6**	**786.3**	**742.3**	**667.7**	mm
	% Difference of Qp with SWAT.OBS	42%	43%	44%	47%	49%	52%	56%	58%	60%	67%	%
SWAT.ARP	Qp for the Return Period T	**1328.9**	**1292.3**	**1240.6**	**1122.8**	**1031.7**	**936.8**	**820.3**	**793.5**	**735.3**	**636.6**	mm
	% Difference of Qp with SWAT.OBS	59%	59%	59%	59%	59%	59%	59%	59%	59%	59%	%

Qp : Stream flow

Maximum monthly flow results:

Figure D3: Gumbel diagram for maximum monthly flow to determine Qp (y) for a given return period

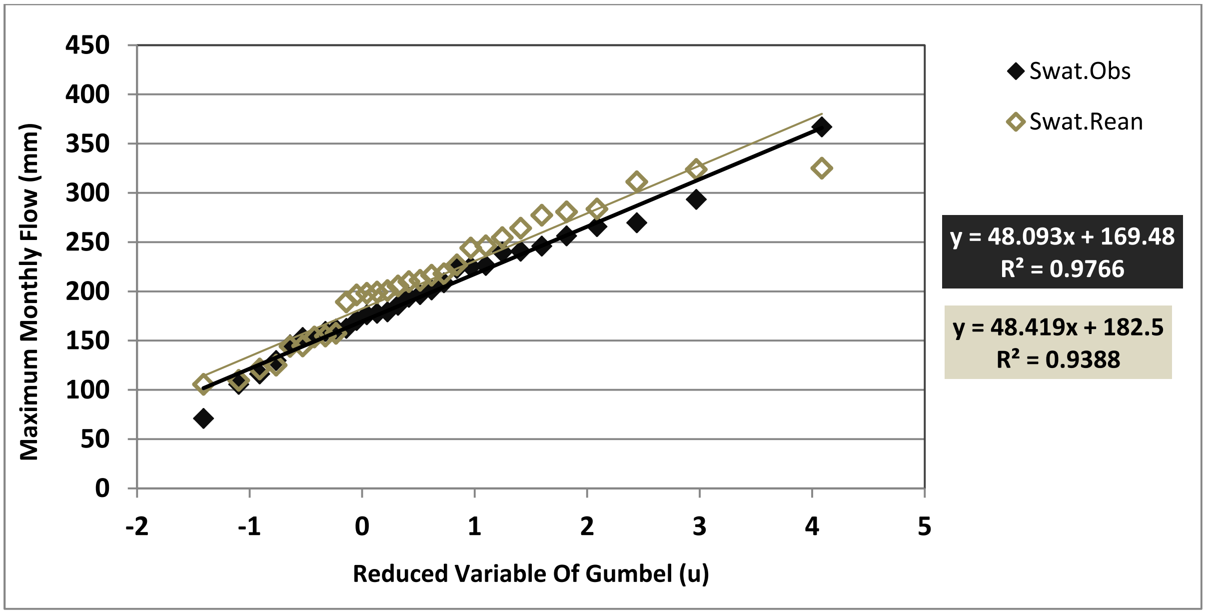

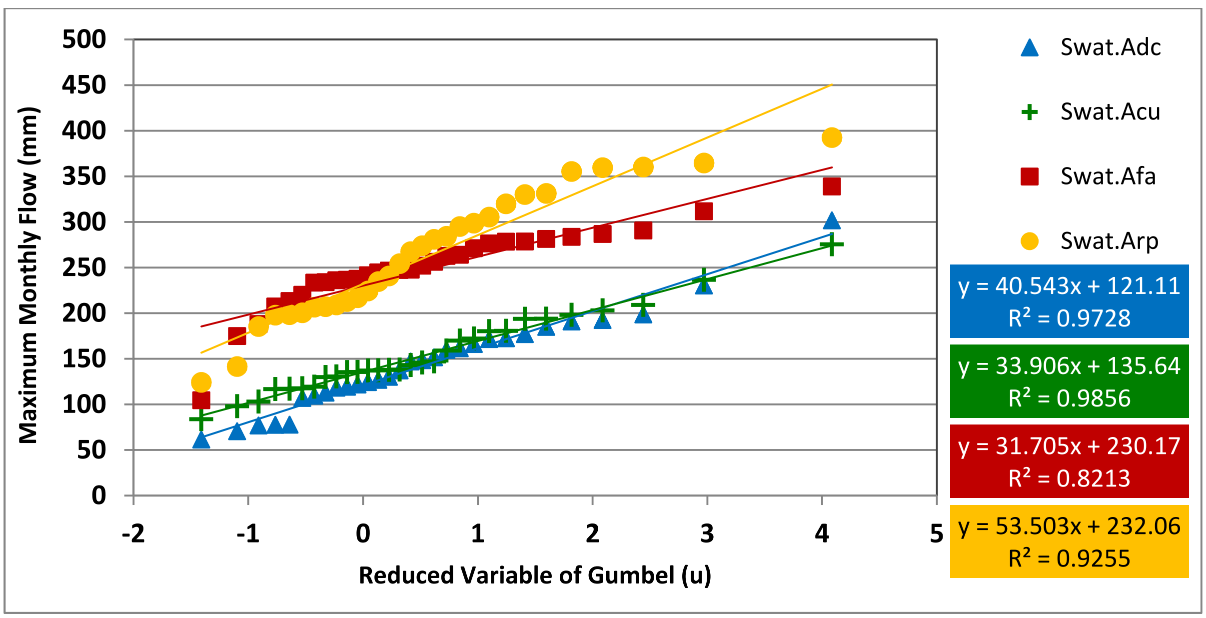

Table D4 Maximum monthly values for different return periods with their probability of exceedence or non-exceedence for each simulation over the historical period (1961-2000)

Return Period T		100	75	50	20	10	5	2.33	2	1.5	1.1	[years]
Non-Exceedence Probability		99%	99%	98%	95%	90%	80%	57%	50%	33%	9%	%
Probability of Exceedence		1%	1%	2%	5%	10%	20%	43%	50%	67%	91%	%
		4.6	4.3	3.9	3.0	2.3	1.5	0.6	0.4	-0.1	-0.9	
SWAT.OBS	Qp for the Return Period T	**390.7**	**376.8**	**357.1**	**312.3**	**277.7**	**241.6**	**197.3**	**187.1**	**165.0**	**127.4**	mm
	Qp for the Return Period T	**405.2**	**391.2**	**371.4**	**326.3**	**291.5**	**255.1**	**210.5**	**200.2**	**177.9**	**140.2**	mm
SWAT.ACZ	% Difference of Qp with Swat.Obs	4%	4%	4%	4%	5%	6%	7%	7%	8%	10%	%
	Qp for the Return Period T	**307.6**	**295.9**	**279.3**	**241.5**	**212.3**	**181.9**	**144.6**	**136**	**117.3**	**85.7**	mm
SWAT.ADC	% Difference of Qp with Swat.Obs	-21%	-21%	-22%	-23%	-24%	-25%	-27%	-27%	-29%	-33%	%
	Qp for the Return Period T	**291.6**	**281.8**	**267.9**	**236.3**	**211.9**	**186.5**	**155.3**	**148.1**	**132.4**	**106.0**	mm
SWAT.ACU	% Difference of Qp with Swat.Obs	-25%	-25%	-25%	-24%	-24%	-23%	-21%	-21%	-20%	-17%	%
	Qp for the Return Period T	**376**	**366.8**	**353.9**	**324.3**	**301.5**	**277.7**	**248.5**	**241.8**	**227.2**	**202.4**	mm
SWAT.AFA	% Difference of Qp with Swat.Obs	-4%	-3%	-1%	4%	9%	15%	26%	29%	38%	59%	%
	Qp for the Return Period T	**478.2**	**462.7**	**440.8**	**391**	**352.5**	**312.3**	**263**	**251.7**	**227**	**185.3**	mm
SWAT.ARP	% Difference of Qp with Swat.Obs	22%	23%	23%	25%	27%	29%	33%	35%	38%	45%	%

APPENDIX E : Values of seasonal and monthly changes

Table E1: 30-Years seasonal averaged change values in mm of water and % for main hydrological components

		Δ Pcp	Δ AET	Δ Wyld	Δ RnQ	Δ SubSQ	Δ Perco (Recharge)
Fall	ADC	24 (8%)	1 (1%)	20 (19%)	-2 (-33%)	22 (22%)	21 (23%)
	ACU	10 (3%)	1 (1%)	-1 (-1%)	-3 (-38%)	2 (2%)	3 (3%)
	AFA	38 (13%)	7 (9%)	34 (20%)	-1 (-11%)	35 (22%)	41 (34%)
	ARP	10 (3%)	-2 (-2%)	7 (4%)	2 (20%)	5 (3%)	17 (13%)
	Average	21(7%)	1.6 (1%)	15(11%)	-0.9(-9%)	16(12%)	20 (18%)
Winter	ADC	42 (21%)	8 (47%)	53 (135%)	19 (59%)	39 (262%)	22 (318%)
	ACU	30 (15%)	8 (47%)	62 (153%)	25 (91%)	43 (219%)	26 (327%)
	AFA	62 (28%)	3 (44%)	65 (216%)	33 (161%)	37 (268%)	17 (316%)
	ARP	30 (11%)	2 (13%)	52 (111%)	19 (66%)	37 (154%)	26 (207%)
	Average	41(18%)	5.5 (37%)	58(148%)	24 (88%)	39(215%)	23(277%)
Spring	ADC	71 (26%)	37 (26%)	24 (9%)	-20 (-19%)	40 (22%)	29 (18%)
	ACU	51 (19%)	32 (22%)	-17 (-6%)	-49 (-42%)	23 (13%)	19 (12%)
	AFA	50 (16%)	19(21%)	23 (5%)	-15 (-8%)	38(14%)	26 (12%)
	ARP	59 (17%)	21 (15%)	18 (4%)	-18 (-12%)	33 (11%)	17 (7%)
	Average	58 (19%)	27 (21%)	12(3%)	-26(-18)	33(14%)	23 (12%)
Summer	ADC	-25 (-5%)	20 (5%)	-35 (-30%)	-1.3 (-49%)	-34 (-30%)	-34 (-29%)
	ACU	-3 (-1%)	22 (6%)	-7 (-8%)	1 (85%)	-7 (-9%)	-8 (-9%)
	AFA	-18 (-4%)	22 (9%)	-33 (-27%)	0.22 (9%)	-33 (-17%)	-30 (-16%)
	ARP	-6 (-1%)	6 (2%)	-2 (-1%)	-2 (-13%)	0 (0%)	-7 (-4%)
	Average	-13 (-3%)	18(5%)	-19(-13%)	-0.4(-9%)	-19 (-13%)	-20 (-14%)
Year	ADC	111 (9%)	66 (10%)	63 (12%)	-4 (-3%)	67 (16%)	38 (10%)
	ACU	89 (7%)	63 (10%)	38 (7%)	-26 (-17%)	60 (15%)	40 (11%)
	AFA	132 (10%)	51 (12%)	89 (11%)	17 (8%)	76 (12%)	54 (10%)
	ARP	93 (6%)	28 (5%)	75 (9%)	1 (1%)	74 (11%)	52 (9%)
	Average	106 (8%)	52(9%)	66(10%)	-3(-2%)	69 (13%)	46 (10%)

Pcp : Precipitation ; **AET** : Actual Evapotranspiration ; **Wyld**:Wateryield (Contribution of total runoff (surface and subsurface) to stream flow) ; **RnQ**: Surface runoff ; **SubSQ** : Subsurface flow ; **Perco:** percolation (Water that percolates past the root zone during the time step. Over a long period of time this variable should equal GW recharge (Neitsch et al., 2004)).

Changes in the table are given in absolute values (mm) and percentage to facilitate comparison and interpretation of results. Percentages values have to be interpreted with caution. For example, fall and summer surface runoff (Qsurf) present high percentage change >15 % for very small absolute changes (a few mm) because reference values of the historical period were already very small. A small increase of a small value can rapidly produce a relative high increase that might not be in fact important.

Also, percentages values are calculated on different bases (historical precipitation, runoff, etc.) to focus on the changes, therefore they don't complete each other to close a water budget.

% Changes or Δ% change $= \frac{(\bar{F}_{pcp} - \bar{C}_{pcp})}{\bar{C}_{pcp}}$

where: $\bar{F} = Seasonal\ future\ Average, and\ \bar{C} = Seasonal\ Average\ over\ the\ control\ period.$

Figure E2: Mean monthly sediment loading as simulated with the different climate inputs, for the current (historical) (1971-2000) and future climates (2041-2070). * indicate significant changes (Paired *t*-test, *P* ≤ 0.05)

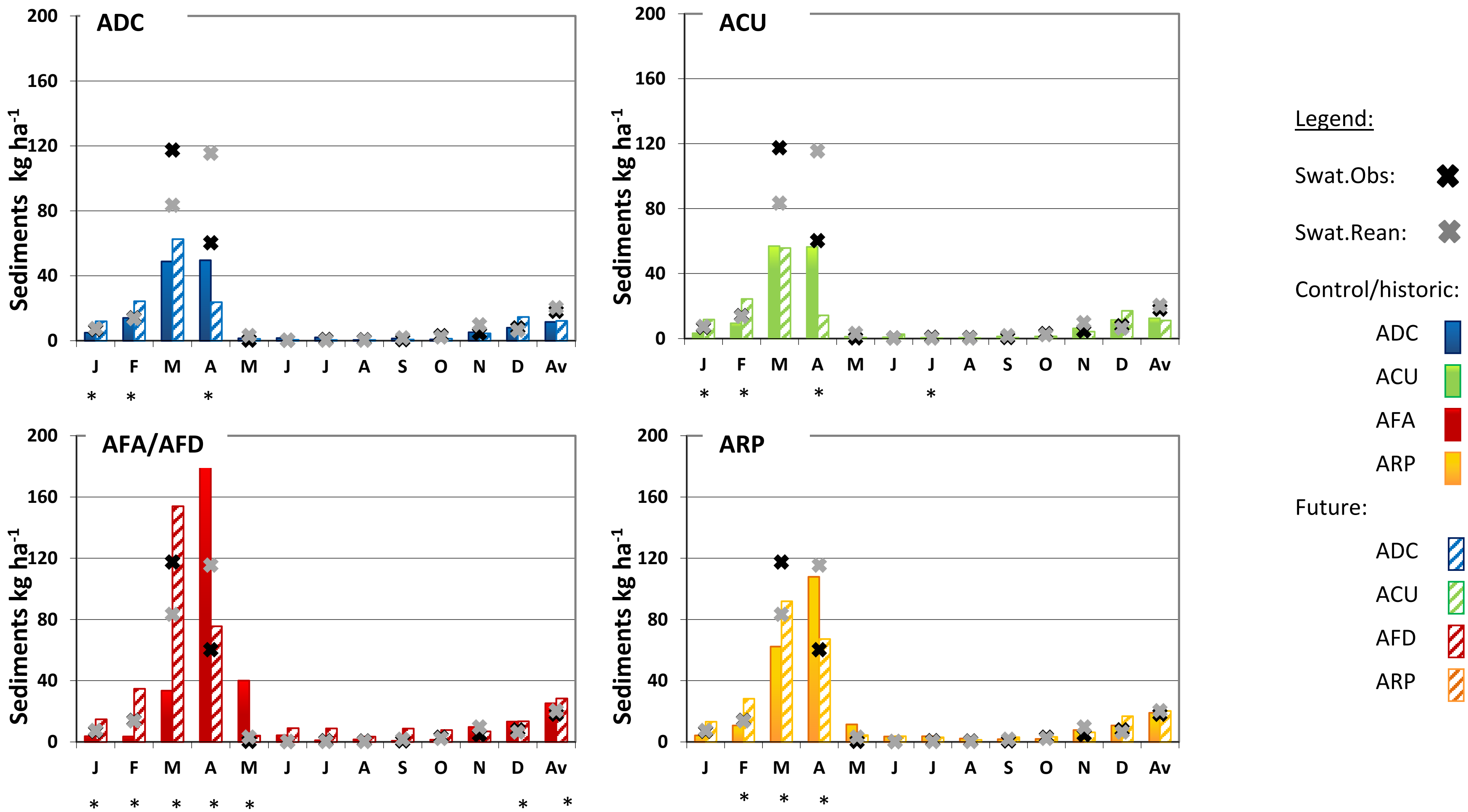

Figure E3: Mean monthly total Phosphorus loading as simulated with the different climate inputs, for the current (historical) (1971-2000) and future climates (2041-2070). * indicate significant changes (Paired *t*-test, $P \leq 0.05$).

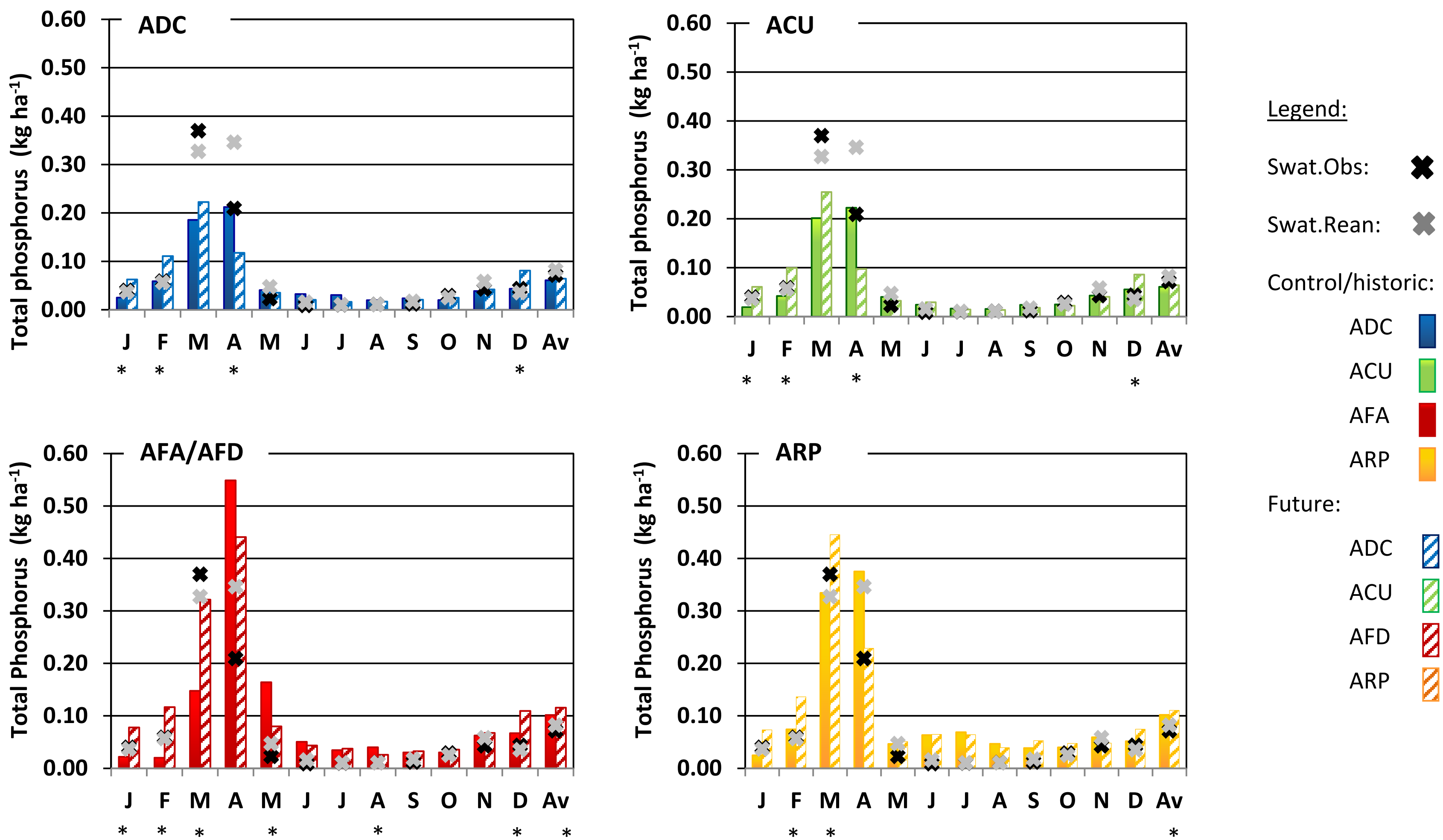

Figure E4: Mean monthly total Nitrogen loading as simulated with the different climate inputs, for the current (historical) (1971-2000) and future climates (2041-2070). * indicate significant changes (Paired t-test, p<0.05).